

Investigation of Flow and Water Constituent Fluxes Through the Tidal Inlets of the Barataria Basin

The Water Institute of the Gulf

Produced for and funded by: Coastal Protection and Restoration Authority (Task Order 55)

December 20, 2019



THE WATER INSTITUTE
OF THE GULF®

Investigation of Flow and Water Constituent Fluxes Through the Tidal Inlets of the Barataria Basin

**CYNDHIA RAMATCHANDIRANE¹, ANDREW COURTOIS^{1,2}, DIANA
R. DI LEONARDO¹, ABIGAIL C. ECKLAND¹, IOANNIS
GEORGIOU^{1,2}, MIKE MINER¹, TARA YOCUM²**

¹The Water Institute of the Gulf, New Orleans, LA, USA

²The University of New Orleans, New Orleans, LA, USA

Produced for and funded by: Coastal Protection and Restoration Authority (Task Order 55)

12/20/2019





INTEGRATING APPLIED RESEARCH | LINKING KNOWLEDGE TO ACTION | BUILDING PARTNERSHIPS

ABOUT THE WATER INSTITUTE OF THE GULF

The Water Institute of the Gulf is a not-for-profit, independent research institute dedicated to advancing the understanding of coastal, deltaic, river and water resource systems, both within the Gulf Coast and around the world. This mission supports the practical application of innovative science and engineering, providing solutions that benefit society. For more information, visit www.thewaterinstitute.org.

SUGGESTED CITATION

Task Order:

Ramatchandirane C., Courtois, A., Di Leonardo D.R., Eckland, A.C., Georgiou, I., Miner, M., and Yocum, T. (2019). Investigation of flow and water constituent fluxes through the tidal inlets of the Barataria Basin. The Water Institute of the Gulf. Prepared for and funded by the Coastal Protection and Restoration Authority. Baton Rouge, LA.



Preface

The Water Institute of the Gulf (the Institute) was contracted by the Coastal Protection and Restoration Authority (CPRA) of Louisiana to characterize water, sediment, salinity, and nutrient fluxes through the tidal inlets of Barataria Basin in south Louisiana in an effort to provide new information that can be applied to improve the performance of numerical models that are applied to inform coastal restoration plans/programs. Field-based measurements were acquired to quantify the exchange of water and attendant constituents (salinity, suspended sediment, and nutrients) through the inlets between the Barataria Basin estuary and the Gulf of Mexico. These data are ultimately intended for application to model calibration that will greatly reduce uncertainty for future simulations related to hydrodynamics in the lower basin. The Institute partnered with the University of New Orleans (UNO) to provide technical and logistical assistance in the field, data processing, and laboratory analyses, and with Louisiana State University (LSU) to provide and adapt data from existing instrument deployments.

The Institute collected information about flow velocities through each of the inlets over the course of nine months (January 15, 2019 through September 26, 2019). Field campaigns involved two components: 1) deploying fixed instruments at three of the nine Barataria Basin tidal inlets (Barataria Pass, Quatre Bayou Pass, and Fontanelle Pass) to continuously measure hydrological and water quality parameters (e.g., flow velocity, water level, turbidity, salinity, temperature, pH, dissolved oxygen, chlorophyll *a*, blue-green algae) during the study period, and 2) conducting vessel-based surveys at each of the nine inlets.

This report details the data collection efforts described above at the Barataria Basin inlets and accompanies a data deliverable provided to CPRA in digital form. This document is intended to be solely a data report and does not contain analytical or interpretative information. Additional data analysis and interpretation, and eventual data integration into the Basin Wide model is anticipated during a second phase of this study.



Table of Contents

Preface	i
List of Figures	iii
List of Tables	iii
List of Appendices Tables	iv
Acknowledgements.....	vi
1.0 Introduction.....	1
1.1. Overview.....	1
1.2. Tidal Inlets and their Role in Basin Hydraulics	2
1.3. Barataria Basin.....	3
1.4. Field Study Description	7
2.0 Data Collection Methods	11
2.1. Overall Vessel-Based Survey Design	11
2.1.1. Research Vessels.....	11
2.1.2. Data Collection Design	12
2.2. Vessel-Based Data Collection.....	17
2.2.1. Current Velocities and Discharge Through Inlets (ADCP)	17
2.2.2. Water Column Profile Casts for Conductivity, Temperature, Depth (CTD)	20
2.2.3. Suspended Sediment Water Sampling	22
2.3. Fixed Position Instrumentation.....	24
2.3.1. Station Positioning and Elevation (Trimble RTK GPS)	24
2.3.2. Continuous Discharge and Water Current Velocity Monitoring (H-ADCP).....	25
2.3.3. Continuous Velocity Record and Index Velocity Calibration	28
2.3.4. Continuous Measurement of Water Quality Constituents and Water Level (EXO2 YSI) ..	28
3.0 Results.....	32
3.1. Synoptic Data Summary	32
3.2. Water Discharge.....	32
3.2.1. Acoustic Doppler Current Profiler (ADCP) Surveys.....	32
3.2.2. Index Velocity Calibration for Barataria Pass and Fontanelle Pass	33
3.3. Suspended Sediment Samples.....	36
3.4. EXO2 YSI Turbidity Sensor Calibration to TSS	36
References.....	38
Appendices.....	41
Appendix A: ADCP File Log and Discharge Summary	42
Appendix B: CTD File Log	55
Appendix C: Suspended Sediment Data Log from Transect Surveys – TSS and LOI	57
Appendix D: Suspended Sediment Data Log from Transect Surveys – TSS and Grain Size.....	68
Appendix E: Water Sample Data Log from Transect Surveys – Nutrients	70
Appendix F: RTK Points Data Log.....	72
Appendix G: Current Meter File Log (Aquadopp, SL-500, and AWAC)	78
Appendix H: YSI File Log.....	79
Appendix I: Suspended Sediment Data Log for YSI Turbidity Calibration	80



List of Figures

Figure 1. Schematic of an idealized tidal inlet system.....	3
Figure 2. Land loss map of Barataria Basin 1932-2001.....	4
Figure 3. Historical bathymetric profiles of Barataria Pass	5
Figure 4. Channel velocity and air pressure plots with cold front passages	6
Figure 5. Typical surface current patterns outside of Barataria Basin from numerical experiments.....	7
Figure 6. Map of the study area showing the nine Barataria Basin tidal inlets.....	8
Figure 7. Close-up maps of western (top) and eastern (bottom) Barataria inlets.....	9
Figure 8. Photographs of the vessels used during this study's vessel-based data collection	11
Figure 9. Two ADCP transects from Barataria Pass illustrating the effect of waves on data coverage	12
Figure 10. Example of an ADCP channel cross-section transect.....	19
Figure 11. CTD and water sampling set-up on the RV <i>Penland</i>	21
Figure 12. Example of processed data recovered from the CTD profiler	22
Figure 13. Photograph of RTK GPS survey of surface elevation	25
Figure 14. Images depicting H-ADCP installations.....	26
Figure 15. Photograph of Nortek Sidelooping Aquadopp current meter	27
Figure 16. Example of a depth-averaged velocity flow rose at Quatre Bayou Pass	27
Figure 17. Photograph of EXO2 YSI multi-sensor hydrological and water quality sonde.....	29
Figure 18. Example of processed hydrological data	31
Figure 19. Plot showing fixed-instrument data collected and processed during study period.....	32
Figure 20. Continuous velocity record at Tx-02	34
Figure 21. ADCP velocity transect from Tx-02 during ebb tide on 9/10/2019 at 20:11 UTC.....	34
Figure 22. Continuous velocity record at Tx-07	35
Figure 23. Index velocity calibration curve for Fontanelle Pass (Tx-07)	36
Figure 24. YSI turbidity sensor correlation with total suspended sediment (TSS).....	37

List of Tables

Table 1. Vessel-based survey transect names and start and endpoint coordinates	10
Table 2. Vessel-based sampling station names and coordinates	10
Table 3. Fixed station names and coordinates	10
Table 4. Data collection activities	12
Table 5. Summary of fixed instrument deployment and servicing trips	14
Table 6. Summary of the data collection activities conducted during each survey	17



List of Appendices Tables

Appendix A: ADCP File Log and Discharge Summary

Table A-A 1. List of ADCP survey files, including discharge, at Caminada Pass (Tx-01).....	42
Table A-A 2. List of ADCP survey files, including discharge, at Barataria Pass (Tx-02)	43
Table A-A 3. List of ADCP survey files, including discharge, at Pass Abel (Tx-03)	45
Table A-A 4. List of ADCP survey files, including discharge, at Quatre Bayou Pass (Tx-04).....	46
Table A-A 5. List of ADCP survey files, including discharge, at Pass Ronquille (Tx-05)	47
Table A-A 6. List of ADCP survey files, including discharge, at Bastian Pass (Tx-06)	48
Table A-A 7. List of ADCP survey files, including discharge, at Fontanelle Pass (Tx-07)	49
Table A-A 8. List of ADCP survey files, including discharge, at Scofield Pass (Tx-08).....	51
Table A-A 9. List of ADCP survey files, including discharge, at Bay Coquette (Tx-09)	54

Appendix B: CTD File Log

Table A-B 1. List of CTD files from vessel-based surveys	55
--	----

Appendix C: Suspended Sediment Data Log from Transect Surveys – TSS and LOI

Table A-C 1. Data log of TSS and LOI from suspended sediment samples at Caminada Pass.....	57
Table A-C 2. Data log of TSS and LOI from suspended sediment samples at Barataria Pass	58
Table A-C 3. Data log of TSS and LOI from suspended sediment samples at Pass Abel	59
Table A-C 4. Data log of TSS and LOI from suspended sediment samples at Quatre Bayou Pass.....	60
Table A-C 5. Data log of TSS and LOI from suspended sediment samples at Pass Ronquille	61
Table A-C 6. Data log of TSS and LOI from suspended sediment samples at Bastian Pass.....	62
Table A-C 7. Data log of TSS and LOI from suspended sediment samples at Fontanelle Pass	64
Table A-C 8. Data log of TSS and LOI from suspended sediment samples at Scofield Pass.....	67
Table A-C 9. Data log of TSS and LOI from suspended sediment samples at Bay Coquette	67

Appendix D: Suspended Sediment Data Log from Transect Surveys – TSS and Grain Size

Table A-D 1. Data log of TSS and grain size from suspended sediment samples at Barataria Pass	68
Table A-D 2. Data log of TSS and grain size from suspended sediment samples at Quatre Bayou Pass... <td>69</td>	69
Table A-D 3. Data log of TSS and grain size from suspended sediment samples at Fontanelle Pass	69

Appendix E: Water Sample Data Log from Transect Surveys - Nutrients

Table A-E 1. Data log of water samples from transect surveys collected for nutrients.....	70
---	----

Appendix F: RTK Points Data Log

Table A-F 1. RTK points collected at the Tx-02 fixed instrumented site.....	72
Table A-F 2. RTK points collected at the Tx-04 fixed instrumented site.....	75
Table A-F 3. RTK points collected at the Tx-07 fixed instrumented site.....	76

Appendix G: Current Meter File Log (Aquadopp, SL-500, and AWAC)

Table A-G 1. List of current meter files (Aquadopp, SL-500, and AWAC)	78
---	----

Appendix H: YSI File Log

Table A-H 1. List of raw YSI files.....	79
Table A-H 2. List of processed YSI files.....	79



Appendix I: Suspended Sediment Data Log for YSI Turbidity Calibration

Table A-I 1. Data log of suspended sediment samples for YSI turbidity calibration 80



Acknowledgements

The authors would like to acknowledge the support of the following individuals for their contribution in the field and in the lab: Francesca Messina and Leland Moss from the Institute, Mike Brown and Leah Tevis from UNO, Dallon Weathers formerly with the Institute, and Jon Bridgeman from CPRA.

Dr. Chunyan Li and Brian Milan from LSU are recognized for their contribution to additional data collection efforts critical for the completion of this study.

Joseph (Wes) LeBlanc, Jon Bridgeman, Darin Lee, and Kazi Sadid from CPRA provided guidance on the scope and management of this task order.

A special thanks to Specialty Diving of LA, Inc. and Gulf Coast Divers for specialized assistance in the field.

This report was internally reviewed by Christopher Esposito.



1.0 Introduction

1.1. OVERVIEW

The tidal inlets situated along the Barataria Basin barrier island shoreline play an important role in governing the fluxes of water and attendant constituents (suspended sediment, salinity, nutrients, etc.) throughout the Basin. The geometries of the inlet channels are highly dynamic and evolve rapidly in response to: (1) increasing open water area and hydraulic connectivity within the basin, and (2) sand supply along the barrier shoreline (e.g., barrier restoration projects). Mississippi River discharge plays an important role in salinity and other water quality constituent fluctuations, especially at the more eastern inlets. This is the first time that all nine tidal inlets of the Barataria Basin have been the focus of a coordinated data collection effort and treated as a single integrated system. The motivation for this data collection effort (and future analyses based upon these new data) is to provide an up-to-date, quantified hydraulics and water quality constituent flux along the entire Barataria Basin barrier shoreline. These data are important to inform improved performance and confidence in numerical model simulations by addressing data gaps relating to present-day conditions and the exchange of water constituents between the Barataria Basin and the Gulf of Mexico. The field data collection effort consisted of numerous vessel-based data collection campaigns that traverse each of the nine tidal inlet channels at their throat and the deployment of fixed-station instruments to provide continuous point measurements of constituents in select “index” inlets over the entire study duration.

Earlier works (e.g. FitzGerald et al., 2007; Howes, 2009; Li et al., 2018; Marmer, 1948; Reed, 1995) consider only four of the nine total Barataria inlets, with inlets east of Barataria Bay being disregarded and treated as a separate tidal basin. However, land loss within the basin has led to increased hydraulic connectivity and potential for Barataria Bay and the attendant four major inlets (Caminada Pass, Barataria Pass, Quatre Bayou Pass, Pass Abel) to be influenced by more eastern portions of the basin via the five tidal inlets (Pass Ronquille, Bastian Pass, Fontanelle Pass, Scofield Pass, Bay Coquette) associated with that region and the Mississippi River during times of high discharge. Moreover, these earlier works that presently inform numerical modeling cannot consider the aggressive barrier island restoration program implemented by the Louisiana Coastal Protection and Restoration Authority (CPRA) undertaken after their completion. Approximately 90% of the Barataria Basin barrier shoreline has been restored over the past decade. Given the near-term goals of the 2012 and 2017 versions of the Louisiana Coastal Master Plan (LA CPRA, 2012; 2017) and subsequently Mid-Barataria Sediment Diversion planning and design efforts, accurate characterization and quantification of inlet tidal hydraulics is critical to improve basin-wide numerical modeling capabilities.

This report is divided into three sections:

1. Introduction
2. Data Collection Methods
3. Study Results

The scope of this project was solely focused on data collection and post-processing those data. No data analysis, interpretations, or application of those for numerical model improvements were included. It is anticipated that future (yet to be funded) work will involve analysis and interpretation of these data



integrated with a wealth of other existing data products from the Barataria Basin tidal inlets, offshore, and within the basin (e.g., Howes, 2009; Li et al., 2011; 2018; 2019) to provide a comprehensive understanding and quantification of inlet hydraulics, their role in basin hydraulics, and attendant water quality and nutrient fluxes.

This methods report covers procedures employed for data collection, processing, and data management. The logs of data files and samples are provided in the Appendices. Digital files, along with metadata, of all processed data accompany the submission of this report. As documented in this report, all data have been processed and have undergone quality assurance/quality control (QA/QC) review.

1.2. TIDAL INLETS AND THEIR ROLE IN BASIN HYDRAULICS

A tidal inlet is an opening along the shoreline that separates barrier islands and serves as a connection between the ocean and backbarrier (Figure 1). Locally, a tidal inlet may be referred to as a pass or *coupe* (French for “cut”). Tidal currents maintain the inlet channel by shore-perpendicular flushing of sediment that is transported to the inlet by wave-driven currents (Brown, 1928; Escoffier, 1940; FitzGerald & Miner, 2013). Tidal inlet formation can occur through breaching of a barrier spit building across an embayment or at the location of a former river channel (Davis, Jr. & FitzGerald, 2009). The volume of water that flows through the inlet during each portion of the tidal cycle (flood or ebb) is termed tidal prism. The tidal prism is a function of the spring tidal range and the area of open water in the backbarrier basin (O’Brien, 1931). Two important relationships at tidal inlets have been identified: (1) an increase in tidal prism correlates with an increase in inlet throat cross-sectional area (O’Brien, 1931), and (2) ebb tidal delta size (sediment volume) increases with an increase in tidal prism (Walton & Adams, 1976). Past studies of these relationships as they relate to the Barataria Basin are discussed further in section 1.3.

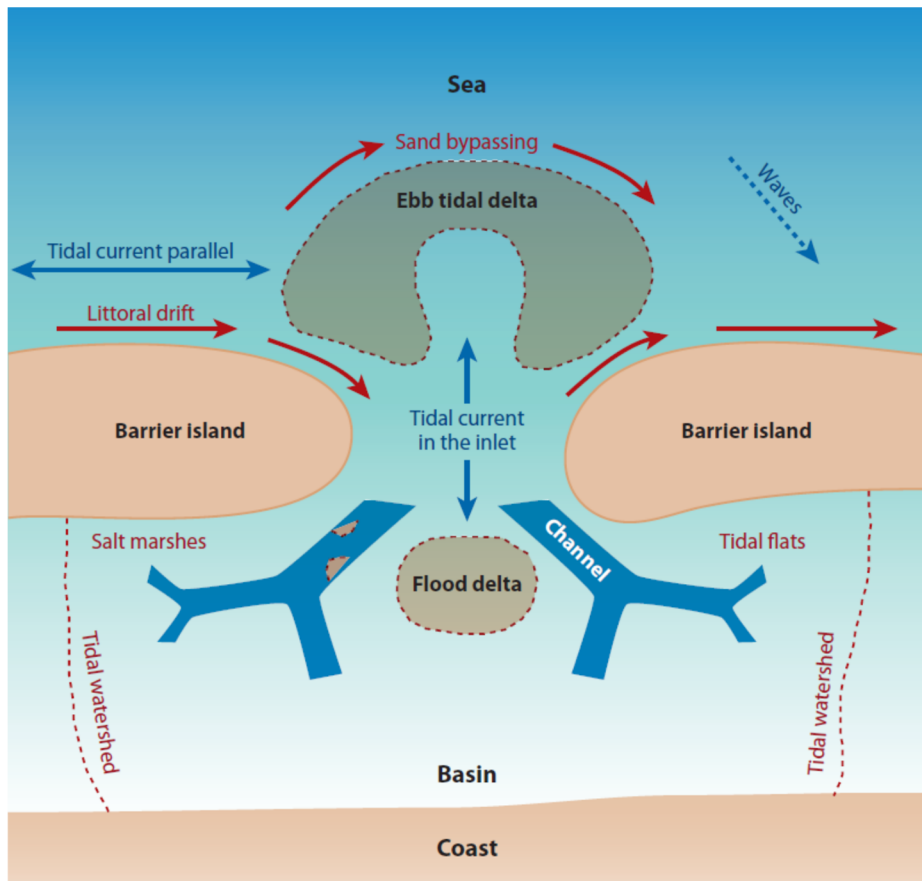


Figure 1. Schematic of an idealized tidal inlet system; reproduced from de Swart & Zimmerman (2009)

1.3. BARATARIA BASIN

The Barataria Basin is an irregularly shaped shallow interdistributary basin bounded by the abandoned distributary Bayou Lafourche to the west, and the active Mississippi River to the east. Barataria Basin is approximately 6,600 square kilometer (km^2) (Turner et al., 2019). The main freshwater source to the basin is from the Mississippi River, through the Davis Pond Diversion, with a flow capacity of 250 cubic meters per second (m^3/s) (Li et al., 2011), direct precipitation and runoff, and through navigation waterways with Mississippi River influence (Georgiou et al., 2010). Other freshwater sources entering the basin via man-made structures are the Naomi and West Pointe à la Hache siphons that operate at a maximum rate of approximately $60 \text{ m}^3/\text{s}$ (Inoue et al., 2008). In the lower part of the basin is Barataria Bay, a shallow estuary (~2 meters [m]) fronted by a chain of barrier islands separated by nine tidal inlets. The barriers fronting Barataria Basin experience diurnal tides with a microtidal range of 0.4 m, which increases to 0.6 m during spring tides (FitzGerald et al., 2004). Previous research by Marmer (1948) measured tidal currents in Barataria Bay over 24 days of observation. Marmer (1948) found the amount of water flowing among Barataria Pass, Quatre Bayou Pass, Caminada Pass, and Pass Abel was estimated to be 66%, 18%, 13%, and 3% respectively, of the total. The barrier islands in this region formed from marine reworking of abandoned delta lobes associated with the St. Bernard, Lafourche and Plaquemines Delta complexes (Frazier, 1967; Penland et al., 1988; Roberts et al., 1997) and subsequent ongoing coastal sediment transport processes (FitzGerald et al., 2004; List et al., 1997; Miner et al., 2009; Penland



et al., 1988). Relative sea-level rise and wetland loss have contributed to the conversion of land to open water throughout Barataria Basin (Figure 2).

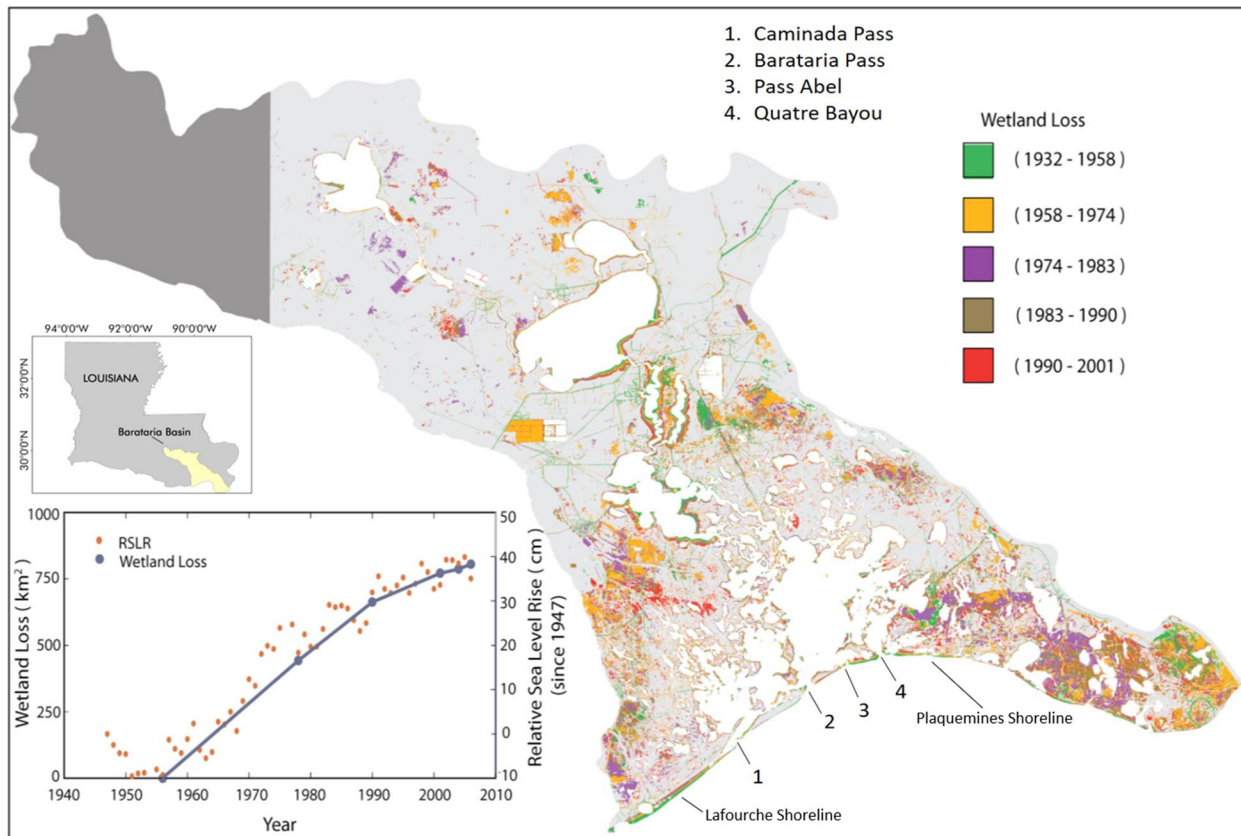


Figure 2. Land loss map of Barataria Basin 1932-2001; modified from (Howes, 2009).

Barataria Basin experienced approximately 1,120 km² of land loss between 1932-2016 (Couvillion et al., 2017). Rates of relative sea level rise in the southern portion of the basin, specifically for Grand Isle, LA, have been documented at 9.1 millimeters per year (mm/yr) (Byrnes et al., 2019). The combined effects of wetland loss and relative sea-level rise has resulted in increased tidal prism. To accommodate the increased volume of water exchanged between Barataria Basin and the Gulf of Mexico, inlets have increased in cross-sectional area and new inlets have formed (Figure 3; FitzGerald et al., 2007, 2004; Howes, 2009; Miner et al., 2009). Increased tidal prism also results in greater sand trapping efficiency at ebb tidal deltas (Figure 3), which (coupled with inlet widening) occurs at the expense of barrier island integrity (FitzGerald et al., 2007; Miner et al., 2009).

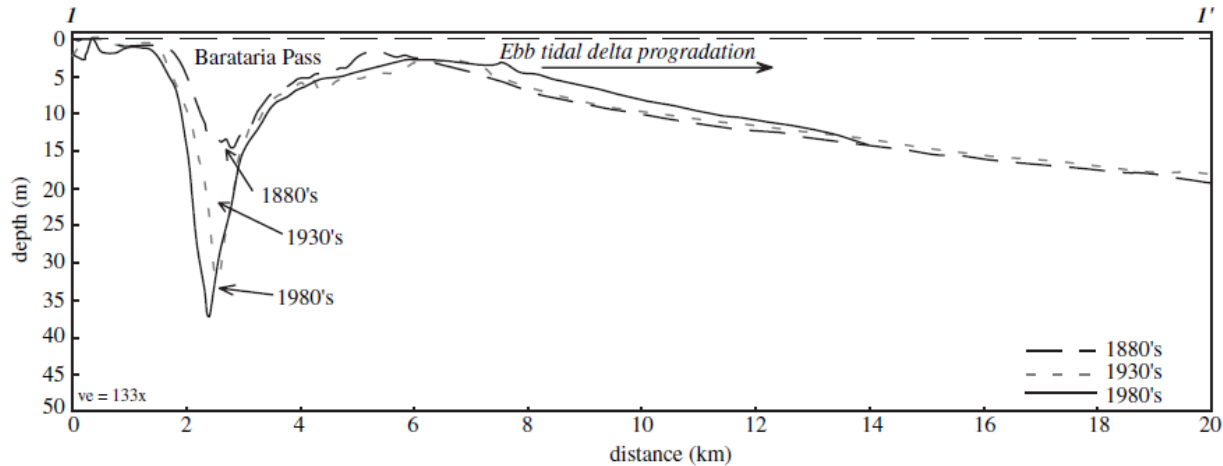


Figure 3. Historical bathymetric profiles of Barataria Pass illustrating inlet cross-sectional area expansion and seaward progradation of the ebb tidal delta; data from List et al. (1994); figure reproduced from Fitzgerald et al. (2004)

The breaching of barriers and formation of new tidal inlets along Louisiana's barrier islands are most commonly attributed to the passage of hurricanes. Some hurricane-cut inlets are ephemeral, while others remain open and become a stable conduit for tidal exchange. Historical bathymetric and shoreline maps of Barataria Basin show the breaching and establishment of stable inlets, such as Pass Abel, (List et al., 1994; Williams et al., 1992). Maps from the 1880s do not show the existence of Pass Abel and it is not present on historical maps until the 1930s, suggesting that it formed sometime between the 1880s and 1930s surveys. The increase in tidal prism for Barataria Basin allowed for Pass Abel to become a stable tidal inlet after initial storm breaching (FitzGerald et al., 2004). For detailed accounts of the formation/closure of tidal inlets in Barataria Basin the reader is referred to Levin (1993); Williams et al. (1992), and FitzGerald et al. (2004).

Other research in Barataria Basin has focused on nutrients, salinity, subtidal flow related to meteorological forcing, and the flushing of the basin. Wissel et al. (2005) and Turner et al. (2019) recorded the introduction of nutrients via Mississippi River water through Barataria Basin. Monthly salinity sampling in Barataria Basin over a 22-year period showed that the annual average salinity decreased within the basin as the annual Mississippi River discharge increased (Turner et al., 2019). This highlights the important role of Mississippi River water within Barataria Basin. The passage of frontal systems (warm or cold) also has a strong influence on subtidal flow within Barataria Basin (Li et al., 2018, 2019). Li et al. (2019) studied the passage of 51 cold fronts and their impact on subtidal exchange in multiple tidal inlets using horizontal acoustic Doppler current profilers (H-ADCPs) and Finite-Volume Coastal Ocean Model (FVCOM; numerical model commonly used in coastal environments) simulations. Results show that when a cold front passes the area, a strong outward flow into the Gulf develops, producing the maximum outward subtidal flow, with the north component of the wind vector being the major contributor to subtidal flow through the inlets (Figure 4). Li et al. (2011) estimated that the flushing time of Barataria Bay is approximately 13-19 days and used numerical simulations to show that fresh water can enter Barataria Bay as a result of the lateral spreading of the Mississippi River plume and the Louisiana Coastal Current (Figure 5). At the inlet scale Li et al. (2009), using 24-hour synoptic surveys at



Barataria Pass, noted a lateral inversion of the flow over a tidal cycle, driven by asymmetric straining across the inlet. The authors documented higher stratification on the eastern side of the inlet during flood tide compared to much lower stratification of the western side. Conversely during ebb flows, the stratification patterns were reversed, a phenomenon that the authors attributed to Mississippi River water masses arriving at the inlet during high river discharge. Cui et al. (2018) studied Barataria Pass further, building on the research of Li et al. (2009) using a validated three-dimensional oceanographic model. They found that partial stratification controls lateral circulation patterns across the inlet; they report that in addition to pressure gradient and vertical stress divergence contributing to lateral circulation, non-linear advection and horizontal stress divergence played a role, causing lateral circulation during ebb to be mostly toward the east part of the inlet, despite cross-sectionally average velocities during both flood and ebb being similar with little, if any, asymmetry (Cui et al., 2018).

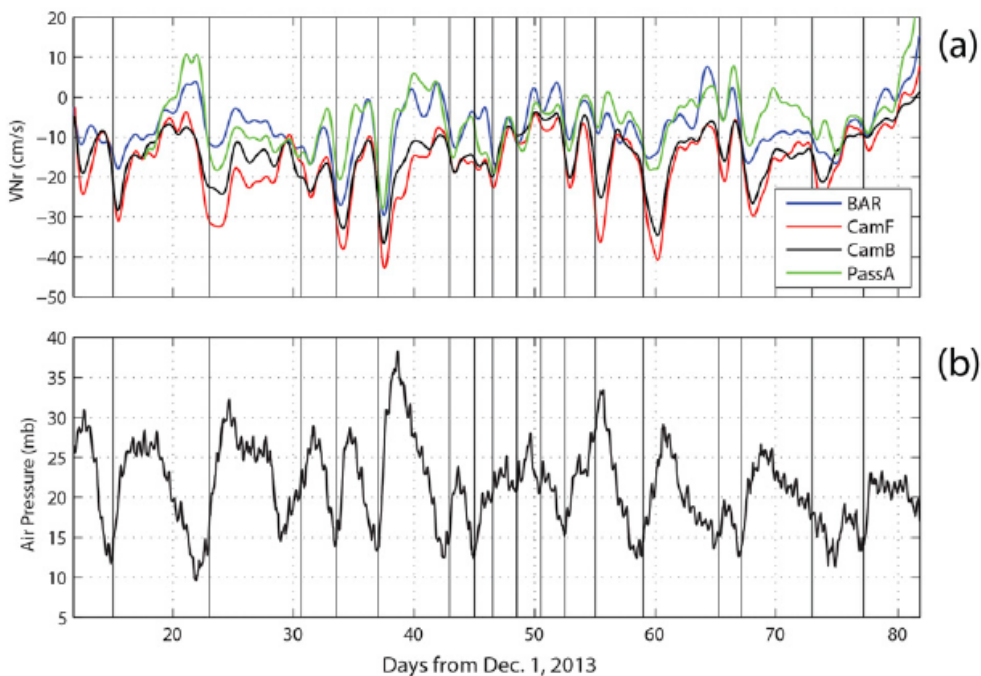


Figure 4. Channel velocity and air pressure plots with cold front passages, (a) low-pass filtered along-channel velocity from H-ADCP measurements at multiple tidal inlets (Barataria Pass- BAR, Caminada Pass- CamF and CamB, and Pass Abel- PassA) during a 2013/2014 time period, (b) air pressure. Vertical lines represent times of cold front passages. Reproduced from (Li et al., 2009).

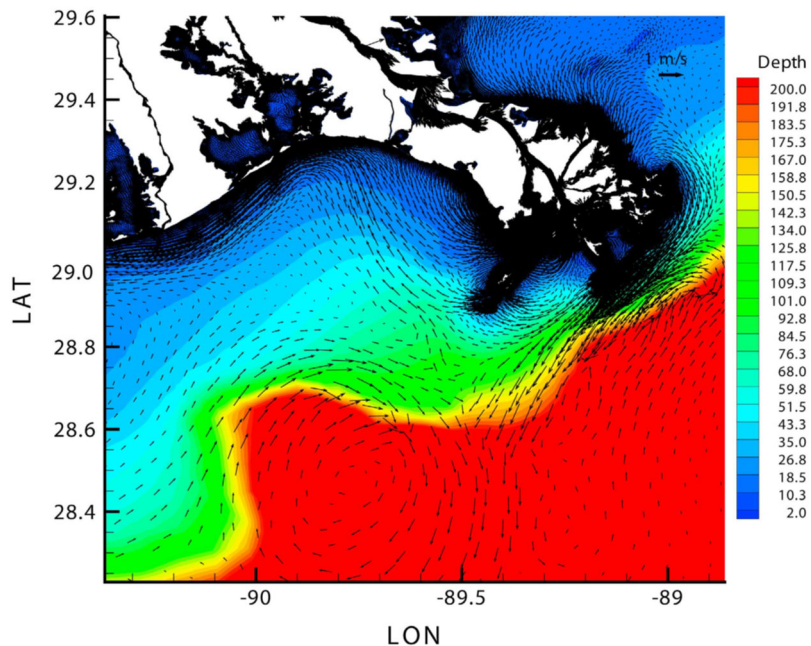


Figure 5. Typical surface current patterns outside of Barataria Basin from numerical experiments; reproduced from Li et al. (2011).

The aforementioned research (FitzGerald et al., 2007, 2004; Howes, 2009; Li et al., 2009, 2011, 2018, 2019; Turner et al., 2019) highlights the wide range of variables (relative sea level rise, delta plain disintegration/wetland loss, Mississippi River discharge, and meteorological events) affecting the exchange of water, sediment, and nutrients at tidal inlets in Barataria Basin.

1.4. FIELD STUDY DESCRIPTION

In order to quantify tidal exchange between Barataria Basin and the Gulf of Mexico, it is essential to have synoptic measurements at all Barataria Basin tidal inlets (Figure 6), including the eastern inlets (Figure 7) that had formerly been assumed independent from the western inlets that directly influence Barataria Bay. Vessel-based surveys (Table 1), vessel-based station casts (Table 2), and fixed position instruments (Table 3) were used to conduct field measurements of flow velocities. These methods have been employed by Howes (2009), Li et al. (2019), and others. Vessel-based surveys of flow velocity measurements were conducted at all nine tidal inlets (Figure 6; details in Section 2.2.1). During select surveys, water column profiling casts and sampling were also conducted at several stations within each inlet (Figure 7; details in Sections 2.2.2 and 2.2.3). The number of stations (A, B, C) within each inlet was determined based on inlet width. At minimum, for each inlet one station was located at the deepest part of the inlet throat. For the wider inlets, an additional one or two stations were selected to capture a representative cross-section of flow at the given inlet. Three tidal inlets (Figure 6) were selected for fixed instrument deployment: Barataria Pass (Tx-02), Quatre Bayou Pass (Tx-04), and Fontanelle Pass (Tx-07). These inlets were selected based on their position along the Barataria basin shoreline, inlet cross-sectional area, and availability of existing structures as suitable instrument mount points. Barataria Pass is the dominant inlet for the Barataria Bay (western) portion of the study area, and has historically been the focus of previous instrument occupation and research (e.g. Howes, 2009; Li et al., 2019). Instrumenting this inlet provides information that is compatible with these previous and ongoing studies. Fontanelle Pass



is one of the larger of the tidal inlets associated with the eastern Barataria Basin and had existing infrastructure suitable for establishing instrument installations. Quatre Bayou Pass was chosen because it has a well-defined channel throat, provided a transitional inlet between the western and eastern inlets, and existing infrastructure for instrument mounting. Various combinations of instruments were deployed at these fixed stations that include H-ADCPs (Sontek SL-500, Nortek Sideloading Aquadopp, and Nortek 2D AWAC) to measure current velocity and direction and hydrological sondes (EXO2 YSI) to measure several water quality parameters. A detailed description of instruments and sampling methodology is provided in Section 2.0.

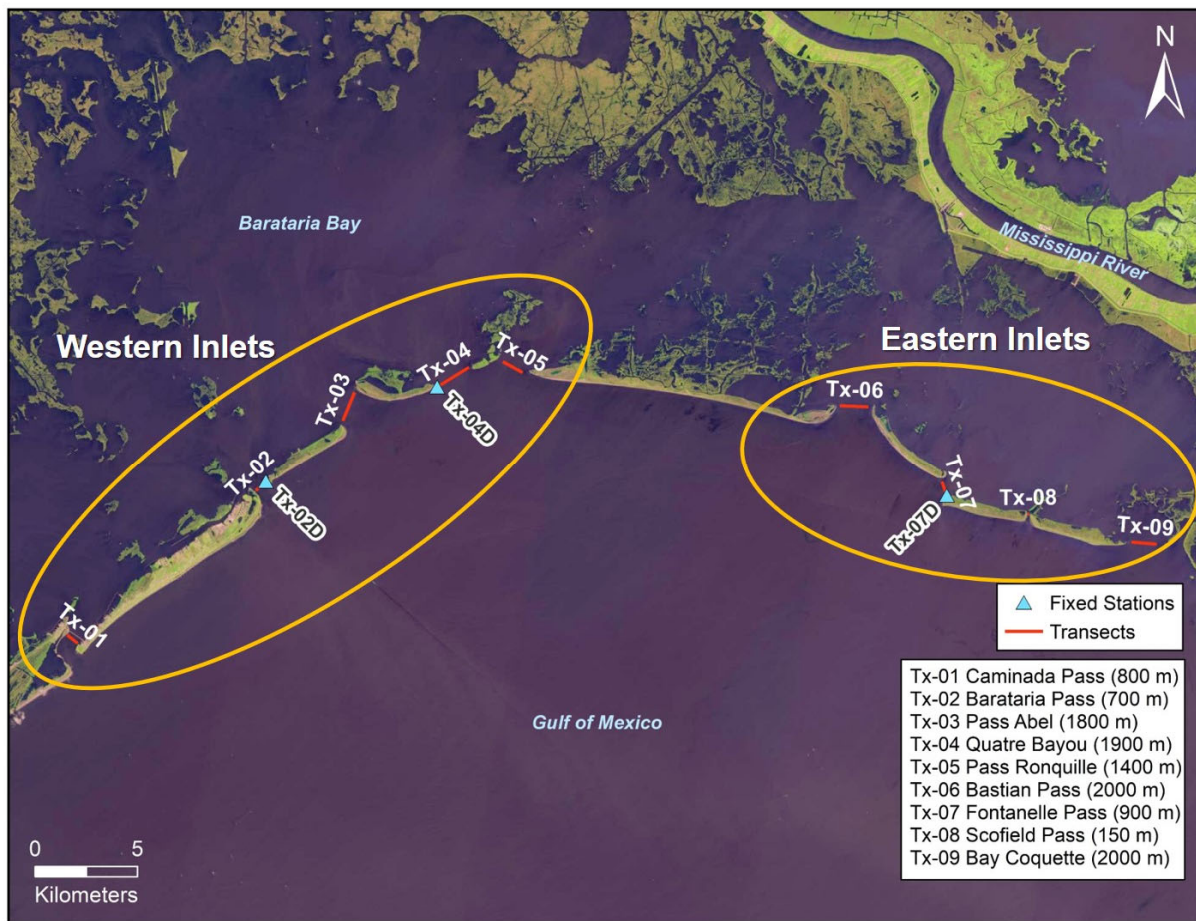


Figure 6. Map of the study area showing the nine Barataria Basin tidal inlets that are the focus of this data collection effort. Red lines represent vessel-based transect locations. Blue triangles represent fixed instrument deployment locations. Transect ID, corresponding tidal inlet name, and approximate transect length are provided in the inset table. Background imagery is from Landsat 8 acquired on 08/29/2019, retrieved from USGS EarthExplorer (<https://earthexplorer.usgs.gov/>).



Figure 7. Close-up maps of western (top) and eastern (bottom) Barataria inlets. Red lines represent vessel-based transects. Blue triangles represent fixed instrument deployment locations. Green circles indicate sampling stations along the survey transects. Background imagery is from Landsat 8 acquired on 08/29/2019, retrieved from USGS EarthExplorer (<https://earthexplorer.usgs.gov/>).



Table 1. Vessel-based survey transect names and start and endpoint coordinates

Transect	Location	Start Latitude	Start Longitude	End Latitude	End Longitude
Tx-01	Caminada Pass	29.207531	-90.048573	29.203743	-90.043357
Tx-02	Barataria Pass	29.268935	-89.951972	29.272909	-89.946796
Tx-03	Pass Abel	29.298837	-89.907379	29.311280	-89.901150
Tx-04	Quatre Bayou Pass	29.312692	-89.859598	29.320904	-89.843325
Tx-05	Pass Ronquille	29.323074	-89.826304	29.317944	-89.816419
Tx-06	Bastian Pass	29.299477	-89.657667	29.298675	-89.643365
Tx-07	Fontanelle Pass	29.264513	-89.607528	29.258300	-89.605305
Tx-08	Scofield Pass	29.249125	-89.565143	29.249105	-89.564238
Tx-09	Bay Coquette	29.235442	-89.513330	29.234203	-89.500713

Table 2. Vessel-based sampling station names and coordinates

Transect	Station	Location	Latitude	Longitude
Tx-01	A	Caminada Pass	29.207116	-90.048001
Tx-01	B	Caminada Pass	29.205844	-90.046249
Tx-01	C	Caminada Pass	29.204292	-90.044114
Tx-02	A	Barataria Pass	29.269453	-89.951297
Tx-02	B	Barataria Pass	29.270710	-89.949660
Tx-02	C	Barataria Pass	29.271996	-89.947985
Tx-03	A	Pass Abel	29.300795	-89.906399
Tx-03	B	Pass Abel	29.303750	-89.904919
Tx-03	C	Pass Abel	29.309220	-89.902181
Tx-04	A	Quatre Bayou Pass	29.313325	-89.858343
Tx-04	B	Quatre Bayou Pass	29.315602	-89.853832
Tx-04	C	Quatre Bayou Pass	29.318988	-89.847121
Tx-05	A	Pass Ronquille	29.321779	-89.823808
Tx-05	B	Pass Ronquille	29.319539	-89.819492
Tx-06	A	Bastian Pass	29.299384	-89.656003
Tx-06	B	Bastian Pass	29.299096	-89.650868
Tx-06	C	Bastian Pass	29.298814	-89.645849
Tx-07	A	Fontanelle Pass	29.263023	-89.606995
Tx-07	B	Fontanelle Pass	29.260113	-89.605954
Tx-08	A	Scofield Pass	29.249116	-89.564748
Tx-09	A	Bay Coquette	29.235266	-89.511530
Tx-09	B	Bay Coquette	29.234880	-89.507605

Table 3. Fixed station names and coordinates

Station	Location	Latitude	Longitude
Tx-02D	Barataria Pass	29.272833	-89.946806
Tx-04D	Quatre Bayou Pass	29.312692	-89.859598
Tx-07D	Fontanelle Pass	29.258289	-89.605301



2.0 Data Collection Methods

2.1. OVERALL VESSEL-BASED SURVEY DESIGN

2.1.1. Research Vessels

Four different research vessels were used to conduct surveys and deploy and service fixed instruments (Figure 8). The Water Institute of the Gulf's RV *Lake Itasca* and RV *Silver Mullet* are configured to run acoustic Doppler current profiler (ADCP) surveys with bow-mounted transducers providing for an optimal location for current velocity measurement that is removed from the influence of "hydraulic noise" produced by the boat hull (Figure 8). The bow-mount also allows for the vessel to acquire measurements while traversing the inlet back and forth in both directions. The research vessels from the University of New Orleans (UNO) are configured to run ADCP surveys with the transducer mounted on the port side, offset from the bow (RV *Penland*) and on the starboard side (RV *Mudlump*) (Figure 8). This configuration significantly decreases the effect of vessel motion (due to waves) on the transducer. Increased wave conditions can result in "blanking" and decreased data coverage (example shown in Figure 9) which is more pronounced with bow-mounted configurations that are more removed from the vessel's center of motion. However, a limitation of the side-mounted ADCP configuration is that surveying is restricted to one direction, with the transducer side of the boat facing up-current when traversing the channel, to prevent hydrodynamic influence of the boat hull on measurements.



Figure 8. Photographs of the vessels used during this study's vessel-based data collection; RV *Penland* (top left), RV *Silver Mullet* (top right), RV *Mudlump* (bottom left), and RV *Lake Itasca* (bottom right)

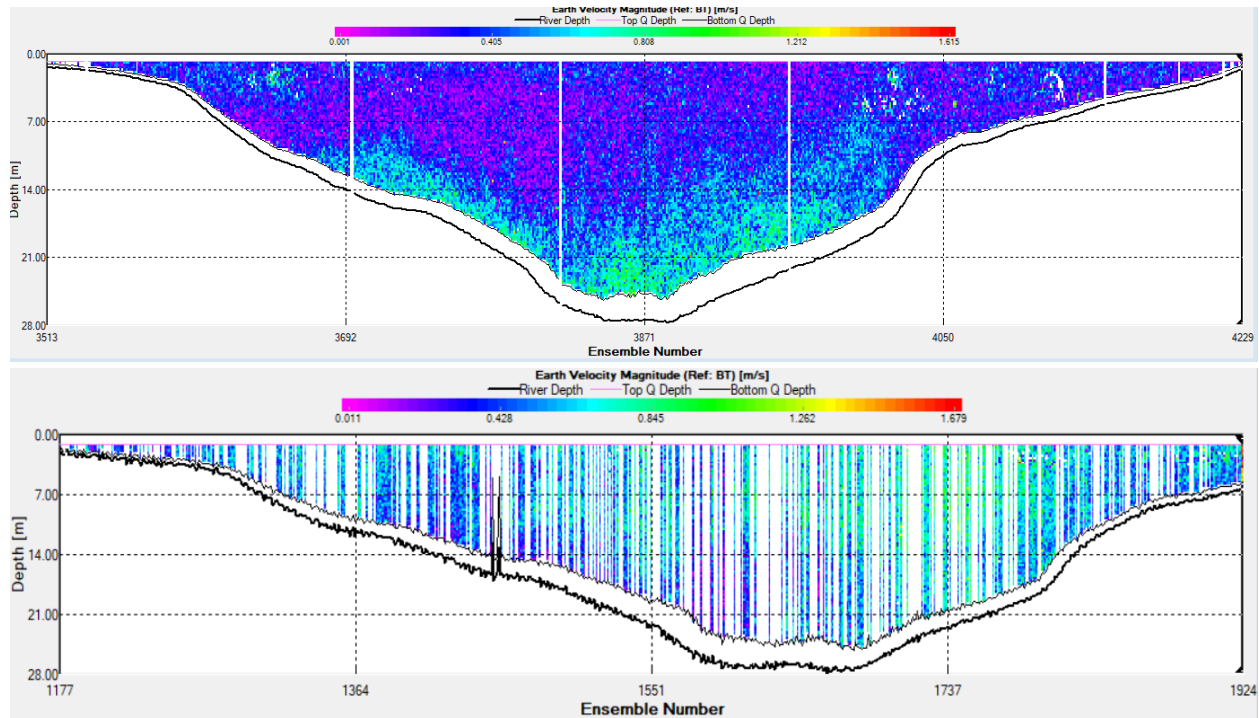


Figure 9. Two ADCP transects from Barataria Pass illustrating the effect of waves on data coverage; white blank areas represent gaps in data coverage caused by waves. The top panel from the *RV Penland* on June 3, 2019 15:50 UTC (approximately 2 m/s winds) has more complete coverage with minimal data gaps, the bottom panel from the *RV Silver Mullet* on May 22, 2019 15:44 UTC has blanked areas during rough conditions (approximately 5 m/s winds) with data gaps indicating that sea-state can have significant influence on data quality. Note that while data gaps such as these are not optimal, discharge at the inlets can be computed with minimal uncertainty if there are regularly-spaced “windows” of measurements for a given channel cross-section.

2.1.2. Data Collection Design

All data collection activities, instruments, and data types are described in Table 4. Fixed instruments were deployed at three stations in late January 2019 (Figure 6), and one remains deployed as of the submission date of this report for continuous monitoring of flow at Fontanelle Pass (Tx-07). A summary of fixed instrument deployment and servicing dates for each of the three fixed stations is listed in Table 5. Vessel-based surveys were conducted between late January 2019 and September 2019 (Figure 7). A summary of all activities conducted during each survey is listed in Table 6.

Table 4. Data collection activities conducted and instruments deployed

Activity	Location	Instruments	Purpose of data collection
*ADCP transects	All 9 inlets	RD Instruments 1200 kHz Rio Grande, RD Instruments 600 kHz RiverRay	Integrated water discharge and current velocities
GPS Positioning	All 9 inlets	Trimble R8, Trimble MPS865, Hemisphere A101	Provide GPS positioning and navigation data for ADCP surveys



Activity	Location	Instruments	Purpose of data collection
Water quality profiler	All 9 inlets	Seabird SBE19 plus Profiler **CTD	Water column profiles for conductivity, temperature, turbidity, pH, dissolved oxygen, and depth
Water sampling: suspended sediment and % organics	All 9 inlets	Electric pump and hose system	Suspended sediment concentrations and % organics at near-surface, mid-depth, and near-bed (0.1, 0.5 and 0.9) fractional depths
Water sampling: grain size and nutrients	Tx-02, Tx-04, Tx-07	Electric pump and hose system	Grain size and nutrients additionally collected at the thalweg station at near-surface, mid-depth, and near-bed (0.1, 0.5 and 0.9) fractional depths
Water quality and water level monitoring	Tx-02D, Tx-04D, Tx-07D	EXO2 YSI	Water level, salinity, turbidity, temperature, dissolved oxygen, and chlorophyll <i>a</i> , blue-green algae
Current velocity monitoring	Tx-02D, Tx-04D, Tx-07D	Sontek SL-500, Nortek Sidelooking Aquadopp, Nortek 2D AWAC	Continuous water discharge calibrated from ADCP transects
Water elevation	Tx-02D, Tx-04D, Tx-07D	Trimble R8 ***RTK GPS	Fixed instrument calibration to water level and vertical datum (NAVD88)

*ADCP = Acoustic Doppler current profiler;

**CTD = Conductivity, depth, temperature;

***RTK = Real Time Kinematic



Table 5. Summary of fixed instrument deployment and servicing trips

Dates	Stations	Location	Instruments	Detail of Activity
01/11/2019	Tx-07	Fontanelle Pass	YSI	Installed structures on pilings to house SL-500 and YSI, deployed YSI
01/15/2019	Tx-02	Barataria Pass	YSI and SL-500	Installed and deployed SL-500 and YSI on USGS piling and platform
01/16/2019	Tx-04	Quatre Bayou Pass	YSI and SL-500	Installed and deployed SL-500 and YSI on piling
01/26/2019	Tx-07	Fontanelle Pass	SL-500	Deployed SL-500
02/05/2019	Tx-02	Barataria Pass	YSI and SL-500	Routine service, water present in SL-500 battery case
02/24/2019	Tx-02	Barataria Pass	YSI and SL-500	Routine service, redeployed SL-500 and YSI
03/12/2019	Tx-04	Quatre Bayou Pass	YSI and SL-500	Instruments discovered missing
03/12/2019	Tx-07	Fontanelle Pass	YSI and SL-500	Routine service, redeployed SL-500 and YSI
03/22/2019	Tx-04	Quatre Bayou Pass	YSI and Aquadopp, Klein 300	Lost instrument recovery attempt, deployed back-up instruments: sled with YSI and Aquadopp
03/22/2019	Tx-02	Barataria Pass	YSI and SL-500	Routine service, issues with SL-500, redeployed YSI
04/02/2019	Tx-04	Quatre Bayou Pass	Divers	Lost instrument recovery with Gulf Coast Divers
04/10/2019	Tx-02	Barataria Pass	YSI and SL-500	Serviced and redeployed YSI, deployed SL-500
04/10/2019	Tx-04	Quatre Bayou Pass	YSI and Aquadopp	Serviced sled with YSI and Aquadopp, unable to redeploy due to sea state
04/28/2019	Tx-04	Quatre Bayou Pass	YSI and Aquadopp	Redeployed sled with YSI and Aquadopp



Dates	Stations	Location	Instruments	Detail of Activity
04/28/2019	Tx-02	Barataria Pass	YSI and SL-500	Routine service, redeployed SL-500 and YSI
05/05/2019	Tx-07	Fontanelle Pass	YSI and SL-500	Routine service, redeployed SL-500 and YSI
05/15/2019	Tx-02	Barataria Pass	YSI and SL-500	Routine service, redeployed SL-500 and YSI
06/02/2019	Tx-04	Quatre Bayou Pass	YSI and Aquadopp	Marker buoy on sled discovered missing, began lost instrument search (drag-line)
06/26/2019	Tx-04	Quatre Bayou Pass	Klein 3000	Lost instrument search, conducted side-scan survey
07/01/2019	Tx-07	Fontanelle Pass	SL-500	Routine service, redeployed SL-500, YSI inaccessible due to high water
07/18/2019	Tx-02	Barataria Pass	YSI and SL-500	SL-500 discovered missing, began lost instrument search, serviced YSI but did not redeploy due to issue with calibration
07/18/2019	Tx-07	Fontanelle Pass	YSI and SL-500	Routine service and redeployed SL-500, YSI experienced water damage, deployed new YSI
07/26/2019	Tx-02	Barataria Pass	Klein 3000	Search for lost instrument, conducted side-scan survey
07/30/2019	Tx-02	Barataria Pass	Klein 3000	Search for lost instrument, conducted side-scan survey
08/08/2019	Tx-02	Barataria Pass	Edgetech 4125	Search for lost instrument, conducted side-scan survey
08/09/2019	Tx-02	Barataria Pass	Edgetech 4125	Search for lost instrument, conducted side-scan survey
08/13/2019	Tx-02	Barataria Pass	Edgetech 4125	Search for lost instrument, conducted side-scan survey
08/16/2019	Tx-02	Barataria Pass	Divers	Search for lost instrument with Specialty Diving of LA, Inc. to investigate side-scan targets, no instruments were recovered



Dates	Stations	Location	Instruments	Detail of Activity
09/05/2019	Tx-02	Barataria Pass	YSI and LSU H-ADCP	Routine service and redeployed LSU's H-ADCP, deployed YSI
09/08/2019	Tx-07	Fontanelle Pass	YSI and SL-500	Routine service, redeployed SL-500 and new YSI
09/17/2019	Tx-02	Barataria Pass	LSU H-ADCP	Routine service, redeployed LSU's H-ADCP
09/25/2019	Tx-02	Barataria Pass	YSI and LSU H-ADCP	Routine service, redeployed LSU's H-ADCP and YSI
09/26/2019	Tx-07	Fontanelle Pass	YSI and SL-500	Routine service, redeployed SL-500 and YSI



Table 6. Summary of the data collection activities conducted during each survey

Transects	Location	Dates	ADCP	CTD & Water Sampling	TSS	LOI	Grain Size
Tx-01	Caminada Pass	4/11/2019	x	x	x	x	
Tx-02	Barataria Pass	2/5/2019	x	x	x	x	x
		5/22/2019	x				
		6/3/2019	x	x	x	x	x
		9/5/2019	x		x	x	
		9/10/2019	x				
Tx-03	Pass Abel	6/2/2019	x	x	x	x	
		9/10/2019	x				
Tx-04	Quatre Bayou Pass	5/20/2019	x	x	x	x	x
		9/19/2019	x				
Tx-05	Pass Ronquille	5/20/2019	x	x	x	x	
		9/9/2019	x				
Tx-06	Bastian Pass	3/17/2019	x	x	x	x	
		5/6/2019	x	x	x	x	
Tx-07	Fontanelle Pass	3/17/2019	x	x	x	x	x
		5/5/2019	x	x	x	x	
		5/6/2019	x	x	x	x	
		7/18/19			x	x	
		9/8/2019	x		x	x	
Tx-08	Scofield Pass	3/17/2019	x	x	x	x	
		6/14/2019	x	x	x	x	
		7/1/2019	x	x	x	x	
Tx-09	Bay Coquette	6/14/2019	x	x	x	x	

2.2. VESSEL-BASED DATA COLLECTION

2.2.1. Current Velocities and Discharge Through Inlets (ADCP)

ADCP surveys were strategically planned to be conducted during the ebb portion of the tidal cycle of spring tides (when astronomically-forced tidal current velocities through the inlets are greatest). Survey duration at each inlet lasted several hours in order to capture changing flow conditions through the ebb portion of the cycle with the goal of capturing both the maximum ebb velocities for that daily cycle and tidal hydraulic behavior for each inlet during the flood-ebb or ebb-flood transitions. Meeting these criteria required that the ebb portion of the cycle occur during daylight hours and when sea-state and weather conditions (fog, thunderstorms, etc.) allowed for the ability to acquire accurate measurements and safely conduct cross-inlet transect surveys. Note that the Barataria Basin inlets are heavily used as navigation routes for commercial and recreational vessel traffic on headings perpendicular to the course bearing of most transects surveyed. Therefore, very few days throughout the year are suitable for conducting the vessel-based surveys.



Two ADCP instruments were used for surveying: (1) the RD Instruments (RDI) 1200 kHz Workhorse Rio Grande ADCP, and (2) the RDI 600 kHz RiverRay ADCP. During the study a compass calibration was completed for both ADCP instruments. The size of the study area (< 64 km between inlets) does not require separate compass calibrations for different inlets. Furthermore, the magnetic declination in Louisiana is less than 1°. Instruments were used interchangeably between the four vessels. Prior to each ADCP survey, the operator input values for the following parameters: Transducer draft offset, maximum boat speed, maximum water speed, and maximum water depth.

Positioning was provided by three different GPS units: The Trimble R8, the Trimble MPS865, and the Hemisphere A101. Additional information about the Trimble R8 can be found in Section 2.3.1. The Trimble MPS865 and Hemisphere A101 provide precise horizontal position using Differential GPS, which uses a network of fixed ground-based reference stations (for example from the U.S. Coast Guard) to improve position accuracy up to about 3 cm. Velocity and discharge for all inlets were measured and referenced to bottom track (BT) of the ADCP transducer and to the global navigation satellite system (GNSS) positioning (i.e., the GGA data string, which is the fixed GPS data) and ship track. WinRiver II software provided by RDI was utilized for data processing and visualization.

The WinRiver II software provided an integrated outward (i.e., Gulfward or ebb) or inward (i.e., basinward or flood) total water discharge by utilizing the measured zone and extrapolating (within the WinRiver software) for the four areas of the channel cross-section not measured (e.g., surface water above the transducer faces, the near bottom, and the right and left banks too shallow to survey). The draft of the transducer was measured and the distances to the banks were input for each survey by the operator. Cross-sections can be visualized in WinRiver II (Figure 10).

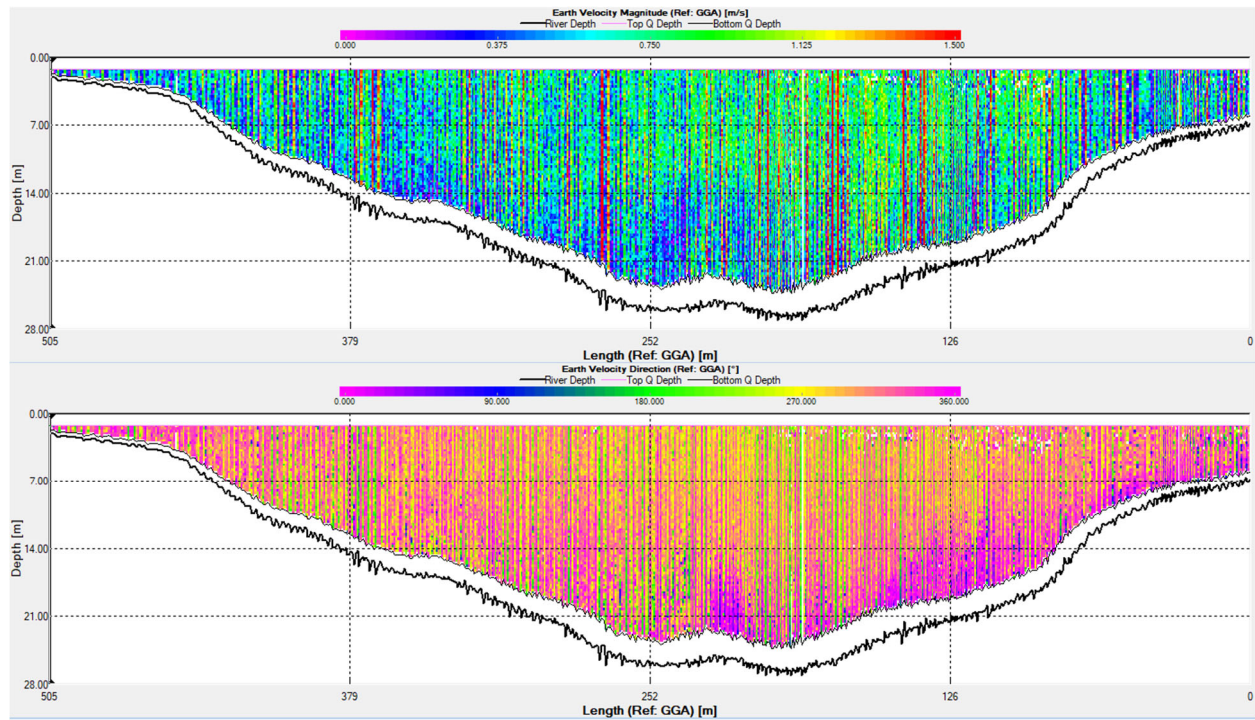


Figure 10. Example of an ADCP channel cross-section transect (at Tx-02, Barataria Pass) from west bank to east bank on May 22, 2019. The top plot shows flow velocity magnitude and the bottom plot shows flow azimuth.

The vertical distribution of the data was sampled at 0.25 m depth bins that spanned the water column starting from the transducer faces (0.25 m-0.75 m below the water surface depending on wave conditions) and extending down to the bed. For discharge calculations, an additional blanking distance of 0.25 m below the transducer is applied (within WinRiver II) to account for acoustic “ringing” proximal to the source (e.g., sound waves reflecting off the transducer, vessel hull, water surface, etc.). Likewise, WinRiver II also applies a variable blanking zone that extends vertically up from the bed a distance equal to 6% of the total distance from the transducers to the bed for discharge calculations (Figure 79 in Teledyne RD Instruments, Inc., 2016). This is due to measurement error inherent to ADCP instruments associated with acoustic “ringing” off the bed resulting in erroneous velocities being reported. A separate measurement file was used for data collection at each inlet in order to specify known maximum water depths to improve data precision.

After each survey, a QA/QC procedure was conducted on each ADCP transect using WinRiver II software to visually inspect data and determine quality. External factors such as dolphin interference with the ADCP, sea state (i.e., waves higher than 1 m; Figure 9), loss/complication of GPS signal, and other vessels (shrimp boats, crew boats, etc.) crossing the transect at time of surveying were experienced during field collection of data and documented in field notes. During data collection, decisions were made by field scientists not to complete some transects where data quality was low due to the factors mentioned above (e.g., dolphin interference, boat traffic). The incomplete transects were disregarded and not carried forward to post-processing activities. Increased wave conditions can also have an impact on data coverage (Figure 9). It is important to note that WinRiver II can competently interpolate across data gaps caused by



waves. One way to minimize the effect wave conditions have on data collection is to increase the ADCP transducer draft. However, this is limited by shallow depths (~1.5 m) over broad intra-inlet platforms (left part of cross-section in Figure 10). ADCP bottom-track referenced velocity and discharge were recorded for all ADCP surveys and were used for the index velocity calibration (section 2.3.3). A file log of all ADCP survey transect data, including discharge, can be found in Appendix A: ADCP File Log and Discharge Summary.

2.2.2. Water Column Profile Casts for Conductivity, Temperature, Depth (CTD)

Water column profile casts were conducted at multiple stations of each inlet (Figure 7) during select ADCP transect surveys to capture changing conditions over the course of each inlet survey. Casts were conducted using a Seabird SBE-19 plus CTD (conductivity/temperature/depth) water column profiler (Figure 11). The unit sampled at 4 Hz and averaged sampled data at a 1 Hz frequency for the following instruments built into the profiler:

1. Microcat CT sensor (records water conductivity and temperature)
2. Paroscientific DigiQuartz pressure sensor
3. Pump flow-through system for dissolved oxygen sensors
4. SBE 18 pH sensor
5. Campbell Scientific OBS-3 optical backscatter turbidity sensor

At the onset of each cast, the profiler was held at the water surface for ~45 seconds to flush water through the system. Only data from the downcast are reported (Figure 12) because there is potential for the introduction of sediment from the bed into the instrument, contaminating sensor readings during the upcast. Data are presented in tabular form with the following columns:

Col A	Year
Col B	Month
Col C	Day
Col D	Hour
Col E	Minute
Col F	Seconds
Col G	Elapsed Time (s)
Col H	Water Depth (m)
Col I	Salinity (PSU)
Col J	Temperature (°C)
Col K	OBS-3 backscatterance (nephelometric turbidity units [NTU])
Col L	Dissolved Oxygen (mg/L)
Col M	Dissolved Oxygen (% saturation)
Col N	Oxygen Saturation (mg/L)
Col O	pH

A file log of CTD cast data can be found in Appendix B: CTD File Log.

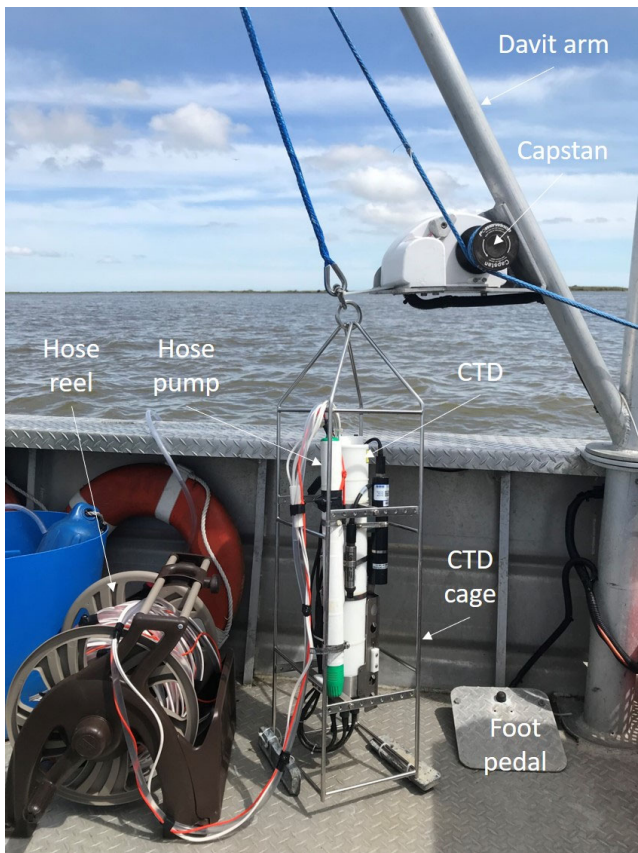


Figure 11. CTD and water sampling set-up on the RV *Penland*

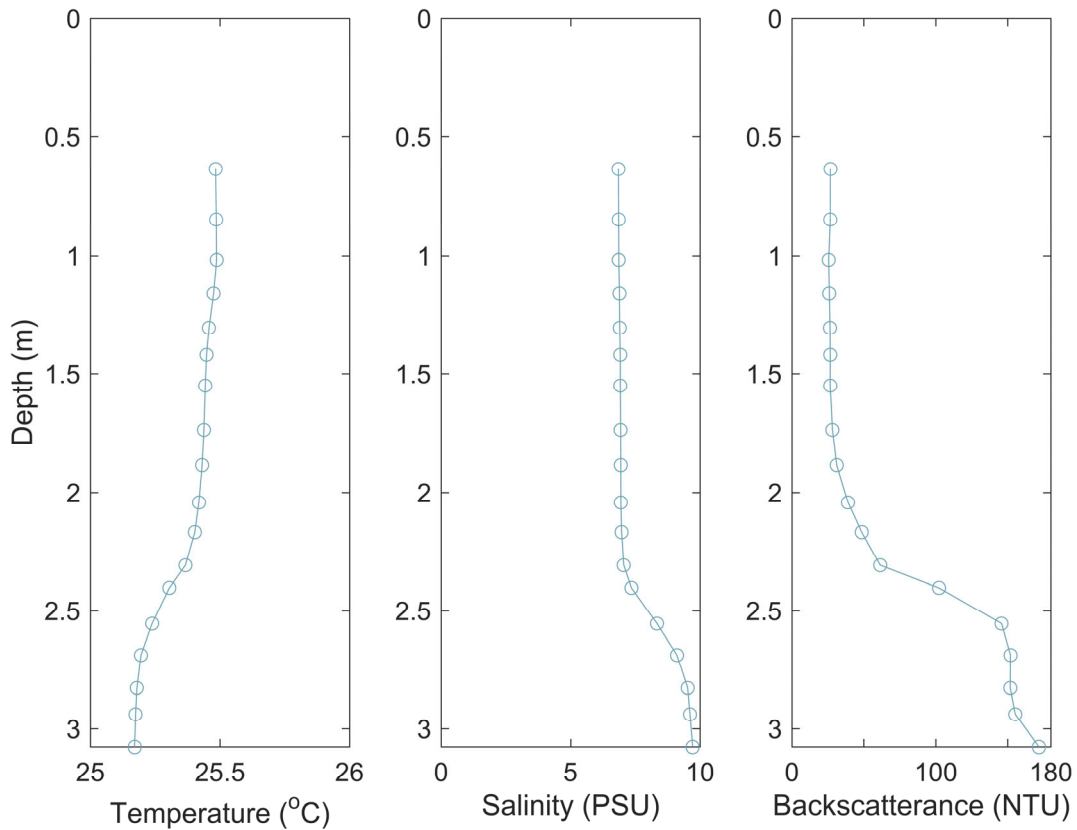


Figure 12. Example of processed data recovered from the CTD profiler at station B along transect Tx-07 (Fontanelle Pass); from left to right, temperature, salinity, and turbidity measured as optical backscatterance

2.2.3. Suspended Sediment Water Sampling

Water samples were collected in 1-liter Nalgene bottles using an electric pump and hose system attached to the CTD cage providing for synchronous data collection (Figure 11). Water sampling took place on the upcast beginning with the 0.9 fractional depth, followed by 0.5 and 0.1 fractional depths. Station depth was determined using the vessel echosounder. Depth of the CTD cage was tracked by counting pre-measured markings on the rope labeled in 1 m increments. The hose was flushed for ~20 seconds at each sampling depth prior to collecting the sample to flush out water stored from the previous depth and/or station.

Water sampling was conducted at multiple stations for each inlet (Figure 7) during select ADCP transect surveys with repeat sampling to capture changing conditions over the course of the survey at each inlet. All collected water samples were analyzed for total suspended sediment (TSS) and loss on ignition (LOI; a proxy for measuring organics). A subset of samples were additionally analyzed for suspended sediment grain size distribution and nutrients. This subset was collected only once at the thalweg station of the three fixed instrumented inlets (Figure 7), Barataria Pass (Tx-02), Quatre Bayou Pass (Tx-04), and



Fontanelle Pass (Tx-07). Detailed sample processing methods of each (TSS, LOI, grain size, and nutrients) are presented below.

Total Suspended Sediment (TSS) on Collected Water Samples

Water samples at varying water depths were analyzed in the laboratory for suspended sediment concentration (2540D in Eaton et al., 2005). The total water volume of each sample was measured with a graduated cylinder. The samples were then vacuum-filtered through pre-weighed 0.7 µm glass fiber or 0.4 µm polycarbonate filters depending on the secondary analysis. The filters and the sediment retained were oven-dried to a constant weight at 100°C. After cooling to room temperature in a desiccator, dry sample weights were measured. Total suspended sediment (TSS) concentrations (in mg/L) were determined using the total measured sediment weight (dry weight - filter weight) and sample volume, where the dry weight consists of both the dried sediment and the filter.

$$TSS = \frac{\text{dry wt (mg)} - \text{filter wt (mg)}}{\text{Sample volume (L)}}$$

A log of TSS sample data from these cross-channel surveys can be found in Appendix C: Suspended Sediment Data Log from Transect Surveys – TSS and LOI. After suspended sediment concentrations were calculated, grain size analysis (polycarbonate filters) and loss on ignition (LOI; glass fiber filters) were carried out on selected samples.

Loss on Ignition (LOI) Analysis on Selected Samples

Samples filtered through glass fiber filters (designated for LOI) were heated in a muffle furnace at 580°C for a minimum of 10 hours (2540E in Eaton et al., 2005). After cooling to room temperature in the oven, combusted sample weights were measured. LOI (mg/L) was determined using the dry weight (dried sediment plus the filter), total measured weight after combustion (combusted sediment plus filter), and sample volume.

$$LOI = \frac{\text{dry wt (mg)} - \text{combustion wt (mg)}}{\text{Sample volume (L)}}$$

A log of LOI sample data from these cross-channel surveys can be found in Appendix C: Suspended Sediment Data Log from Transect Surveys – TSS and LOI.

Grain Size Analysis on Selected Samples

Samples filtered through polycarbonate filters (designated for grain size analysis) were re-wet and disaggregated using 0.1% sodium hexametaphosphate solution (Chilingar, 1952; Manfredini et al., 1990) and sonication (Malvern, 2015). Each filter was removed from the sonicator after fines were released (~2 minutes) to prevent damage to the filter and contamination of the sample from damaged filter pieces. The sample was sonicated for 30 minutes before measurement due to the high propensity for flocculation in fine sediments. Samples were then quantitatively analyzed at UNO using the Malvern Mastersizer 3000E laser diffraction particle size analyzer with a HydroEV dispersion unit. The measurement is accomplished by passing sediment, suspended in a solution of deionized water, between two narrow panes of glass in front of a laser. Large particles scatter light at small angles relative to the laser beam and small particles



scatter light at large angles. The angular scattering intensity data is then analyzed to calculate the size of the particles and is reported as a volume equivalent sphere diameter. Particles can be binned into any number of desired size classes. For this study, particles are binned into 86 size classes from 0.393 μm to 1090 μm (clay to very coarse sand). Each grain size distribution is an average of five measurements.

A log of grain size sample data from these cross-channel surveys can be found in Appendix D: Suspended Sediment Data Log from Transect Surveys – TSS and Grain Size. Analyses for TSS were also conducted on these samples and are included.

Nutrients Collected on Selected Samples

Triplicate water samples were collected at 0.1, 0.5, and 0.9 fraction depths at the thalweg station of fixed instrumented inlets, Barataria Pass (Tx-02), Quatre Bayou Pass (Tx-04), and Fontanelle Pass (Tx-07) to measure: ammonium (NH_4), nitrite + nitrate (NO_3+NO_2), phosphate (PO_4), silicate (SiO_2), total nitrogen (TN), and total phosphorus (TP). Constituents of TN and TP were not filtered immediately in the field, while those for NH_4 , NO_3 , PO_4 , and SiO_2 were filtered immediately in the field using a Whatman GF/F filter (porosity of 0.7 μm) and a syringe filtering apparatus (Zhang, 1997; Zhang & Berberian, 1997). All samples were kept on ice until transferred to a freezer at the Baton Rouge Institute office in the Center of Coastal and Deltaic Solutions.

A log of nutrient samples collected from these cross-channel surveys can be found in Appendix E: Water Sample Data Log from Transect Surveys – Nutrients. Future processing and analysis of these samples are planned for Phase II of this study.

2.3. FIXED POSITION INSTRUMENTATION

2.3.1. Station Positioning and Elevation (Trimble RTK GPS)

Precision positioning and water surface elevation data were collected at each fixed station site on each visit using a Trimble R8 Real-Time Kinematic (RTK) system; the GPS antenna was mounted on top of a 2 m survey pole (Figure 13). RTK correction was provided via mobile internet through the LSU Center for Geoinformatics (C4G) (<http://c4gnet.lsu.edu/c4g>). Survey points were taken by continuously logging at least 10 position and elevation points (Trimble Access "rapid-point" method) in fixed RTK ($\pm 3.0 \text{ cm}$ x, y, z location). The horizontal datum of the survey was Universal Transverse Mercator (UTM) Zone 15N in the North American Datum of 1983 (NAD83). The vertical datum was the North American Vertical Datum of 1988 (NAVD88) and was calculated referencing the 2012a Geoid (Geoid12A). Both the horizontal and vertical units are in meters. All water levels logged at fixed station and survey instruments were corrected to the NAVD88 in Geoid 12A. These RTK data points are reported in Appendix F: RTK Points Data Log.

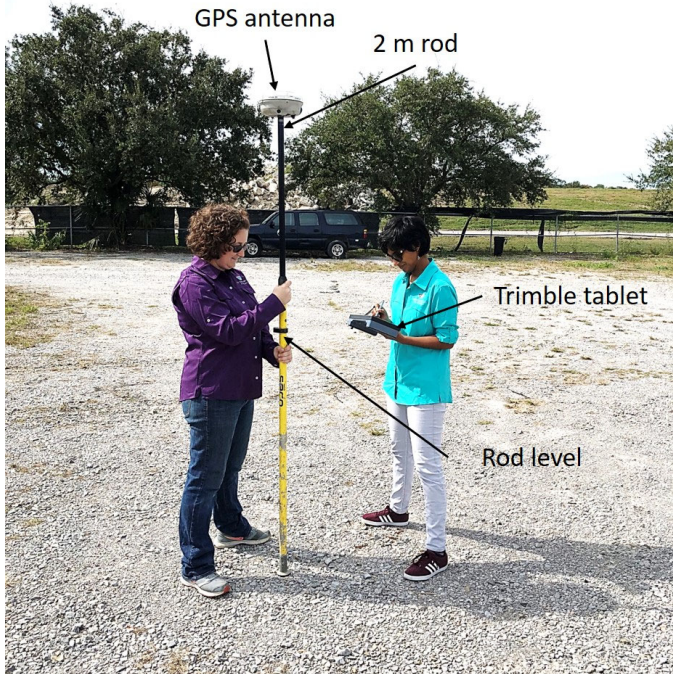


Figure 13. Photograph of RTK GPS survey of surface elevation

2.3.2. Continuous Discharge and Water Current Velocity Monitoring (H-ADCP)

H-ADCPs were installed at Barataria Pass (Tx-02D), Quatre Bayou Pass (Tx-04D), and Fontanelle Pass (Tx-07D) to measure continuous discharge (Figure 14). The H-ADCPs were SL-500s from Sontek operating at a frequency of 500 kHz. They have a range of 1.5-120 m and a cell resolution of up to 10 cells. The water velocity accuracy of the SL-500 is $\pm 1\%$ of measured velocity, or ± 0.005 m/s (± 0.015 ft/s). Water velocity profile data were collected horizontally in 10 bins, each 8 m long, with a 1.5 m blanking distance from the transducers. Data were collected and logged for 10 minutes every hour.

At the three sites, the H-ADCP were installed approximately 1 m from the water surface at mid-tide, oriented across the channel. Because the transducer beams expand with distance from the transducer, the depths of deployment were determined by considering two factors: (1) Water surface interference with H-ADCP transducer beams during lowest water levels, and (2) seabed interference with the H-ADCP transducer beams. H-ADCPs were deployed and serviced according to the schedule in Table 5.

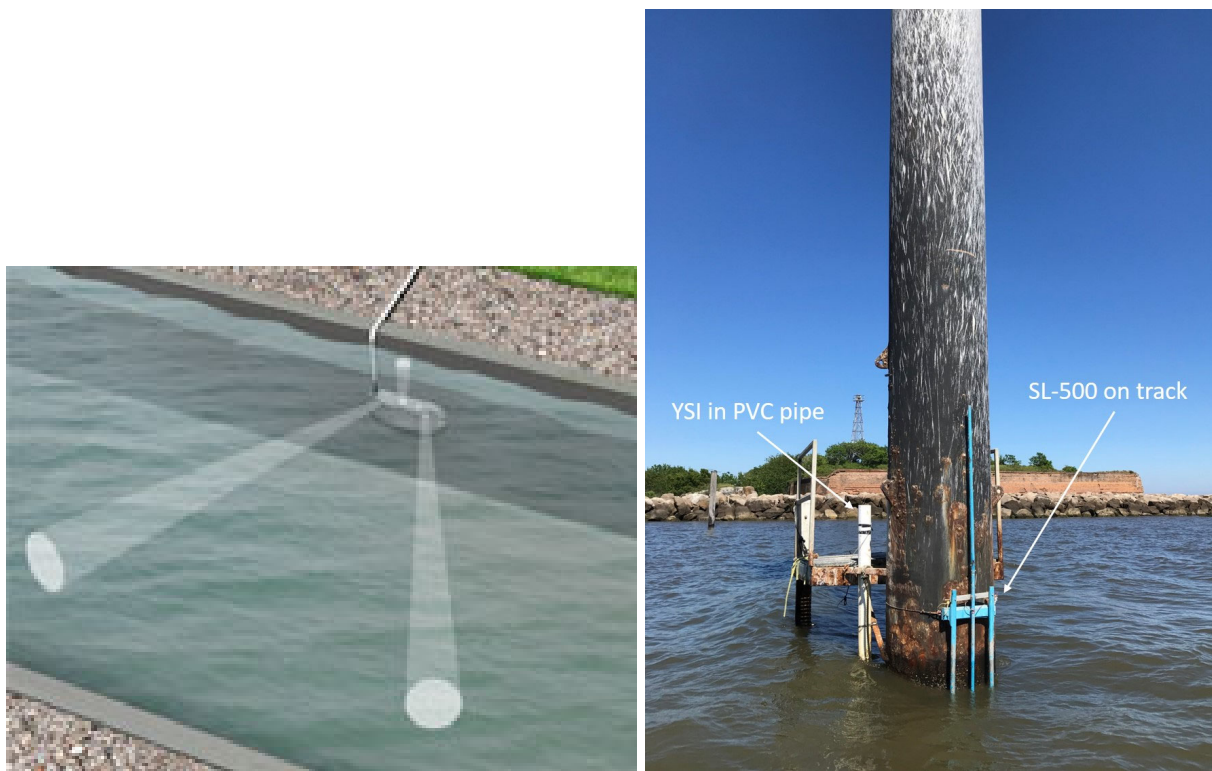


Figure 14. Images depicting H-ADCP installations. Image on the left shows a schematic of a deployed H-ADCP where the two acoustic transducers record water velocities at one fixed depth (image from Sontek: <http://www.sontek.com/productsdetail.php?SonTek-SL-8>). Right image shows the H-ADCP installation at Barataria Pass (Tx-02D) mounted to a “track and trolley” that is fixed to a steel piling at USGS Water Data Gauge 073802516 Barataria Pass at Grand Isle, LA.

During a servicing visit on March 12, 2019 it was observed that the Quatre Bayou Pass (Tx-04D) station instrumentation and mount had been compromised and was no longer fixed to the structure where it had been installed. It was determined that instead of the SL-500 H-ADCP, a Nortek Sideloading Aquadopp current profiler on an x-shaped sled bottom mount (Figure 15) deployed on the inlet floor was better suited for this location. The bottom mount sled was deployed on the western flank of Quatre Bayou Pass at ~8 m depth with the Aquadopp mounted horizontally and its transducers facing up ~0.25 m above the seabed. Current profile data were collected vertically in 0.5 m bins starting from a 0.4 m blanking distance above the transducers up to the air-water interface and logged hourly from samples collected at 1 Hz and averaged over 10 minutes then depth-averaged. Example processed data are shown in Figure 16.

On April 2, 2019, subsequent to installing this second station at Quatre Bayou Pass, efforts to recover the missing SL-500 rig using side-scan sonar and divers were successful. However, on the following check-up visit to Quatre Bayou Pass on June 6, 2019, the Aquadopp rig described above was discovered missing (likely due to shrimping activity) and multiple instrument recovery attempts failed to locate the rig (Table 5). Due to the risky deployment location, no further continuous velocity measurements were collected at Quatre Bayou Pass (Tx-04D) thereafter.



Figure 15. Photograph of Nortek Sidelooking Aquadopp current meter on sled mount resting on the vessel deck

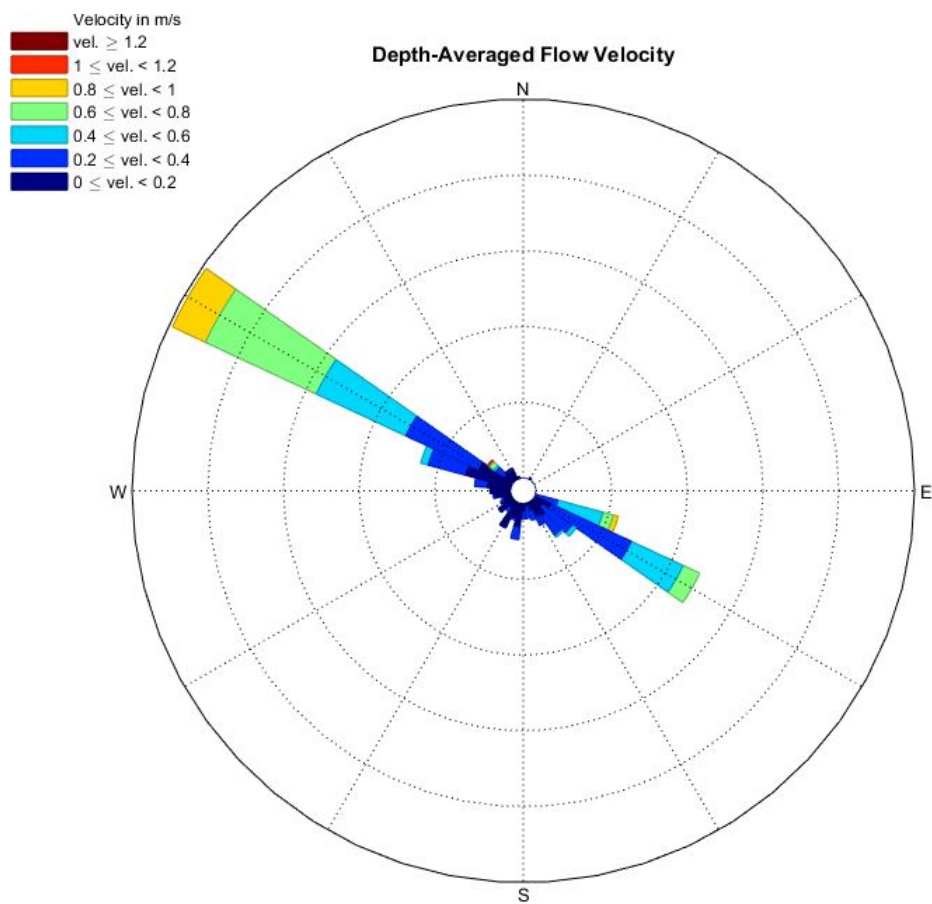


Figure 16. Example of a depth-averaged velocity flow rose at Quatre Bayou Pass from 03/22/2019 to 4/10/2019, where the compass direction indicates the direction the water is flowing toward

After Hurricane Barry made landfall in Louisiana on July 13th, the SL-500 at Barataria Pass (Tx-02D), could not be located, despite several search attempts including bottom imaging and diver searches (Table 5). Through a partnership with Chunyan Li at LSU, continuous H-ADCP measurements were obtained for



this inlet from a station that was located approximately 40 m Gulf-ward of the original station. Velocity measurements at this station were collected by a Nortek 2D AWAC 400kHz Profiler. The instrument was deployed approximately 0.75 m below the water surface, and oriented across the channel. Data was collected in 20 bins, each 5 m long. The frequency of data collection varied between 1 and 5 minutes, but all data collected during the first 10 minutes of every hour was averaged to approximate the data collection settings of the SL-500 deployed at Fontanelle Pass (Tx-07D). The data for this instrument were also collected in an East-North-Up reference frame. It was rotated into a streamwise (X) and cross-stream (Y) velocity during processing to match the reference used at Fontanelle Pass (Tx-07D).

A log of fixed current profiler data files can be found in Appendix G: Current Meter File Log (Aquadopp, SL-500, and AWAC).

2.3.3. Continuous Velocity Record and Index Velocity Calibration

Continuous velocity measurements from H-ADCP instruments can yield information about discharge if properly calibrated with measurements of the total discharge. The method used here is the USGS Index Velocity Method (Levesque & Oberg, 2012; Ruhl & Simpson, 2005). The velocity measured by the instrument is indexed to the mean channel velocity from boat-based ADCP measurements. This method requires only that the H-ADCP measure the velocity in a representative portion of the channel.

Continuous velocity measurements from Barataria Pass (Tx-02) and Fontanelle Pass (Tx-07) were calibrated using the mean velocity measured during the ADCP surveys of the inlets described in section 2.2.1 and provided in Appendix A (Table A-A 2 for Barataria Pass and Table A-A 7 for Fontanelle Pass). The calculation of the index curve for each of the two inlets is described in section 3.2.2. For all velocities, positive velocities record flow toward the Gulf of Mexico, and negative velocities record flow toward the interior of Barataria Bay.

A continuous velocity record can be constructed using the data provided in this report (H-ADCP velocity, index curve, stage, channel shape), but this additional analysis is beyond the scope of this task.

2.3.4. Continuous Measurement of Water Quality Constituents and Water Level (EXO2 YSI)

Three multiparameter hydrological and water quality sondes (EXO2 YSI Xylem, Inc.

<https://www.y si.com/EXO2>; Figure 17) were deployed at each of the three fixed instrument sites, Barataria Pass (Tx-02), Quatre Bayou Pass (Tx-04), and Fontanelle Pass (Tx-07). The parameters that were measured at all stations included water level, conductivity, temperature, turbidity, dissolved oxygen, pH, chlorophyll *a*, and blue-green algae. Data were continuously recorded at 20-minute intervals. All recorded data were then averaged hourly. The sondes were serviced (cleaning/removing biofouling, data downloading, and battery replacement) according to the schedule listed in Table 5 and regularly calibrated with standard solutions provided by the manufacturer (<https://www.exowater.com/manuals-software.php>).

Surface water samples of 1-liter Nalgene bottles co-located with the deployed YSIs were collected during servicing trips to calibrate the YSI turbidity sensor measured in Formazin Nephelometric Units (FNU) to TSS in mg/L. These suspended sediment samples were processed using the same TSS methods described in section 2.2.3. YSI turbidity sensor calibration is described in section 3.4.



Water level data were adjusted using sea level barometric pressure data from the Galliano South Lafourche Airport (<https://www.ncdc.noaa.gov/cdo-web/datasets/LCD/stations/WBAN:12993/detail>) to account for local barometric changes. Quality control included statistical filtering, as well as inter-comparison with nearby USGS water quality and hydrological stations. An example of processed YSI data is shown in Figure 18.

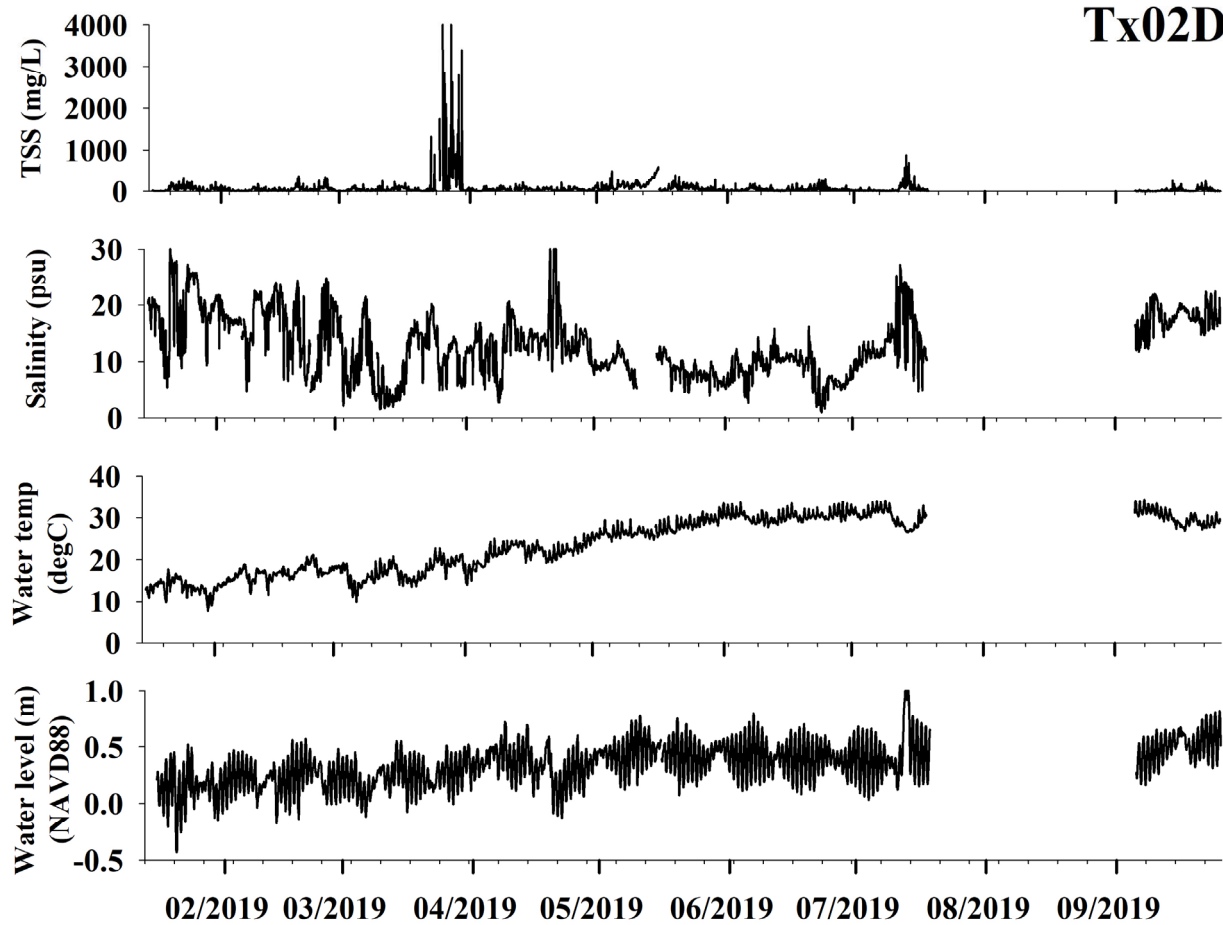
A log of fixed YSI data files (Appendix H: YSI File Log) and the associated suspended sediment samples for the turbidity to TSS calibration (Appendix I: Suspended Sediment Data Log for YSI Turbidity Calibration) can be found in the Appendices.



Figure 17. Photograph of EXO2 YSI multi-sensor hydrological and water quality sonde (image from <https://www.y si.com/EXO2>)



Tx02D





Tx02D

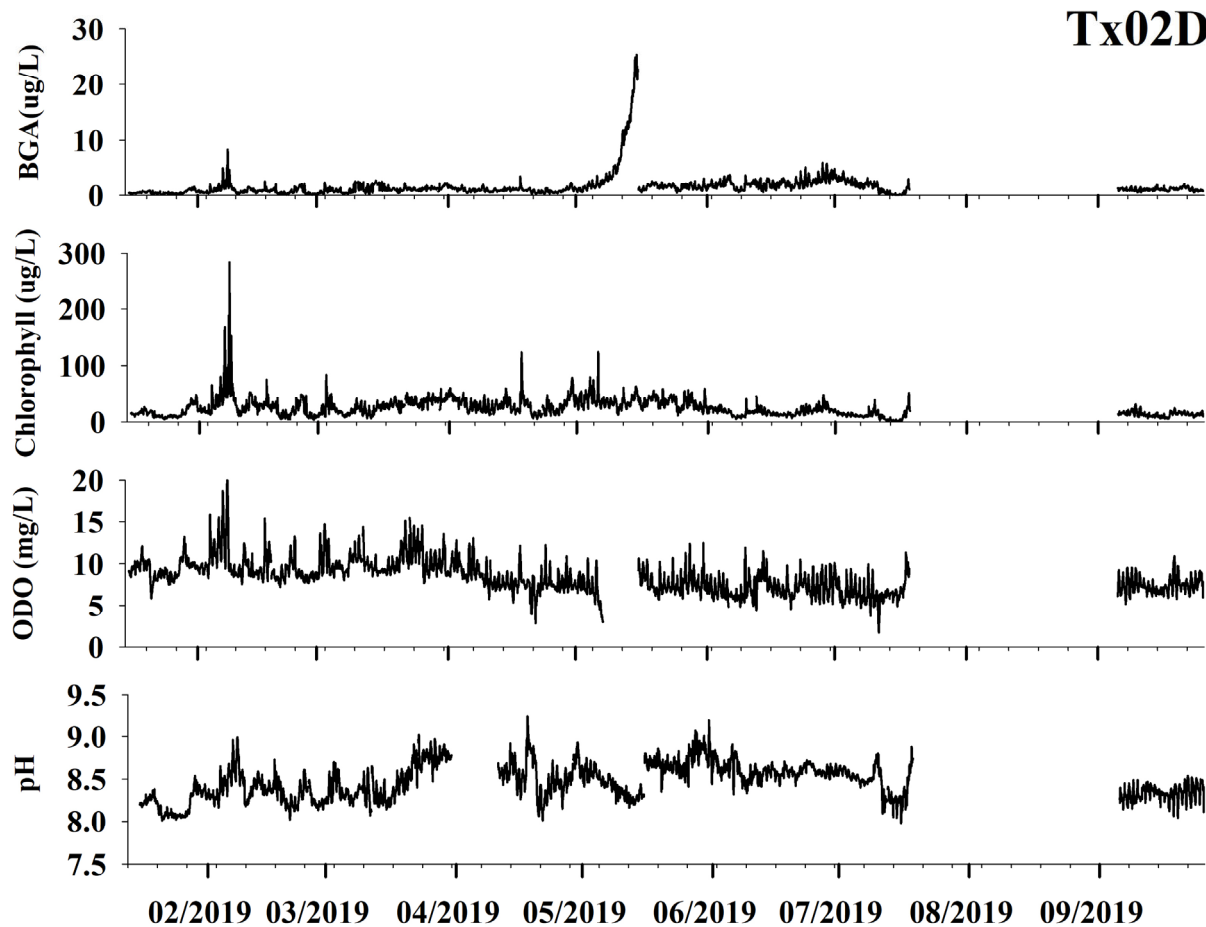


Figure 18. Example of processed hydrological data at Tx02D from January to September 2019 (TSS, water salinity, water temperature, water elevation in NAVD88, blue-green algae, chlorophyll *a*, dissolved oxygen, and pH)



3.0 Results

3.1. SYNOPTIC DATA SUMMARY

A summary of final data coverage from the three fixed-instrument stations compared to timing of individual inlet ADCP surveys is presented in Figure 19.

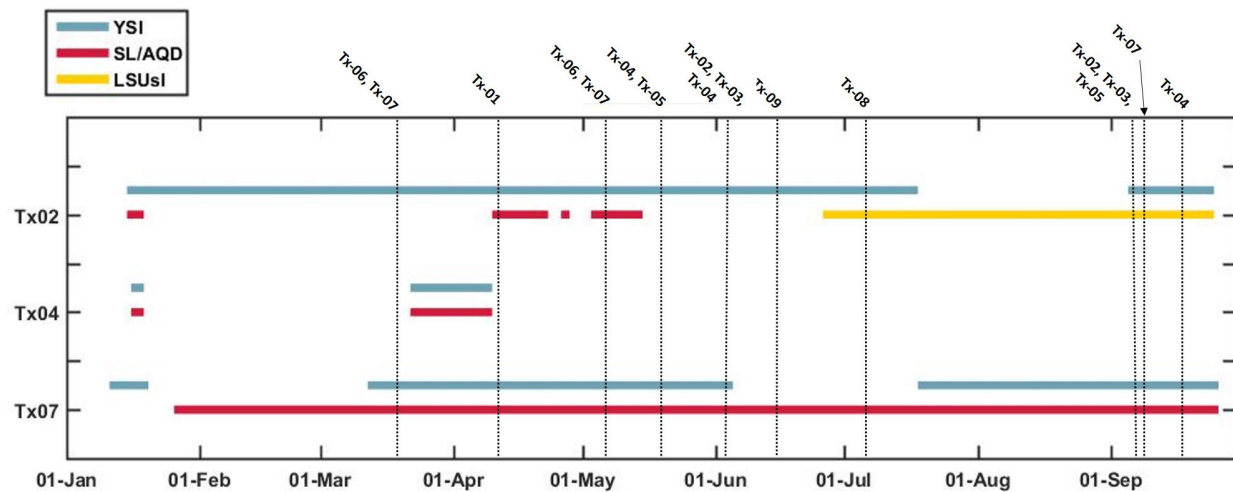


Figure 19. Plot showing fixed-instrument data collected and processed during study period (YSI = multi-sensor water quality sonde; SL/AQD = H-ADCP or Aquadopp current profiler; LSUsI = LSU H-ADCP at Barataria Pass). Vessel-based ADCP surveys are indicated by dashed black vertical lines. Fixed stations are indicated on the y-axis (Barataria Pass = Tx02; Quatre Bayou Pass = Tx04; Fontanelle Pass = Tx07). The gaps represent data loss due to weather, instrument failure, or displaced instrument (see text).

Presented in the following sections are the results of ADCP discharge calculations for transect surveys at each inlet, calibration of water discharge index velocity, and YSI turbidity sensor to total suspended sediment. Processed data from the fixed instruments, CTD, and water sampling are presented as digital files that accompany this report.

3.2. WATER DISCHARGE

3.2.1. Acoustic Doppler Current Profiler (ADCP) Surveys

ADCP discharges are calculated automatically (considering user-inputs described in Section 2.2.1) within WinRiver II ADCP survey and post-processing software. A file log and summary of discharges for each inlet survey can be found in Appendix A. Both Bottom Track and GGA discharges are reported, where available.

Bottom Track allows the ADCP to measure the distance travelled without the use of external positioning, such as a GPS, and is the most accurate way to measure velocity and discharge (p. 218, Teledyne RD Instruments, 2016). The use of Bottom Track is appropriate for channels where the bed sediment is not in rapid transport and where near-bed suspended sediment concentrations are not excessive (e.g. saltation in the boundary layer). The Barataria tidal inlets meet both of these conditions. For this reason, Bottom



Track derived discharge data was used for all analysis. GPS GGA position data, was also collected in case a mobile bed was present, however, no mobile bed was observed during the surveys. If, for any reason, a differential GPS or an RTK GPS position cannot be achieved during the survey, the GGA velocity and discharge will differ from the Bottom Track velocity and discharge. The differences that can be observed between the Bottom Track and GGA data in this report serve to illustrate the benefit of using Bottom Track data, especially in areas where an accurate GPS position can be challenging to achieve. The WinRiverII measurement files for each survey will be provided accompanying this report.

3.2.2. Index Velocity Calibration for Barataria Pass and Fontanelle Pass

Barataria Pass (Tx-02)

The H-ADCP at Tx-02D was programmed to measure the flow velocity in 20 bins covering 100 m of channel width; these measurements were averaged to create a single velocity measurement for the index calibration. However, the signal strength of the measurement from each velocity bin decreases with distance from the instrument. Only velocity bins that recorded a signal at least 6 dB greater than the noise floor (12 dB) were used in the average. The noise floor is defined as the approximate minimum amplitude of the return signal. The number of bins used in the average ranged from 0 bins to 20 bins. At times when no bins have good data are interpreted as times of instrument burial by moving sediment (Dr. Chunyan Li, personal communication Oct 9, 2019). This location in Barataria Pass is highly dynamic where wave-currents interact with tidal currents to develop and migrate swash bars and marginal flood channel bedforms (Hayes, 1980) that may intermittently bury or interfere with instruments. In a recent H-ADCP deployment in Pass Abel by Dr. Li, the instrument was also buried during the experiment (Li et al., 2019). The periodic burial and exhumation of the H-ADCP demonstrates the morphodynamics associated with tidal inlets. The velocity record from the H-ADCP is shown in Figure 20, along with the measurements from the ADCP survey at the transect. As can be seen in Figure 20, the flow patterns around the instrument are complex, often with larger velocity magnitudes in the cross-stream direction than the streamwise direction. In addition, due to the channel shape and constraints on instrument deployment location, the H-ADCP was only able to measure flow on a shallow shelf in the northeast part of the channel (Figure 21). As is the case with measurements derived on the flanks of any tidal inlet channel that do not extend the entire distance across the inlet throat, the velocity measured on this shallow shelf must be compared to cross-inlet survey ADCP data to gain an understanding of tidal inlet hydraulics at this location because local hydraulic behavior at this position is not always a simple representation of the flow field across the entire channel.

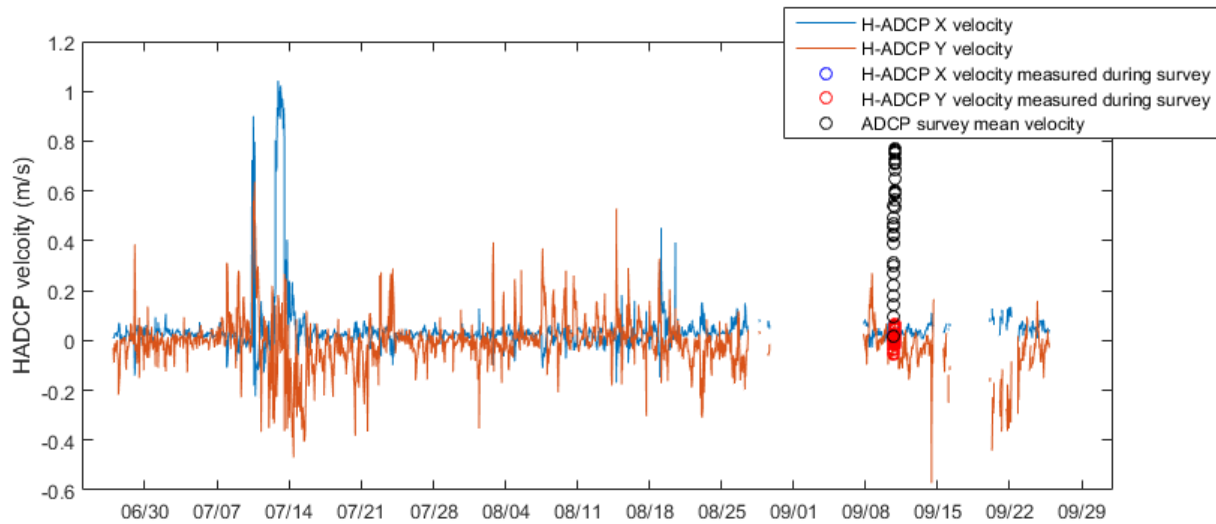


Figure 20. Continuous velocity record at Tx-02 with the measurements from the ADCP surveys highlighted to show the points used in the index calibration. The X velocity is the streamwise velocity. The Y velocity is the cross-stream velocity. The H-ADCP X velocity measurements during the survey (blue circles) plot behind the red circles for the H-ADCP Y velocity. Note that the large spike in July represents Hurricane Barry.

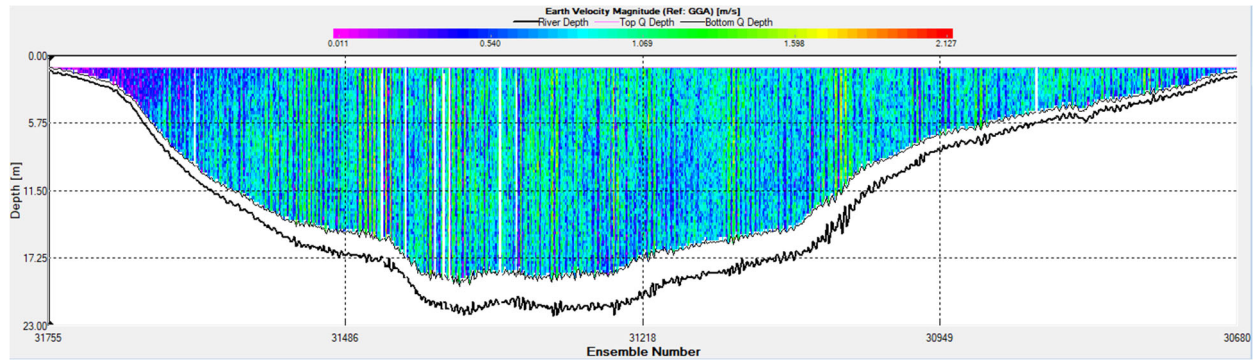


Figure 21. ADCP velocity transect from Tx-02 during ebb tide on 9/10/2019 at 20:11 UTC. The transect orientation is from northeast to southwest from left to right.

Fontanelle Pass (Tx-07)

The shallow depths at the deployment site combined with beam spreading inherent in any acoustic measurement resulted in some of the data bins being contaminated by reflections off the surface of the water. Only the first 2 velocity bins at Tx-07 yielded data that was never influenced by this reflection. These bins measure the velocities in a 16 m section of the channel between 1.5 m and 17.5 m from the instrument. Additionally, due to complex flow conditions at this site, only Beam 2 of the H-ADCP instrument measured representative velocities in the channel. Beam 1 velocities were evaluated as not being representative of channel flow; Beam 1 velocities were too low, in comparison with the ADCP measured velocities, to be representative of channel flow conditions. The velocity record from the H-ADCP is shown in Figure 22. Only velocities from Beam 2 were used to calculate the index velocity. The index curve calculated for Tx-07 is as follows:



$$V = 2.07v_i - 0.179$$

where V represents the mean channel velocity, and v_i represents the measured H-ADCP velocities (Figure 23). The coefficient of determination (r^2) for the index curve is 0.94.

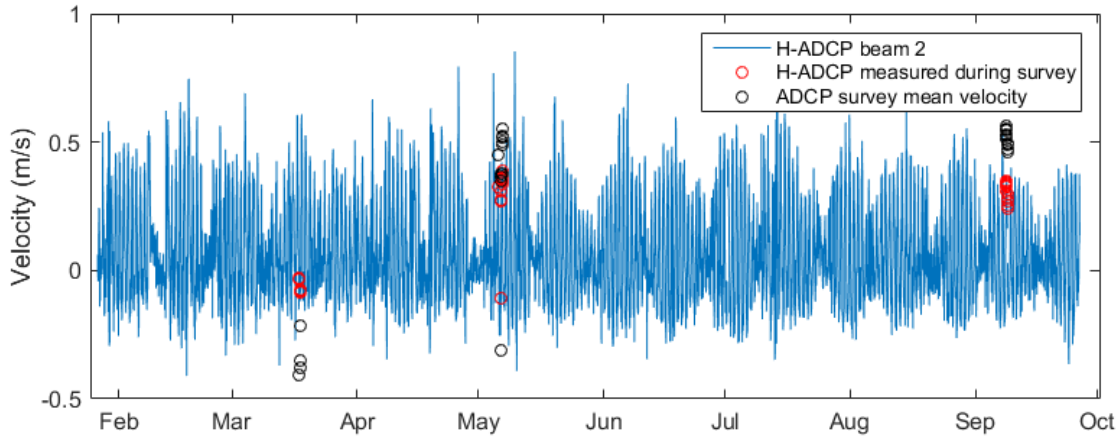


Figure 22. Continuous velocity record at Tx-07 with the measurements from the ADCP surveys highlighted to show the points used in the index calibration

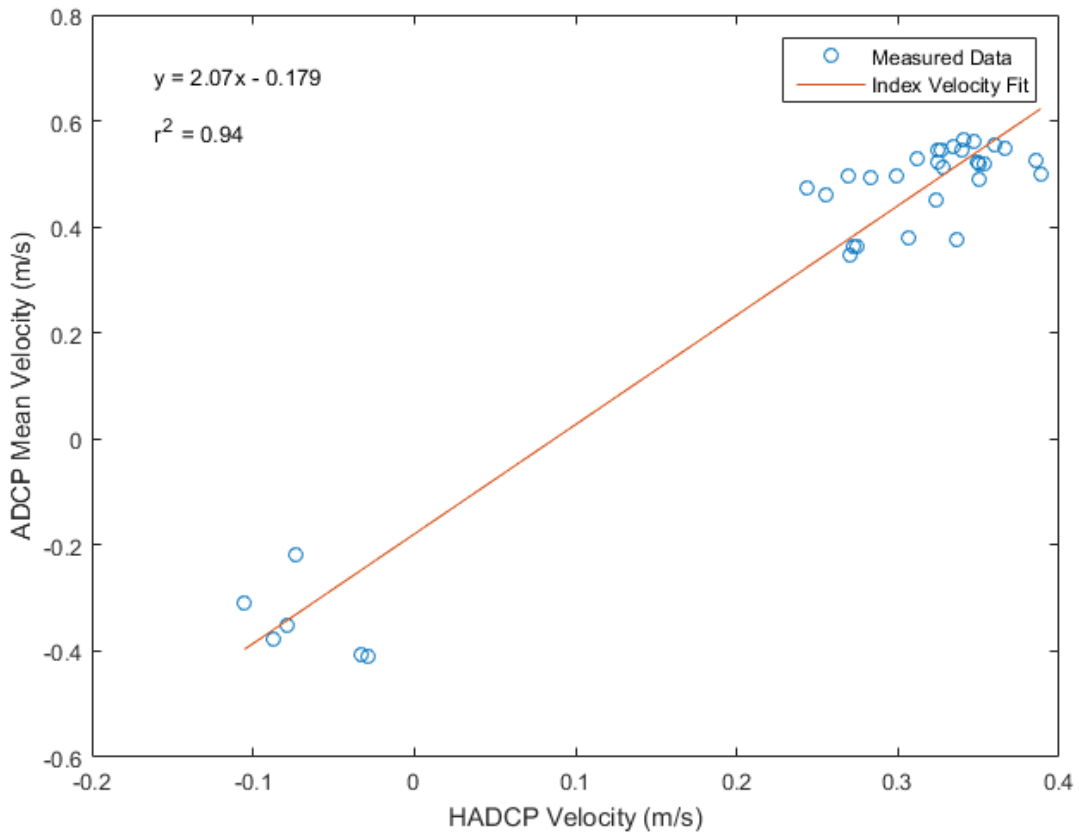


Figure 23. Index velocity calibration curve for Fontanelle Pass (Tx-07)

3.3. SUSPENDED SEDIMENT SAMPLES

Results from suspended sediment sampling collected during vessel-based survey transects are included in the data log tables in Appendix C for TSS and LOI, and Appendix D for TSS and grain size.

3.4. EXO2 YSI TURBIDITY SENSOR CALIBRATION TO TSS

YSI turbidity sensor values were converted to TSS in mg/L using correlations derived from local water samples, described in Section 2.3.3. The suspended sediment mass (in mg/L) was correlated with each sonde turbidity value (in FNU) (Figure 24). A linear regression model was derived for all the YSIs (equation 1), where x is the turbidity sensor value in FNU. Separate regression models for Barataria Pass (Tx-02), Quatre Bayou Pass (Tx-04), and Fontanelle Pass (Tx-07) were also derived and their equations are shown as equations 2, 3, and 4, respectively. The turbidity correlation at Barataria Pass is very good ($R^2 = 0.97$). Due to the lost instrument at Quatre Bayou Pass, only two points are used, hence the $R^2 = 1$. The correlation at Fontanelle Pass could improve from additional bottles collected during periods of higher turbidity. The regression equation for all YSIs (4) was used to calculate continuous TSS for all sondes. The TSS and FNU values used for this calibration can be found in Appendix I.

$$\text{TSS} = 1.35x - 3.76, R^2 = 0.81 \quad (1)$$

$$\text{TSS} = 1.56x + 2.04, R^2 = 0.97 \quad (2)$$



$$\text{TSS} = -0.13x + 12.20, R^2 = 1.00 \quad (3)$$

$$\text{TSS} = 0.74x + 8.69, R^2 = 0.60 \quad (4)$$

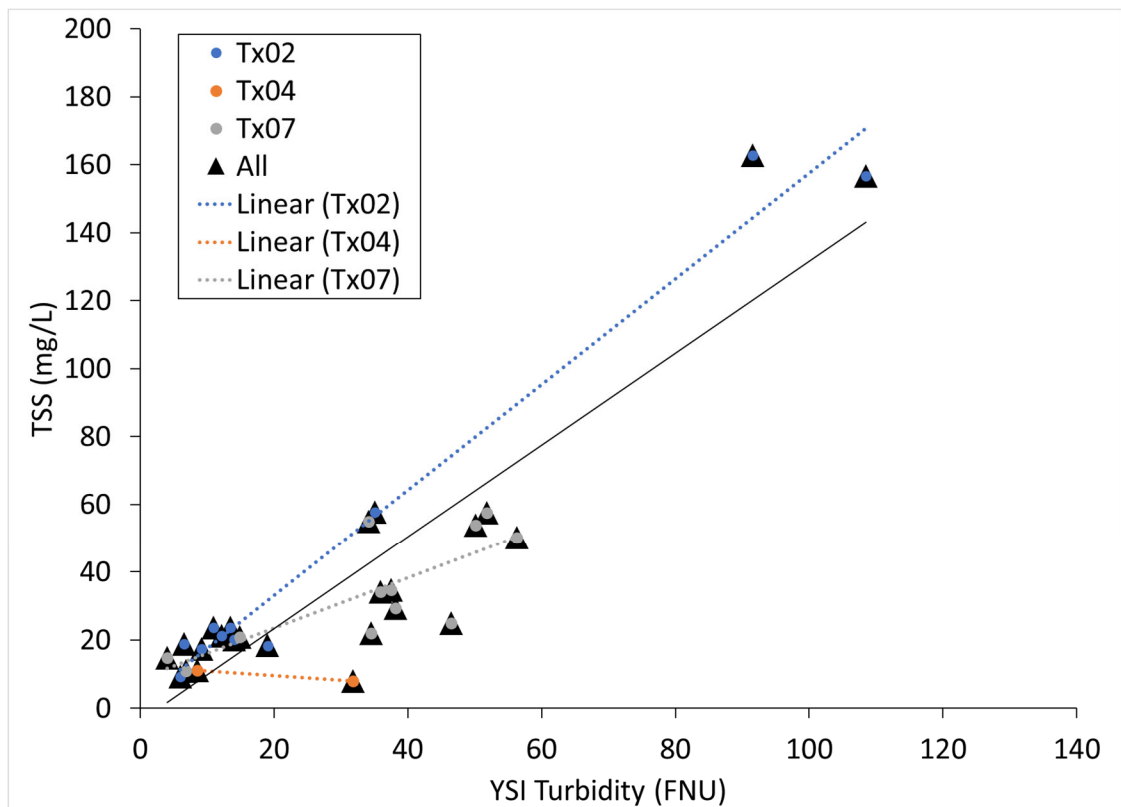


Figure 24. YSI turbidity sensor correlation with total suspended sediment (TSS)



References

- Brown, E. I. (1928). Inlets on sandy coasts. *Proceedings of the American Society of Civil Engineers*, 54(2), 505–554.
- Byrnes, M. R., Britsch, L. D., Berlinghoff, J. L., Johnson, R., & Khalil, S. (2019). Recent subsidence rates for Barataria Basin, Louisiana. *Geo-Marine Letters*, 39(4), 265–278.
- Chilingar, G. V. (1952). Study of the dispersing agents. *Journal of Sedimentary Research*, 22(4), 229–233.
- Couvillion, B. R., Beck, H., Schoolmaster, D., & Fischer, M. (2017). Land Area Change in Coastal Louisiana (1932 to 2016), 26.
- Cui, L., Huang, H., Li, C., & Justic, D. (2018). Lateral circulation in a partially stratified tidal inlet. *Journal of Marine Science and Engineering*, 6(4), 159.
- Davis, Jr., R. A., & FitzGerald, D. M. (2009). *Beaches and coasts*. John Wiley & Sons.
- de Swart, H. E., & Zimmerman, J. T. F. (2009). Morphodynamics of tidal inlet systems. *Annual Review of Fluid Mechanics*, 41(1), 203–229.
- Eaton, A., Clesceri, L., Rice, E., & Greenberg, A. (Eds.). (2005). 2540 Solids. In *Standard Methods for the examination of water and wastewater* (21st ed., pp. 55–61). American Public Health Association.
- Escoffier, F. F. (1940). *The stability of tidal inlets*. United States Engineer Office Mobile United States.
- FitzGerald, D., Kulp, M., Hughes, Z., Georgiou, I., Miner, M., Penland, S., & Howes, N. (2007). Impacts of rising sea level to backbarrier wetlands, tidal inlets, and barrier islands: Barataria coast, Louisiana. In *Coastal Sediments '07* (pp. 1179–1192). New Orleans, Louisiana, United States: American Society of Civil Engineers.
- FitzGerald, D. M., Kulp, M., Penland, S., Flocks, J., & Kindinger, J. (2004). Morphologic and stratigraphic evolution of muddy ebb-tidal deltas along a subsiding coast: Barataria Bay, Mississippi River delta. *Sedimentology*, 51(6), 1157–1178.
- FitzGerald, D. M., & Miner, M. D. (2013). Tidal inlets and lagoons along siliciclastic barrier coasts. In *Treatise on Geomorphology* (John F. Shroder, Vol. 10, pp. 149–165). San Diego, CA.
- Frazier, D. E. (1967). Recent deltaic deposits of the Mississippi River: Their development and chronology. *Transactions of the Gulf Coast Association of Geological Societies*, 17, 287–315.
- Georgiou, I. Y., McCorquodale, A. J., Neupani, J. A., Howes, N., Hughes, Z., FitzGerald, D. M., & Schindler, J. K. (2010). *Modeling the hydrodynamics of diversions into Barataria Basin* (p. 102). Metairie, Louisiana: Pontchartrain Institute for Environmental Sciences.
- Hayes, M. O. (1980). General morphology and sediment patterns in tidal inlets. *Sedimentary Geology*, 26(1–3), 139–156.
- Howes, N. C. (2009). The impact of wetland loss on inlet morphology and tidal range within Barataria Bay, Louisiana. *Boston University*, 107.
- Inoue, M., Park, D., Justic, D., & Wisemanjr, W. (2008). A high-resolution integrated hydrology–hydrodynamic model of the Barataria Basin system. *Environmental Modelling & Software*, 23(9), 1122–1132.
- LA CPRA. (2012). *Louisiana's comprehensive master plan for a sustainable coast: Committed to our coast* (p. 192). Baton Rouge, LA: Coastal Protection and Restoration Authority of Louisiana.
- LA CPRA. (2017). *Louisiana's comprehensive master plan for a sustainable coast: Committed to our coast* (p. 392). Baton Rouge, LA: Coastal Protection and Restoration Authority of Louisiana.
- Levesque, V. A., & Oberg, K. A. (2012). *Computing discharge using the index velocity method: U.S. Geological Survey Techniques and Methods 3-A23* (p. 148). Reston, VA: U.S. Geological Survey.



- Levin, D. R. (1993). Tidal inlet evolution in the Mississippi River delta plain. *Journal of Coastal Research*, 9(2), 462–480.
- Li, C., Huang, W., & Milan, B. (2019). Atmospheric cold front-induced exchange flows through a microtidal multi-inlet bay: Analysis using multiple horizontal ADCPs and FVCOM simulations. *Journal of Atmospheric and Oceanic Technology*, 36(3), 443–472.
- Li, C., Swenson, E., Weeks, E., & White, J. R. (2009). Asymmetric tidal straining across an inlet: Lateral inversion and variability over a tidal cycle. *Estuarine, Coastal and Shelf Science*, 85(4), 651–660.
- Li, C., Weeks, E., Huang, W., Milan, B., & Wu, R. (2018). Weather-induced transport through a tidal channel calibrated by an unmanned boat. *Journal of Atmospheric and Oceanic Technology*, 35(2), 261–279.
- Li, C., White, J. R., Chen, C., Lin, H., Weeks, E., Galvan, K., & Bargu, S. (2011). Summertime tidal flushing of Barataria Bay: Transports of water and suspended sediments. *Journal of Geophysical Research: Oceans*, 116(C4), C04009.
- List, J. H., Jaffe, B. E., Jr., A. H. S., & Hansen, M. E. (1997). Bathymetric comparisons adjacent to the Louisiana barrier islands: Processes of large-scale change. *Journal of Coastal Research*, 13(3), 670–678.
- List, J. H., Jaffe, B. E., Sallenger, A. H., Williams, S. J., McBride, R. A., & Penland, S. (1994). *Louisiana barrier island erosion study: atlas of sea-floor changes from 1878 to 1989*.
- Malvern. (2015). Manual: Mastersizer 3000 user manual (MAN0474), 198.
- Manfredini, T., Pellacani, G. C., Pozzi, P., & Corradi, A. B. (1990). Monomeric and oligomeric phosphates as deflocculants of concentrated aqueous clay suspensions. *Applied Clay Science*, 5(3), 193–201.
- Marmer, H. A. (1948). *The currents in Barataria Bay* (p. 30). College Station, Texas: Texas A&M Research Foundation.
- Miner, M. D., Kulp, M. A., FitzGerald, D. M., Flocks, J. G., & Weathers, H. D. (2009). Delta lobe degradation and hurricane impacts governing large-scale coastal behavior, South-central Louisiana, USA. *Geo-Marine Letters*, 29(6), 441–453.
- O'Brien, M. P. (1931). Estuary tidal prisms related to entrance area. *Civil Engineering*, 1(8), 738–739.
- Penland, S., Boyd, R., & Suter, J. R. (1988). Transgressive depositional systems of the Mississippi delta plain: A model for barrier shoreline and shelf sand development. *Journal of Sedimentary Petrology*, 58(6), 932–949.
- Reed, D. J. (1995). Status and Trends of Hydrologic Modification, Reduction in Sediment Availability, and Habitat Loss/Modification in the Barataria-Terrebonne Estuarine System. *Barataria-Terrebonne National Estuary Program*, 20, 752.
- Roberts, H. H., Walker, N., Kemp, G. P., & Majersky, S. (1997). Evolution of sedimentary architecture and surface morphology: Atchafalaya and Wax Lake deltas, Louisiana (1973–1994). *Gulf Coast Association of Geological Societies Transactions*, 47, 477–484.
- Ruhl, C. A., & Simpson, M. R. (2005). *Computation of discharge using the index-velocity method in tidally affected areas* (Scientific Investigations Report No. 2005–5004) (p. 31). Reston, VA: U.S. Geological Survey.
- Teledyne RD Instruments. (2016). WinRiver II Software User's Guide, 310.
- Teledyne RD Instruments, Inc. (2016). *WorkHorse Sentinel, Monitor, & Mariner operation manual* (No. P/N 957-6150-00) (pp. 1–232).
- Turner, R. E., Swenson, E. M., Milan, C. S., & Lee, J. M. (2019). Spatial variations in chlorophyll a, C, N, and P in a Louisiana estuary from 1994 to 2016. *Hydrobiologia*, 834(1), 131–144.
- Walton, T. L., & Adams, W. D. (1976). Capacity of inlet outer bars to store sand. *Coastal Engineering*, 112, 1919–1937.
- Williams, S. J., Penland, S., & Sallenger, A. H. (1992). Atlas of shoreline changes in Louisiana, 109.
- Wissel, B., Gače, A., & Fry, B. (2005). Tracing river influences on phytoplankton dynamics in two Louisiana estuaries. *Ecology*, 86(10), 2751–2762.



- Zhang, J.-Z. (1997). Determination of Nitrate and Nitrite in Estuarine and Coastal Waters by Gas Segmented Continuous Flow Colorimetric Analysis, 20.
- Zhang, J.-Z., & Berberian, G. A. (1997). Determination of Dissolved Silicate in Estuarine and Coastal Waters by Gas Segmented Continuous Flow Colorimetric Analysis, 13.



Appendices



APPENDIX A: ADCP FILE LOG AND DISCHARGE SUMMARY

Table A-A 1. List of ADCP survey files, including discharge, at Caminada Pass (Tx-01)

Folder Name	Filename	Lap Start Time (UTC)	Lap End Time (UTC)	Direction	Total Q, BT (cms)	Total Q, GGA (cms)
TO55_Tx01_0	CMD_0_000_19-04-11_195014.PD0	19:52	-	L > R	-494.567	-510.365
TO55_Tx01_0	CMD_0_001_19-04-11_200207.PD0	20:06	-	R > L	-490.181	-707.036
TO55_Tx01_0	CMD_0_002_19-04-11_201430.PD0	20:20	-	L > R	-281.069	-303.702
TO55_Tx01_0	CMD_0_003_19-04-11_203015.PD0	20:31	-	R > L	-156.326	-373.87
TO55_Tx01_0	CMD_0_004_19-04-11_204142.PD0	20:43	-	L > R	-9.375	-23.46
TO55_Tx01_0	CMD_0_006_19-04-11_205636.PD0	21:08	-	R > L	218.864	312.862
TO55_Tx01_0	CMD_0_007_19-04-11_212356.PD0	21:27	-	L > R	567.324	66.419
TO55_Tx01_0	CMD_0_008_19-04-11_213719.PD0	21:38	-	R > L	714.552	-219.102
TO55_Tx01_0	CMD_0_009_19-04-11_215447.PD0	21:55	-	L > R	938.352	1210.038
TO55_Tx01_0	CMD_0_010_19-04-11_222253.PD0	22:25	-	R > L	1478.748	1148.726
TO55_Tx01_0	CMD_0_011_19-04-11_223739.PD0	22:42	-	L > R	1640.829	1463.637
TO55_Tx01_0	CMD_0_012_19-04-11_225512.PD0	22:55	-	R > L	1789.039	-686.716
TO55_Tx01_0	CMD_0_013_19-04-11_231158.PD0	23:12	-	L > R	1723.43	251.038
TO55_Tx01_0	CMD_0_014_19-04-11_232433.PD0	23:32	-	R > L	1899.721	-1523.549
TO55_Tx01_0	CMD_0_015_19-04-11_234822.PD0	23:49	-	L > R	1987.157	-2161.982

Table A-A 2. List of ADCP survey files, including discharge, at Barataria Pass (Tx-02)

Folder Name	Filename	Lap Start Time (UTC)	Lap End Time (UTC)	Direction	Total Q, BT (cms)	Total Q, GGA (cms)
TO55_Tx02_0	TO55-Tx-02_0_000_19-02-05_211429.PD0	21:16	21:24	L > R	-3027.048	-2660.784
TO55_Tx02_0	TO55-Tx-02_0_001_19-02-05_212428.PD0	21:27	21:37	R > L	-2957.136	-2862.524
TO55_Tx02_0	TO55-Tx-02_0_003_19-05-22_154319.PD0	15:44	15:52	L > R	-4250.366	-4322.974
TO55_Tx02_0	TO55-Tx-02_0_005_19-05-22_160106.PD0	16:03	16:12	R > L	-3884.437	-4325.421
T055_Tx02_2_Penland	TO55_Tx02_2_0_000_19-06-03_152102.PD0	15:34	15:38	R > L	-3013.582	no GGA
T055_Tx02_2_Penland	TO55_Tx02_2_0_001_19-06-03_153817.PD0	15:44	15:50	R > L	-2277.015	no GGA
T055_Tx02_2_Penland	TO55_Tx02_2_0_002_19-06-03_155055.PD0	16:00	16:08	L > R	-1707.777	no GGA
T055_Tx02_2_Penland	TO55_Tx02_2_0_003_19-06-03_160839.PD0	16:21	16:27	R > L	-1277.923	no GGA
T055_Tx02_2_Penland	TO55_Tx02_2_0_004_19-06-03_162715.PD0	16:34	16:40	L > R	-1074.503	no GGA
T055_Tx02_2_Penland	TO55_Tx02_2_0_005_19-06-03_164048.PD0	16:44	16:50	R > L	-743.555	no GGA
T055_Tx02_2_Penland	TO55_Tx02_2_0_006_19-06-03_165025.PD0	17:57	18:03	R > L	2025.404	no GGA
T055_Tx02_2_Penland	TO55_Tx02_2_0_008_19-06-03_180935.PD0	18:22	18:28	R > L	2888.291	no GGA
T055_Tx02_2_Penland	TO55_Tx02_2_0_009_19-06-03_182857.PD0	18:41	18:48	R > L	3715.184	no GGA
T055_Tx02_2_Penland	TO55_Tx02_2_0_012_19-06-03_185735.PD0	18:57	19:04	R > L	4337.063	no GGA
T055_Tx02_2_Penland	TO55_Tx02_2_0_013_19-06-03_190443.PD0	19:13	19:20	L > R	4901.687	no GGA
T055_Tx02_2_Penland	TO55_Tx02_2_0_014_19-06-03_192058.PD0	19:22	19:32	R > L	5252.176	no GGA
T055_Tx02_2_Penland	TO55_Tx02_2_0_015_19-06-03_193202.PD0	20:45	20:53	R > L	7209.081	no GGA
T055_Tx02_2_Penland	TO55_Tx02_2_0_016_19-06-03_205319.PD0	20:53	21:00	L > R	7146.375	no GGA
T055_Tx02_2_Penland	TO55_Tx02_2_0_017_19-06-03_210014.PD0	21:01	21:09	R > L	7264.104	no GGA
TO55_Tx02_LSU_SM	T055_Tx02_LSU_0_004_19-09-05_181419.PD0	18:51	18:59	R > L	4825.038	4700.701
TO55_Tx02_LSU_SM	T055_Tx02_LSU_0_005_19-09-05_185934.PD0	19:02	19:09	L > R	4814.752	5099.689
TO55_Tx02_LSU_SM	T055_Tx02_LSU_0_006_19-09-05_190949.PD0	19:16	19:24	R > L	4696.076	4573.948
TO55_Tx02_LSU_SM	T055_Tx02_LSU_0_007_19-09-05_192415.PD0	19:26	19:34	L > R	4686.887	4972.755
TO55_Tx02_SM	TO55_Tx02_SM_0_000_19-09-10_140959.PD0	14:21	14:29	L > R	119.834	67.914
TO55_Tx02_SM	TO55_Tx02_SM_0_002_19-09-10_143918.PD0	14:46	14:54	L > R	735.569	718.589
TO55_Tx02_SM	TO55_Tx02_SM_0_003_19-09-10_145500.PD0	14:57	15:05	R > L	1109.011	886.322
TO55_Tx02_SM	TO55_Tx02_SM_0_004_19-09-10_150542.PD0	15:10	15:18	L > R	1348.329	1026.431
TO55_Tx02_SM	TO55_Tx02_SM_0_005_19-09-10_151815.PD0	15:18	15:27	R > L	1714.801	1659.308

Folder Name	Filename	Lap Start Time (UTC)	Lap End Time (UTC)	Direction	Total Q, BT (cms)	Total Q, GGA (cms)
TO55_Tx02_SM	TO55_Tx02_SM_0_006_19-09-10_152751.PD0	15:29	15:37	L > R	2075.896	2113.653
TO55_Tx02_SM	TO55_Tx02_SM_0_007_19-09-10_153753.PD0	15:40	15:50	R > L	2378.841	2193.245
TO55_Tx02_SM	TO55_Tx02_SM_0_008_19-09-10_155001.PD0	15:51	15:59	L > R	2442.708	2708.065
TO55_Tx02_SM	TO55_Tx02_SM_0_009_19-09-10_155943.PD0	16:01	16:11	R > L	3016.878	2779.946
TO55_Tx02_SM	TO55_Tx02_SM_0_010_19-09-10_161103.PD0	16:13	16:22	L > R	3332.571	3426.7
TO55_Tx02_SM	TO55_Tx02_SM_0_011_19-09-10_162218.PD0	16:24	16:34	R > L	3373.294	3164.409
TO55_Tx02_SM	TO55_Tx02_SM_0_012_19-09-10_163456.PD0	16:38	16:47	L > R	3564.577	3797.024
TO55_Tx02_SM	TO55_Tx02_SM_0_013_19-09-10_164723.PD0	16:48	16:58	R > L	3828.901	3659.712
TO55_Tx02_SM	TO55_Tx02_SM_0_014_19-09-10_165807.PD0	17:00	17:09	L > R	3654.919	3950.471
TO55_Tx02_SM	TO55_Tx02_SM_0_015_19-09-10_170905.PD0	17:10	17:19	R > L	4219.193	4011.59
TO55_Tx02_SM	TO55_Tx02_SM_0_016_19-09-10_171940.PD0	17:20	17:29	L > R	4152.588	4373.882
TO55_Tx02_SM	TO55_Tx02_SM_0_017_19-09-10_172915.PD0	17:30	17:40	R > L	4383.176	4317.214
TO55_Tx02_SM	TO55_Tx02_SM_0_018_19-09-10_174015.PD0	17:43	17:51	L > R	4452.767	4681.914
TO55_Tx02_SM	TO55_Tx02_SM_0_019_19-09-10_175149.PD0	17:53	18:02	R > L	4532.38	4448.193
TO55_Tx02_SM	TO55_Tx02_SM_0_020_19-09-10_180243.PD0	18:03	18:12	L > R	4679.635	4882.371
TO55_Tx02_SM	TO55_Tx02_SM_0_021_19-09-10_181206.PD0	18:14	18:23	R > L	4533.032	4390.033
TO55_Tx02_SM	TO55_Tx02_SM_0_022_19-09-10_182346.PD0	18:28	18:37	L > R	5017.798	5258.198
TO55_Tx02_SM	TO55_Tx02_SM_0_023_19-09-10_183740.PD0	18:39	18:48	R > L	5268.263	5134.713
TO55_Tx02_SM	TO55_Tx02_SM_0_024_19-09-10_184832.PD0	18:49	18:58	L > R	5365.893	5629.73
TO55_Tx02_SM	TO55_Tx02_SM_0_025_19-09-10_185830.PD0	19:00	19:08	R > L	5476.872	5398.354
TO55_Tx02_SM	TO55_Tx02_SM_0_026_19-09-10_190848.PD0	19:11	19:19	L > R	5555.298	5808.852
TO55_Tx02_SM	TO55_Tx02_SM_0_027_19-09-10_191903.PD0	19:20	19:29	R > L	5546.907	5523.716
TO55_Tx02_SM	TO55_Tx02_SM_0_028_19-09-10_192938.PD0	19:31	19:40	L > R	5836.687	6082.731
TO55_Tx02_SM	TO55_Tx02_SM_0_029_19-09-10_194010.PD0	19:43	19:52	R > L	5829.06	5761.774
TO55_Tx02_SM	TO55_Tx02_SM_0_030_19-09-10_195213.PD0	19:58	20:08	L > R	5961.566	6237.21
TO55_Tx02_SM	TO55_Tx02_SM_0_032_19-09-10_201122.PD0	20:11	20:22	R > L	5775.242	5752.133
TO55_Tx02_SM	TO55_Tx02_SM_0_033_19-09-10_202236.PD0	20:24	20:33	L > R	6033.986	6331.949
TO55_Tx02_SM	TO55_Tx02_SM_0_034_19-09-10_203313.PD0	20:34	20:44	R > L	5695.583	5620.197

Table A-A 3. List of ADCP survey files, including discharge, at Pass Abel (Tx-03)

Folder Name	Filename	Lap Start Time (UTC)	Lap End Time (UTC)	Direction	Total Q, BT (cms)	Total Q, GGA (cms)
TO55_Tx03_0_Penland	TO55_Tx03_0_000_19-06-02_165307.PD0	17:45	17:59	R>L	1491.734	no GGA
TO55_Tx03_0_Penland	TO55_Tx03_0_001_19-06-02_175958.PD0	18:12	18:24	R>L	1692.968	no GGA
TO55_Tx03_0_Penland	TO55_Tx03_0_002_19-06-02_182445.PD0	19:26	19:37	R>L	2354.743	no GGA
TO55_Tx03_0_Penland	TO55_Tx03_0_003_19-06-02_193734.PD0	19:46	19:57	R>L	2350.976	no GGA
TO55_Tx03_0_Penland	TO55_Tx03_0_004_19-06-02_195711.PD0	20:05	20:16	R>L	2391.954	no GGA
TO55_Tx03_0_Penland	TO55_Tx03_0_005_19-06-02_201648.PD0	22:35	22:45	R>L	2096.371	no GGA
TO55_Tx03_0_Penland	TO55_Tx03_0_006_19-06-02_224446.PD0	22:52	23:02	R>L	2099.931	no GGA
TO55_Tx03_0_Penland	TO55_Tx03_0_007_19-06-02_230230.PD0	23:10	23:21	R>L	2107.423	no GGA
TO55_Tx03_mudlump_0	Tx03_mudlump_0_001_19-09-10_143706.PD0	15:05	15:23	L>R	328.248	366.816
TO55_Tx03_mudlump_0	Tx03_mudlump_0_003_19-09-10_153305.PD0	15:41	15:58	L>R	704.24	251.987
TO55_Tx03_mudlump_0	Tx03_mudlump_0_004_19-09-10_155843.PD0	16:13	16:32	L>R	954.812	426.848
TO55_Tx03_mudlump_0	Tx03_mudlump_0_005_19-09-10_163255.PD0	16:48	17:06	L>R	1245.312	657.415
TO55_Tx03_mudlump_0	Tx03_mudlump_0_006_19-09-10_170605.PD0	17:17	17:35	L>R	1447.561	500.414
TO55_Tx03_mudlump_0	Tx03_mudlump_0_007_19-09-10_173527.PD0	17:49	18:07	L>R	1608.921	299.052
TO55_Tx03_mudlump_0	Tx03_mudlump_0_008_19-09-10_180731.PD0	18:21	18:39	L>R	1803.578	262.131
TO55_Tx03_mudlump_0	Tx03_mudlump_0_009_19-09-10_183946.PD0	18:55	19:13	L>R	2061.955	22.645
TO55_Tx03_mudlump_0	Tx03_mudlump_0_010_19-09-10_191319.PD0	19:25	19:44	L>R	2153.737	419.703
TO55_Tx03_mudlump_0	Tx03_mudlump_0_011_19-09-10_194425.PD0	19:56	20:14	L>R	2161.414	255.54
TO55_Tx03_mudlump_0	Tx03_mudlump_0_012_19-09-10_201450.PD0	20:31	20:50	L>R	2103.875	481.289

Table A-A 4. List of ADCP survey files, including discharge, at Quatre Bayou Pass (Tx-04)

Folder Name	Filename	Lap Start Time (UTC)	Lap End Time (UTC)	Direction	Total Q, BT (cms)	Total Q, GGA (cms)
TO55_Tx04_0	TO55-Tx04_0_000_19-05-20_144112.PD0	14:44	15:04	R > L	-2464.671	-2901.513
TO55_Tx04_0	TO55-Tx04_0_001_19-05-20_150405.PD0	15:04	15:28	L > R	-2113.154	-2160.185
TO55_Tx04_0	TO55-Tx04_0_002_19-05-20_152808.PD0	15:28	15:53	R > L	-1918.368	-2234.813
TO55_Tx04_0	TO55-Tx04_0_003_19-05-20_155340.PD0	15:54	16:18	L > R	-1431.957	-1463.596
TO55_Tx04_0	TO55-Tx04_0_004_19-05-20_161830.PD0	16:20	16:44	R > L	-1131.774	-1453.483
TO55_Tx04_0	TO55-Tx04_0_005_19-05-20_164442.PD0	16:45	17:08	L > R	-362.533	-419.753
TO55_Tx04_0	TO55-Tx04_0_006_19-05-20_170816.PD0	17:08	17:34	R > L	13.401	-276.877
TO55_Tx04_0	TO55-Tx04_0_007_19-05-20_173417.PD0	17:35	17:58	L > R	281.682	305.296
TO55_Tx04_0	TO55-Tx04_0_008_19-05-20_175850.PD0	18:00	18:26	R > L	963.881	729.174
TO55_Tx04_0	TO55-Tx04_0_009_19-05-20_182609.PD0	18:26	18:48	L > R	1767.442	1789.429
TO55_Tx04_0	TO55-Tx04_0_010_19-05-20_184822.PD0	18:50	19:17	R > L	1989.439	1753.413
TO55_Tx04_0	TO55-Tx04_0_011_19-05-20_191755.PD0	19:18	19:40	L > R	2770.052	2778.969
TO55_Tx04_0	TO55-Tx04_0_012_19-05-20_194057.PD0	19:41	20:06	R > L	3045.301	2818.756
TO55_Tx04_0	TO55-Tx04_0_013_19-05-20_200611.PD0	20:06	20:29	L > R	3533.745	3610.202
TO55_Tx04_0	TO55-Tx04_0_014_19-05-20_202906.PD0	20:29	20:57	R > L	3390.565	3188.764
TO55_Tx04_0	TO55-Tx04_0_015_19-05-20_205727.PD0	20:58	21:18	L > R	3438.362	3601.762
TO55_Tx04_SM2_0	to55_tx04_smullet2_0_000_19-09-19_124725.PDO	12:48	13:11	L > R	2866.825	2922.167
TO55_Tx04_SM2_0	to55_tx04_smullet2_0_001_19-09-19_131137.PDO	13:12	13:39	R > L	2889.839	2531.046
TO55_Tx04_SM2_0	to55_tx04_smullet2_0_002_19-09-19_133957.PDO	13:41	14:03	L > R	2613.93	2689.809
TO55_Tx04_SM2_0	to55_tx04_smullet2_0_003_19-09-19_140336.PDO	14:04	14:31	R > L	2541.457	2162.723
TO55_Tx04_SM2_0	to55_tx04_smullet2_0_005_19-09-19_145449.PDO	14:55	15:23	R > L	2529.916	2188.37
TO55_Tx04_SM2_0	to55_tx04_smullet2_0_006_19-09-19_152313.PDO	15:23	15:45	L > R	2358.832	2433.968
TO55_Tx04_SM2_0	to55_tx04_smullet2_0_007_19-09-19_154543.PDO	15:46	16:11	R > L	2212.406	1802.994
TO55_Tx04_SM2_0	to55_tx04_smullet2_0_008_19-09-19_161148.PDO	16:15	16:37	L > R	1917.155	1877.81
TO55_Tx04_SM2_0	to55_tx04_smullet2_0_011_19-09-19_173442.PDO	17:35	18:07	R > L	917.005	741.53
TO55_Tx04_SM2_0	to55_tx04_smullet2_0_012_19-09-19_180739.PDO	18:08	18:31	L > R	742.898	630.417
TO55_Tx04_SM2_0	to55_tx04_smullet2_0_014_19-09-19_185942.PDO	19:00	19:24	L > R	337.849	267.166

Table A-A 5. List of ADCP survey files, including discharge, at Pass Ronquille (Tx-05)

Transect	Filename	Lap Start Time (UTC)	Lap End Time (UTC)	Direction	Total Q, BT (cms)	Total Q, GGA (cms)
TO55_Tx05_0_Penland	tx05_0_000_19-05-20_163924.PD0	16:45	17:05	R > L	199.758	1488.296
TO55_Tx05_0_Penland	tx05_0_001_19-05-20_170549.PD0	17:22	17:47	R > L	481.217	1532.027
TO55_Tx05_0_Penland	tx05_0_002_19-05-20_174720.PD0	17:56	18:10	R > L	595.352	2699.552
TO55_Tx05_0_Penland	tx05_0_004_19-05-20_181725.PD0	18:19	18:31	R > L	773.113	3053.028
TO55_Tx05_0_Penland	tx05_0_005_19-05-20_183147.PD0	18:39	18:52	R > L	821.013	2667.13
TO55_Tx05_0_Penland	tx05_0_006_19-05-20_185220.PD0	19:00	19:12	R > L	978.74	2822.74
TO55_Tx05_0_Penland	tx05_0_007_19-05-20_191235.PD0	19:19	19:30	R > L	1123.498	3378.47
TO55_Tx05_0_Mullet	TO55-Tx05_0_000.PD0	21:54	22:07	R > L	1523.31	1489.835
TO55_Tx05_0_Mullet	TO55-Tx05_0_001.PD0	22:09	22:17	L > R	1684.17	1724.631
TO55_Tx05_SM	TO55_Tx05_SM_0_001_19-09-09_162305.PD0	16:40	16:57	L > R	1439.125	1670.907
TO55_Tx05_SM	TO55_Tx05_SM_0_002_19-09-09_165713.PD0	16:59	17:23	R > L	1485.634	1468.388
TO55_Tx05_SM	TO55_Tx05_SM_0_003_19-09-09_172322.PD0	17:26	17:42	L > R	1580.881	1858.977
TO55_Tx05_SM	TO55_Tx05_SM_0_004_19-09-09_174258.PD0	17:45	18:09	R > L	1581.734	1567.234
TO55_Tx05_SM	TO55_Tx05_SM_0_005_19-09-09_180930.PD0	18:14	18:30	L > R	1508.796	1822.947
TO55_Tx05_SM	TO55_Tx05_SM_0_006_19-09-09_183019.PD0	18:32	18:55	R > L	1551.993	1544.676
TO55_Tx05_SM	TO55_Tx05_SM_0_007_19-09-09_185546.PD0	18:57	19:15	L > R	1634.38	1831.512
TO55_Tx05_SM	TO55_Tx05_SM_0_008_19-09-09_191519.PD0	19:17	19:41	R > L	1491.941	1461.929
TO55_Tx05_SM	TO55_Tx05_SM_0_009_19-09-09_194131.PD0	19:44	20:01	L > R	1376.637	1647.617
TO55_Tx05_SM	TO55_Tx05_SM_0_011_19-09-09_200212.PD0	20:07	20:32	R > L	1307.394	1256.575
TO55_Tx05_SM	TO55_Tx05_SM_0_012_19-09-09_203211.PD0	20:34	20:50	L > R	1150.943	1383.094
TO55_Tx05_SM	TO55_Tx05_SM_0_013_19-09-09_205038.PD0	20:52	21:15	R > L	1153.965	1087.642
TO55_Tx05_SM	TO55_Tx05_SM_0_014_19-09-09_211501.PD0	21:16	21:32	L > R	1046.366	1279.555
TO55_Tx05_SM	TO55_Tx05_SM_0_015_19-09-09_213207.PD0	21:34	21:59	R > L	911.745	814.861
TO55_Tx05_SM	TO55_Tx05_SM_0_016_19-09-09_215925.PD0	22:00	22:16	L > R	679.755	891.188

Table A-A 6. List of ADCP survey files, including discharge, at Bastian Pass (Tx-06)

Folder Name	Filename	Lap Start Time (UTC)	Lap End Time (UTC)	Direction	Total Q, BT (cms)	Total Q, GGA (cms)
TO55_Tx06_0	TO55_Tx06_0_000_19-03-17_172003.PD0	17:44	17:54	L > R	-755.731	-754.074
TO55_Tx06_0	TO55_Tx06_0_001_19-03-17_180034.PD0	18:04	18:23	L > R	-1436.394	-110.63
TO55_Tx06_0	TO55_Tx06_0_003_19-03-17_182951.PD0	18:33	18:56	R > L	-1651.67	-885.741
TO55_Tx06_0	TO55_Tx06_0_004_19-03-17_185642.PD0	14:51	15:11	L > R	-1254.222	-1276.763
TO55_Tx06_0	TO55_Tx06_0_005_19-05-06_151110.PD0	15:11	15:35	R > L	-916.416	-881.466
TO55_Tx06_0	TO55_Tx06_0_006_19-05-06_153545.PD0	15:36	15:54	L > R	-407.906	-325.844
TO55_Tx06_0	TO55_Tx06_0_007_19-05-06_155419.PD0	19:29	19:49	L > R	2591.922	2817.192
TO55_Tx06_0	TO55_Tx06_0_008_19-05-06_194918.PD0	19:49	20:09	R > L	2779.787	2846.972
TO55_Tx06_0	TO55_Tx06_0_009_19-05-06_200920.PD0	20:09	20:28	L > R	2877.536	3066.05

Table A-A 7. List of ADCP survey files, including discharge, at Fontanelle Pass (Tx-07)

Folder Name	Filename	Lap Start Time (UTC)	Lap End Time (UTC)	Direction	Total Q, BT (cms)	Total Q, GGA (cms)
TO55_Tx07_0	TO55-Tx07_0_000_19-03-17_160501.PD0	16:10	16:21	L > R	-1196.361	-1185.898
TO55_Tx07_0	TO55-Tx07_0_001_19-03-17_162121.PD0	16:21	16:31	R > L	-1212.736	-1383.658
TO55_Tx07_0	TO55-Tx07_0_004_19-03-17_195630.PD0	20:50	21:09	L > R	-972.584	-1278.456
TO55_Tx07_0	TO55-Tx07_0_005_19-03-17_210941.PD0	21:10	21:22	R > L	-970.924	-508.444
TO55_Tx07_0	TO55-Tx07_0_006_19-03-17_223152.PD0	22:31	22:45	L > R	-1148	-1320.108
TO55_Tx07_0	TO55-Tx07_0_007_19-03-17_224512.PD0	22:46	22:57	R > L	-984.878	no GGA
TO55_Tx07_0	TO55-Tx07_0_008_19-03-17_225727.PD0	23:11	23:21	R > L	-657.992	-760.326
TO55_Tx07_0	TO55-Tx07_0_010_19-05-05_231336.PD0	23:16	23:25	R > L	1463.156	1422.322
TO55_Tx07_0	TO55-Tx07_0_011_19-05-05_232535.PD0	23:25	23:36	L > R	1436.819	1429.665
TO55_Tx07_0	TO55-Tx07_0_012_19-05-05_233627.PD0	14:02	14:11	R > L	-1081.079	-1008.934
TO55_Tx07_0	TO55-Tx07_0_015_19-05-06_142615.PD0	17:57	18:08	L > R	1203.745	1311.886
TO55_Tx07_0	TO55-Tx07_0_016_19-05-06_180827.PD0	18:08	18:20	R > L	1257.015	1308.521
TO55_Tx07_0	TO55-Tx07_0_017_19-05-06_182350.PD0	18:25	18:35	L > R	1159.189	1269.129
TO55_Tx07_0	TO55-Tx07_0_018_19-05-06_183555.PD0	18:36	18:49	R > L	1216.369	1242
TO55_Tx07_0	TO55-Tx07_0_019_19-05-06_184932.PD0	18:50	19:01	L > R	1182.784	1296.717
TO55_Tx07_0	TO55-Tx07_0_021_19-05-06_192745.PD0	20:56	21:06	R > L	1594.405	1650.445
TO55_Tx07_0	TO55-Tx07_0_022_19-05-06_210652.PD0	21:07	21:18	L > R	1492.894	1605.39
TO55_Tx07_0	TO55-Tx07_0_023_19-05-06_211810.PD0	21:18	21:29	R > L	1566.627	1625.118
TO55_Tx07_0	TO55-Tx07_0_024_19-05-06_212927.PD0	21:29	21:40	L > R	1522.878	1668.236
TO55_Tx07_0	TO55-Tx07_0_025_19-05-06_214020.PD0	21:40	21:51	R > L	1653.899	1725.899
TO55_Tx07_0	TO55-Tx07_0_026_19-05-06_215151.PD0	21:52	22:03	L > R	1628.909	1728.099
TO55_Tx07_0	TO55-Tx07_0_027_19-05-06_220314.PD0	22:03	22:14	R > L	1615.77	1691.424
TO55_Tx07_0	TO55-Tx07_0_028_19-05-06_221443.PD0	22:15	22:25	L > R	1506.476	1630.119
TO55_Tx07_0	TO55-Tx07_0_029_19-05-06_222533.PD0	22:28	22:39	R > L	1565.021	1679.769
TO55_Tx07_0	TO55-Tx07_0_030_19-05-06_223904.PD0	22:39	22:50	L > R	1488.496	1593.89
TO55_Tx07_SM_0	TO55_Tx07_0_000_19-09-08_161302.PD0	16:32	16:46	L > R	1500.281	1555.851
TO55_Tx07_SM_0	TO55_Tx07_0_001_19-09-08_164627.PD0	16:50	16:59	R > L	1512.169	1324.288
TO55_Tx07_SM_0	TO55_Tx07_0_002_19-09-08_165903.PD0	17:01	17:15	L > R	1570.806	1631.757
TO55_Tx07_SM_0	TO55_Tx07_0_003_19-09-08_171555.PD0	17:21	17:31	R > L	1605.551	1421.119

Folder Name	Filename	Lap Start Time (UTC)	Lap End Time (UTC)	Direction	Total Q, BT (cms)	Total Q, GGA (cms)
TO55_Tx07_SM_0	TO55_Tx07_0_004_19-09-08_173121.PD0	17:33	17:49	L > R	1602.949	1667.164
TO55_Tx07_SM_0	TO55_Tx07_0_005_19-09-08_174902.PD0	17:51	18:00	R > L	1613.86	1416.825
TO55_Tx07_SM_0	TO55_Tx07_0_006_19-09-08_180030.PD0	18:03	18:15	L > R	1517.626	1571.313
TO55_Tx07_SM_0	TO55_Tx07_0_007_19-09-08_181552.PD0	18:18	18:27	R > L	1531.061	1365.516
TO55_Tx07_SM_0	TO55_Tx07_0_008_19-09-08_182702.PD0	18:29	18:40	L > R	1477.198	1546.608
TO55_Tx07_SM_0	TO55_Tx07_0_009_19-09-08_184046.PD0	18:42	18:51	R > L	1424.763	1267.15
TO55_Tx07_SM_0	TO55_Tx07_0_010_19-09-08_185135.PD0	18:54	19:06	L > R	1381.684	1435.188
TO55_Tx07_SM_0	TO55_Tx07_0_011_19-09-08_190637.PD0	19:09	19:19	R > L	1299.233	1148.475
TO55_Tx07_SM_0	TO55_Tx07_0_012_19-09-08_191903.PD0	19:22	19:34	L > R	1300.077	1362.239
TO55_Tx07_SM_0	TO55_Tx07_0_013_19-09-08_193411.PD0	19:36	19:45	R > L	1342.394	1158.2

Table A-A 8. List of ADCP survey files, including discharge, at Scofield Pass (Tx-08)

Folder Name	Filename	Lap Start Time (UTC)	Lap End Time (UTC)	Direction	Total Q, BT (cms)	Total Q, GGA (cms)
TO55_Tx08_0	TO55_Tx08_0_000_19-03-17_215424.PD0	21:57	21:58	R > L	-91.986	-166.786
TO55_Tx08_0	TO55_Tx08_0_001_19-03-17_215843.PD0	22:00	22:01	L > R	-107.521	132.518
TO55_Tx08_2_SM	TO55_Tx08_2_0_000_19-06-14_172552.PD0	17:29	17:30	R > L	64.685	no GGA
TO55_Tx08_2_SM	TO55_Tx08_2_0_001_19-06-14_173033.PD0	17:33	17:34	R > L	74.391	no GGA
TO55_Tx08_2_SM	TO55_Tx08_2_0_002_19-06-14_173426.PD0	17:38	17:39	R > L	86.284	no GGA
TO55_Tx08_2_SM	TO55_Tx08_2_0_003_19-06-14_173957.PD0	17:41	17:42	L > R	84.214	no GGA
TO55_Tx08_2_SM	TO55_Tx08_2_0_004_19-06-14_174253.PD0	17:43	17:45	R > L	85.893	no GGA
TO55_Tx08_2_SM	TO55_Tx08_2_0_005_19-06-14_174516.PD0	17:46	17:47	L > R	91.83	no GGA
TO55_Tx08_2_SM	TO55_Tx08_2_0_006_19-06-14_174713.PD0	17:48	17:49	R > L	78.889	no GGA
TO55_Tx08_0_Mudlump	TO55_TX08_0_000_19-07-01_170133.PD0	17:06	17:08	L > R	104.246	110.305
TO55_Tx08_0_Mudlump	TO55_TX08_0_002_19-07-01_171216.PD0	17:13	17:15	L > R	131.125	117.844
TO55_Tx08_0_Mudlump	TO55_TX08_0_003_19-07-01_171514.PD0	17:17	17:19	L > R	108.767	99.231
TO55_Tx08_0_Mudlump	TO55_TX08_0_004_19-07-01_171920.PD0	17:23	17:25	L > R	115.974	116.682
TO55_Tx08_0_Mudlump	TO55_TX08_0_005_19-07-01_172511.PD0	17:27	17:29	L > R	116.37	118.88
TO55_Tx08_0_Mudlump	TO55_TX08_0_006_19-07-01_172938.PD0	17:31	17:34	L > R	109.309	113.997
TO55_Tx08_0_Mudlump	TO55_TX08_0_007_19-07-01_173448.PD0	17:37	17:39	L > R	114.784	119.566
TO55_Tx08_0_Mudlump	TO55_TX08_0_008_19-07-01_173945.PD0	17:42	17:44	L > R	105.692	115.417
TO55_Tx08_0_Mudlump	TO55_TX08_0_009_19-07-01_174459.PD0	17:47	17:49	L > R	125.566	121.85
TO55_Tx08_0_Mudlump	TO55_TX08_0_010_19-07-01_174914.PD0	17:51	17:53	L > R	122.888	127.853
TO55_Tx08_0_Mudlump	TO55_TX08_0_011_19-07-01_175347.PD0	17:56	17:58	L > R	123.795	125.523
TO55_Tx08_0_Mudlump	TO55_TX08_0_012_19-07-01_175852.PD0	18:01	18:04	L > R	128.846	128.194
TO55_Tx08_0_Mudlump	TO55_TX08_0_013_19-07-01_180412.PD0	18:06	18:09	L > R	138.523	141.427
TO55_Tx08_0_Mudlump	TO55_TX08_0_014_19-07-01_180907.PD0	18:11	18:13	L > R	112.557	117.834
TO55_Tx08_0_Mudlump	TO55_TX08_0_015_19-07-01_181351.PD0	18:54	18:56	L > R	161.025	174.785
TO55_Tx08_0_Mudlump	TO55_TX08_0_016_19-07-01_185611.PD0	18:58	19:00	L > R	137.217	157.894
TO55_Tx08_0_Mudlump	TO55_TX08_0_018_19-07-01_190318.PD0	19:04	19:06	L > R	140.818	153.53
TO55_Tx08_0_Mudlump	TO55_TX08_0_019_19-07-01_190614.PD0	19:08	19:10	L > R	147.58	152.161
TO55_Tx08_0_Mudlump	TO55_TX08_0_020_19-07-01_191013.PD0	19:12	19:14	L > R	118.825	122.742

Folder Name	Filename	Lap Start Time (UTC)	Lap End Time (UTC)	Direction	Total Q, BT (cms)	Total Q, GGA (cms)
TO55_Tx08_0_Mudlump	TO55_TX08_0_021_19-07-01_191406.PD0	19:16	19:17	L > R	145.136	151.715
TO55_Tx08_0_Mudlump	TO55_TX08_0_022_19-07-01_191740.PD0	19:19	19:20	L > R	136.438	159.014
TO55_Tx08_0_Mudlump	TO55_TX08_0_023_19-07-01_192100.PD0	19:22	19:24	L > R	122.857	146.75
TO55_Tx08_0_Mudlump	TO55_TX08_0_024_19-07-01_192405.PD0	19:26	19:27	L > R	189.616	152.415
TO55_Tx08_0_Mudlump	TO55_TX08_0_025_19-07-01_192735.PD0	19:29	19:31	L > R	163.128	159.102
TO55_Tx08_0_Mudlump	TO55_TX08_0_027_19-07-01_193644.PD0	19:37	19:38	L > R	161.144	163.646
TO55_Tx08_0_Mudlump	TO55_TX08_0_028_19-07-01_193901.PD0	19:40	19:42	L > R	187.676	160.353
TO55_Tx08_0_Mudlump	TO55_TX08_0_029_19-07-01_194211.PD0	19:43	19:44	L > R	135.503	166.33
TO55_Tx08_0_Mudlump	TO55_TX08_0_030_19-07-01_194501.PD0	19:46	19:47	L > R	155.9	156.846
TO55_Tx08_0_Mudlump	TO55_TX08_0_031_19-07-01_194754.PD0	19:50	19:52	L > R	111.648	160.805
TO55_Tx08_0_Mudlump	TO55_TX08_0_032_19-07-01_195227.PD0	19:54	19:55	L > R	142.782	175.474
TO55_Tx08_0_Mudlump	TO55_TX08_0_033_19-07-01_195542.PD0	19:57	19:58	L > R	151.764	146.641
TO55_Tx08_0_Mudlump	TO55_TX08_0_034_19-07-01_195836.PD0	20:00	20:01	L > R	138.371	161.095
TO55_Tx08_0_Mudlump	TO55_TX08_0_035_19-07-01_200143.PD0	20:03	20:04	L > R	89.041	166.008
TO55_Tx08_0_Mudlump	TO55_TX08_0_036_19-07-01_200422.PD0	20:06	20:07	L > R	106.307	139.059
TO55_Tx08_0_Mudlump	TO55_TX08_0_037_19-07-01_200732.PD0	20:08	20:10	L > R	148.242	153.351
TO55_Tx08_0_Mudlump	TO55_TX08_0_038_19-07-01_201009.PD0	20:11	20:13	L > R	132.829	155.479
TO55_Tx08_0_Mudlump	TO55_TX08_0_039_19-07-01_201303.PD0	20:14	20:15	L > R	138.26	160.847
TO55_Tx08_0_Mudlump	TO55_TX08_0_040_19-07-01_201527.PD0	20:16	20:17	L > R	133.791	139.512
TO55_Tx08_0_Mudlump	TO55_TX08_0_041_19-07-01_201802.PD0	20:19	20:20	L > R	140.422	137.59
TO55_Tx08_0_Mudlump	TO55_TX08_0_042_19-07-01_202034.PD0	20:22	20:23	L > R	156.25	154.841
TO55_Tx08_0_Mudlump	TO55_TX08_0_043_19-07-01_202350.PD0	20:25	20:26	L > R	107.421	146.038
TO55_Tx08_0_Mudlump	TO55_TX08_0_044_19-07-01_202637.PD0	20:28	20:29	L > R	135.58	134.191
TO55_Tx08_0_Mudlump	TO55_TX08_0_046_19-07-01_203118.PD0	20:32	20:33	L > R	143.148	156.026
TO55_Tx08_0_Mudlump	TO55_TX08_0_047_19-07-01_203339.PD0	20:35	20:36	L > R	130.646	105.149
TO55_Tx08_0_Mudlump	TO55_TX08_0_048_19-07-01_203655.PD0	20:39	20:40	L > R	117.71	133.967
TO55_Tx08_0_Mudlump	TO55_TX08_0_049_19-07-01_204034.PD0	20:42	20:43	L > R	130.218	97.321
TO55_Tx08_0_Mudlump	TO55_TX08_0_050_19-07-01_204353.PD0	20:45	20:46	L > R	111.212	133.962
TO55_Tx08_0_Mudlump	TO55_TX08_0_051_19-07-01_204655.PD0	20:48	20:49	L > R	108.798	118.657

Folder Name	Filename	Lap Start Time (UTC)	Lap End Time (UTC)	Direction	Total Q, BT (cms)	Total Q, GGA (cms)
TO55_Tx08_0_Mudlump	TO55_TX08_0_052_19-07-01_204937.PD0	20:51	20:52	L > R	108.61	125.822
TO55_Tx08_0_Mudlump	TO55_TX08_0_053_19-07-01_205230.PD0	20:53	20:55	L > R	125.746	117.671
TO55_Tx08_0_Mudlump	TO55_TX08_0_054_19-07-01_205514.PD0	20:56	20:58	L > R	118.596	99.33
TO55_Tx08_0_Mudlump	TO55_TX08_0_055_19-07-01_205807.PD0	21:00	21:01	L > R	112.752	105.917
TO55_Tx08_0_Mudlump	TO55_TX08_0_056_19-07-01_210157.PD0	21:03	21:05	L > R	125.754	110.628
TO55_Tx08_0_Mudlump	TO55_TX08_0_057_19-07-01_210512.PD0	21:07	21:08	L > R	137.857	131.537
TO55_Tx08_0_Mudlump	TO55_TX08_0_058_19-07-01_210841.PD0	21:10	21:11	L > R	82.506	103.171
TO55_Tx08_0_Mudlump	TO55_TX08_0_059_19-07-01_211149.PD0	21:12	21:14	L > R	115.135	121.826
TO55_Tx08_0_Mudlump	TO55_TX08_0_060_19-07-01_211426.PD0	21:15	21:17	L > R	86.504	117.216
TO55_Tx08_0_Mudlump	TO55_TX08_0_061_19-07-01_211715.PD0	21:20	21:21	L > R	83.086	100.137

Table A-A 9. List of ADCP survey files, including discharge, at Bay Coquette (Tx-09)

Folder Name	Filename	Lap Start Time (UTC)	Lap End Time (UTC)	Direction	Total Q, BT (cms)	Total Q, GGA (cms)
TO55_Tx09_0_SM	TO55_Tx09_0_001_19-06-14_194513.PD0	19:46	19:51	L>R	668.579	no GGA
TO55_Tx09_0_SM	TO55_Tx09_0_002_19-06-14_195135.PD0	19:53	20:01	R>L	612.089	no GGA
TO55_Tx09_0_SM	TO55_Tx09_0_003_19-06-14_200115.PD0	20:02	20:08	L>R	596.511	no GGA
TO55_Tx09_0_SM	TO55_Tx09_0_004_19-06-14_200815.PD0	20:09	20:17	R>L	552.097	no GGA
TO55_Tx09_0_SM	TO55_Tx09_0_005_19-06-14_201744.PD0	20:18	20:23	L>R	499.833	no GGA
TO55_Tx09_0_SM	TO55_Tx09_0_006_19-06-14_202354.PD0	20:24	20:30	R>L	491.501	no GGA
TO55_Tx09_0_SM	TO55_Tx09_0_007_19-06-14_203052.PD0	20:31	20:36	L>R	434.851	no GGA
TO55_Tx09_2_SM	TO55_Tx09_2_0_000_19-06-14_210325.PD0	21:09	21:13	L>R	344.298	461.527
TO55_Tx09_2_SM	TO55_Tx09_2_0_001_19-06-14_211357.PD0	21:14	21:22	R>L	343.708	234.327
TO55_Tx09_2_SM	TO55_Tx09_2_0_002_19-06-14_212305.PD0	21:23	21:28	L>R	324.339	415.486

APPENDIX B: CTD FILE LOG

Table A-B 1. List of CTD files from vessel-based surveys. The “L” in the filename corresponds to the number of laps surveyed across a given inlet that were conducted in one day.

Inlet	Station	Date Time (UTC)	Processed Filename
Caminada Pass	A	4/11/2019 18:08	TO55-Tx01-A-L1-2019-04-11-0030.csv
Caminada Pass	A	4/11/2019 18:27	TO55-Tx01-A-L1-2019-04-11-0031.csv
Caminada Pass	B	4/11/2019 18:42	TO55-Tx01-B-L1-2019-04-11-0032.csv
Caminada Pass	C	4/11/2019 18:54	TO55-TX01-C-L1-2019-04-11-0033.csv
Barataria pass	A	6/3/2019 17:14	TO55-Tx02-A-L1-2019-06-03-0020.csv
Barataria pass	A	2/5/2019 17:40	TO55-Tx02-A-L1-2019-02-05-0002.csv
Barataria pass	A	6/3/2019 19:46	TO55-Tx02-A-L2-2019-06-03-0024.csv
Barataria pass	B	6/3/2019 17:33	TO55-Tx02-B-L1-2019-06-03-0022.csv
Barataria pass	B	6/3/2019 20:11	TO55-Tx02-B-L2-2019-06-03-0026.csv
Barataria pass	C	2/5/2019 20:04	TO55-Tx02-C-L1-2019-02-05-0004.csv
Barataria pass	C	6/3/2019 17:26	TO55-Tx02-C-L1-2019-06-03-0021.csv
Barataria pass	C	6/3/2019 19:38	TO55-Tx02-C-L2-2019-06-03-0023.csv
Barataria pass	C	6/3/2019 19:59	TO55-Tx02-C-L2-2019-06-03-0025.csv
Pass Abel	A	6/2/2019 18:53	TO55-Tx03-A-L1-2019-06-02-0011.csv
Pass Abel	A	6/2/2019 20:36	TO55-Tx03-A-L2-2019-06-02-0014.csv
Pass Abel	A	6/2/2019 23:36	TO55-Tx03-A-L3-2019-06-02-0015.csv
Pass Abel	B	2/5/2019 19:02	TO55-Tx02-B-L1-2019-02-05-0003.csv
Pass Abel	B	6/2/2019 19:07	TO55-Tx03-B-L1-2019-06-02-0012.csv
Pass Abel	B	6/2/2019 20:27	TO55-Tx03-B-L2-2019-06-02-0013.csv
Pass Abel	B	6/2/2019 23:48	TO55-Tx03-B-L3-2019-06-02-0017.csv
Quatre Bayou Pass	A	5/20/2019 15:03	TO55-Tx04-A-L1-2019-05-20-0003.csv
Quatre Bayou Pass	A	5/20/2019 15:08	TO55-Tx04-A-L1-2019-05-20-0004.csv
Quatre Bayou Pass	A	5/20/2019 21:35	TO55-Tx04-A-L2-2019-05-20-0010.csv
Quatre Bayou Pass	B	5/20/2019 14:54	TO55-Tx04-B-L1-2019-05-20-0002.csv
Quatre Bayou Pass	B	5/20/2019 20:48	TO55-Tx04-B-L2-2019-05-20-0008.csv
Quatre Bayou Pass	C	5/20/2019 14:44	TO55-Tx04-C-L1-2019-05-20-0001.csv
Quatre Bayou Pass	C	5/20/2019 21:14	TO55-Tx04-C-L2-2019-05-20-0009.csv
Pass Ronquille	A	5/20/2019 15:25	TO55-Tx05-A-L1-2019-05-20-0005.csv
Pass Ronquille	A	5/20/2019 19:46	TO55-Tx05-A-L2-2019-05-20-0007.csv
Pass Ronquille	B	5/20/2019 15:45	TO55-Tx05-B-L1-2019-05-20-0006.csv
Bastian Pass	A	3/17/2019 20:14	TO55-Tx06-A-L1-2019-03-17-0023.csv
Bastian Pass	A	5/6/2019 15:21	TO55-Tx06-A-L1-2019-05-06-0047.csv
Bastian Pass	A	5/6/2019 19:53	TO55-Tx06-A-L3-2019-05-06-0055.csv
Bastian Pass	A	5/6/2019 20:38	TO55-Tx06-A-L4-2019-05-06-0059.csv
Bastian Pass	B	3/17/2019 19:50	TO55-Tx06-C-L1-2019-03-17-0021.csv
Bastian Pass	B	3/17/2019 20:02	TO55-Tx06-B-L1-2019-03-17-0022.csv

Inlet	Station	Date Time (UTC)	Processed Filename
Bastian Pass	B	5/6/2019 15:13	TO55-Tx06-B-L1-2019-05-06-0046.csv
Bastian Pass	B	5/6/2019 19:45	TO55-Tx06-B-L3-2019-05-06-0054.csv
Bastian Pass	B	5/6/2019 20:30	TO55-Tx06-B-L4-2019-05-06-0058.csv
Bastian Pass	C	5/6/2019 14:57	TO55-Tx06-C-L1-2019-05-06-0045.csv
Bastian Pass	C	5/6/2019 15:42	TO55-Tx06-C-L2-2019-05-06-0048.csv
Bastian Pass	C	5/6/2019 19:38	TO55-TxTx06C-L3-2019-05-06-0053.csv
Bastian Pass	C	5/6/2019 20:17	TO55-Tx06-C-L4-2019-05-06-0056.csv
Fontanelle Pass	A	3/17/2019 19:21	TO55-Tx07-A-L1-2019-03-17-0020.csv
Fontanelle Pass	A	5/5/2019 19:15	TO55-Tx07-A-L1-2019-05-05-0035.csv
Fontanelle Pass	A	5/6/2019 22:35	TO55-Tx07-A-L10-2019-05-06-0064.csv
Fontanelle Pass	A	3/17/2019 21:17	TO55-Tx07-A-L2-2019-03-17-0025.csv
Fontanelle Pass	A	5/5/2019 21:22	TO55-Tx07-A-L2-2019-05-05-0037.csv
Fontanelle Pass	A	3/17/2019 22:52	TO55-Tx07-A-L3-2019-03-17-0027.csv
Fontanelle Pass	A	5/5/2019 22:04	TO55-Tx07-A-L3-2019-05-05-0039.csv
Fontanelle Pass	A	5/5/2019 22:40	TO55-Tx07-A-L4-2019-05-05-0041.csv
Fontanelle Pass	A	5/6/2019 14:05	TO55-Tx07-A-L5-2019-05-06-0043.csv
Fontanelle Pass	A	5/6/2019 17:58	TO55-Tx07-A-L6-2019-05-06-0049.csv
Fontanelle Pass	A	5/6/2019 18:49	TO55-Tx07-A-L7-2019-05-06-0051.csv
Fontanelle Pass	A	5/6/2019 21:05	TO55-Tx07-A-L8-2019-05-06-0060.csv
Fontanelle Pass	A	5/6/2019 21:50	TO55-Tx07-A-L9-2019-05-06-0062.csv
Fontanelle Pass	B	3/17/2019 17:08	TO55-Tx07-B-L1-2019-03-17-0018.csv
Fontanelle Pass	B	5/5/2019 19:25	TO55-Tx07-B-L1-2019-05-05-0036.csv
Fontanelle Pass	B	5/6/2019 22:44	TO55-Tx07-B-L10-2019-05-06-0065.csv
Fontanelle Pass	B	3/17/2019 21:01	TO55-Tx07-B-L2-2019-03-17-0024.csv
Fontanelle Pass	B	5/5/2019 21:32	TO55-Tx07-B-L2-2019-05-05-0038.csv
Fontanelle Pass	B	3/17/2019 23:03	TO55-Tx07-B-L3-2019-03-17-0028.csv
Fontanelle Pass	B	5/5/2019 22:14	TO55-Tx07-B-L3-2019-05-05-0040.csv
Fontanelle Pass	B	5/5/2019 22:50	TO55-Tx07-B-L4-2019-05-05-0042.csv
Fontanelle Pass	B	5/6/2019 14:24	TO55-Tx07-B-L5-2019-05-06-0044.csv
Fontanelle Pass	B	5/6/2019 18:09	TO55-Tx07-B-L6-2019-05-06-0050.csv
Fontanelle Pass	B	5/6/2019 18:58	TO55-Tx07-B-L7-2019-05-06-0052.csv
Fontanelle Pass	B	5/6/2019 21:12	TO55-Tx07-B-L8-2019-05-06-0061.csv
Fontanelle Pass	B	5/6/2019 22:01	TO55-Tx07-B-L9-2019-05-06-0063.csv
Scofield Bayou	A	3/17/2019 22:09	TO55-Tx08-A-L1-2019-03-17-0026.csv
Scofield Bayou	A	6/14/2019 18:11	TO55-Tx08-A-L1-2019-06-14-0027.csv
Scofield Bayou	A	7/1/2019 18:38	TO55-Tx08-A-L1-2019-07-01-0031.csv
Bay Coquette	B	6/14/2019 19:07	TO55-Tx09-B-L1-2019-06-14-0029.csv

APPENDIX C: SUSPENDED SEDIMENT DATA LOG FROM TRANSECT SURVEYS – TSS AND LOI

Table A-C 1. Data log of TSS and LOI from suspended sediment samples at Caminada Pass. The “S” in the filename corresponds to the visit number for a given inlet, the “L” corresponds to the number of laps surveyed across a given inlet that were conducted in one day.

Sample Name	Date/Time (UTC)	Station	Fractional Depth	Total Depth (m)	Actual depth (m)	TSS (mg/L)	LOI (mg/L)	% Organic
Tx-01-A-TSS Surf	4/11/2019 22:08	A	0.1		Surface	19.47	7.70	39.56
Tx-01-A Surf	4/11/2019 23:35	A	0.1		Surface	23.45	5.63	24.02
Tx-01-B-TSS Surf (1)	4/11/2019 23:39	B	0.1		Surface	21.34	5.42	25.41
Tx-01-B-Tss Surf	4/11/2019 22:16	B	0.1		Surface	14.24	4.34	30.50
Tx-01-C-TSS Surf (2)	4/11/2019 22:16	C	0.1		Surface	12.90	4.90	37.98
T01C TSS Surf	4/11/2019 23:45	C	0.1		Surface	27.55	6.02	21.85
TO55-S2-L1-Tx-01-A-01	4/11/2019 18:33	A	0.1	4.5	0.45	19.25	6.63	34.44
TO55-S2-L1-Tx-01-A-05	4/11/2019 18:31	A	0.5	4.5	2.25	37.41	8.11	21.68
TO55-S2-L1-Tx-01-A-09	4/11/2019 18:29	A	0.9	4.5	4.05	45.09	8.41	18.66
TO55-S2-L1-Tx-01-B-01	4/11/2019 18:47	B	0.1	7.7	0.77	23.84	6.87	28.81
TO55-S2-L1-Tx-01-B-05	4/11/2019 18:45	B	0.5	7.7	3.85	29.78	7.31	24.55
TO55-S2-L1-Tx-01-B-09	4/11/2019 18:43	B	0.9	7.7	6.93	37.96	13.27	34.96
TO55-S2-L1-Tx-01-C-01	4/11/2019 18:59	C	0.1	5.2	0.52	25.44	6.15	24.19
TO55-S2-L1-Tx-01-C-05	4/11/2019 18:57	C	0.5	5.2	2.60	38.05	10.46	27.49
TO55-S1-L1-Tx-01-C-09	4/11/2019 18:55	C	0.9	5.5	4.95	43.56	10.12	23.24
TO55-S2-L2-Tx-01-A-01 Surface	4/11/2019 20:39	A	0.1		Surface	13.72	4.77	34.75
TO55-S2-L2-Tx-01-B-01 Surface	4/11/2019 20:41	B	0.1		Surface	18.93	7.30	38.54
TO55-S2-L2-TX-01-C01 Surface	4/11/2019 20:44	C	0.1		Surface	17.76	6.33	35.63

Table A-C 2. Data log of TSS and LOI from suspended sediment samples at Barataria Pass

Sample Name	Date/Time (UTC)	Station	Fractional Depth	Total Depth (m)	Actual depth (m)	TSS (mg/L)	LOI (mg/L)	% Organic
TO55-S1-L1-Tx-02-A-01	2/5/2019 16:50	A	0.1	3.0	0.30	17.37	9.58	55.17
TO55-S1-L1-Tx-02-A-05	2/5/2019 17:30	A	0.5	3.0	1.50	22.33	10.78	48.26
TO55-S1-L1-Tx-02-A-09	2/5/2019 17:33	A	0.9	3.0	2.70	12.86	6.38	49.58
TO55-S1-L1-Tx-02-B-01	2/5/2019 18:35	B	0.1	22.2	2.22	14.47	7.87	54.41
TO55-S1-L1-Tx-02-B-05	2/5/2019 18:42	B	0.5	22.2	11.10	16.14	8.43	52.24
TO55-S1-L1-Tx-02-B-09	2/5/2019 18:50	B	0.9	22.2	19.98	25.89	12.67	48.93
TO55-S1-L1-Tx-02-C-01	2/5/2019 19:20	C	0.1	11.4	1.14	16.94	8.63	50.97
TO55-S1-L1-Tx-02-C-05	2/5/2019 19:31	C	0.5	11.4	5.70	15.60	7.23	46.31
TO55-S1-L1-Tx-02-C-09	2/5/2019 19:50	C	0.9	11.4	10.26	21.88	9.27	42.35
TO55-S5-L1-Tx-02-A-01	6/3/2019 17:16	A	0.1	3.7	0.37	11.35	7.77	68.47
TO55-S5-L1-Tx-02-A-05	6/3/2019 17:15	A	0.5	3.7	1.85	14.21	6.71	47.18
TO55-S5-L1-Tx-02-A-09	6/3/2019 17:14	A	0.9	3.7	3.33	18.38	7.14	38.86
TO55-S5-L1-Tx-02-B-01	6/3/2019 17:39	B	0.1	22.6	2.26	10.20	6.24	61.22
TO55-S5-L1-Tx-02-B-05	6/3/2019 17:37	B	0.5	22.6	11.30	12.74	6.42	50.41
TO55-S5-L1-Tx-02-B-09	6/3/2019 17:35	B	0.9	22.6	20.34	19.37	7.23	37.30
TO55-S5-L1-Tx-02-C-01	6/3/2019 17:29	C	0.1	11.0	1.10	16.72	7.72	46.20
TO55-S5-L1-Tx-02-C-05	6/3/2019 17:28	C	0.5	11.0	5.50	37.33	11.46	30.70
TO55-S5-L1-Tx-02-C-09	6/3/2019 17:27	C	0.9	11.0	9.90	62.15	14.87	23.93
TO55-S5-L2-Tx-02-A-01	6/3/2019 19:51	A	0.1	3.9	0.39	11.79	5.85	49.57
TO55-S5-L2-Tx-02-A-05	6/3/2019 19:50	A	0.5	3.9	1.95	47.58	8.95	18.81
TO55-S5-L2-Tx-02-A-09	6/3/2019 19:49	A	0.9	3.9	3.51	160.00	16.18	10.11
TO55-S5-L2-Tx-02-B-01	6/3/2019 20:25	B	0.1	24.2	2.42	13.33	7.28	54.62
TO55-S5-L2-Tx-02-B-05	6/3/2019 20:13	B	0.5	24.2	12.10	58.49	12.32	21.07
TO55-S5-L2-Tx-02-B-09	6/3/2019 20:11	B	0.9	24.2	21.78	74.74	15.26	20.42
TO55-S5-L2-Tx-02-C-01	6/3/2019 20:04	C	0.1	13.1	1.31	38.22	10.68	27.95
TO55-S5-L2-Tx-02-C-05	6/3/2019 20:01	C	0.5	13.1	6.55	86.05	19.83	23.05
TO55-S5-L2-Tx-02-C-09	6/3/2019 19:58	C	0.9	13.1	11.79	N/D	N/D	N/D

Table A-C 3. Data log of TSS and LOI from suspended sediment samples at Pass Abel

Sample Name	Date/Time (UTC)	Station	Fractional Depth	Total Depth (m)	Actual depth (m)	TSS (mg/L)	LOI (mg/L)	% Organic
TO55-S5-L1-Tx-03-A-01	6/2/2019 18:55	A	0.1	8.3	0.83	14.30	6.80	47.55
TO55-S5-L1-Tx-03-A-05	6/2/2019 18:57	A	0.5	8.3	4.15	19.69	8.35	42.41
TO55-S5-L1-Tx-03-A-09	6/2/2019 18:59	A	0.9	8.3	7.47	59.90	14.35	23.95
TO55-S5-L1-Tx-03-B-01	6/2/2019 19:10	B	0.1	2.1	0.21	36.12	9.95	27.55
TO55-S5-L1-Tx-03-B-05	6/2/2019 19:09	B	0.5	2.1	1.05	100.51	23.38	23.27
TO55-S5-L2-Tx-03-A-01	6/2/2019 20:41	A	0.1	8.4	0.84	34.85	10.51	30.14
TO55-S5-L2-Tx-03-A-05	6/2/2019 20:39	A	0.5	8.4	4.20	33.00	10.13	30.70
TO55-S5-L2-Tx-03-A-09	6/2/2019 20:38	A	0.9	8.4	7.56	89.74	12.21	13.60
TO55-S5-L2-Tx-03-B-01	6/2/2019 20:30	B	0.1	2.1	0.21	42.10	10.12	24.05
TO55-S5-L2-Tx-03-B-05	6/2/2019 20:28	B	0.5	2.1	1.05	48.79	12.32	25.26
TO55-S5-L3-Tx-03-A-01	6/2/2019 23:40	A	0.1	8.4	0.84	34.24	8.93	26.07
TO55-S5-L3-Tx-03-A-05	6/2/2019 23:38	A	0.5	8.4	4.20	45.33	9.65	21.30
TO55-S5-L3-Tx-03-A-09	6/2/2019 23:37	A	0.9	8.4	7.56	79.38	15.46	19.48
TO55-S5-L3-Tx-03-B-01	6/2/2019 23:49	B	0.1	2.1	0.21	31.02	7.86	25.33
TO55-S5-L3-Tx-03-B-05	6/2/2019 23:49	B	0.5	2.1	1.05	55.66	9.29	16.70

Table A-C 4. Data log of TSS and LOI from suspended sediment samples at Quatre Bayou Pass

Sample Name	Date/Time (UTC)	Station	Fractional Depth	Total Depth (m)	Actual depth (m)	TSS (mg/L)	LOI (mg/L)	% Organic
TO55-S4-L1-Tx-04-A-01	5/20/2019 15:12	A	0.1	11.2	1.12	36.63	6.94	18.94
TO55-S4-L1-Tx-04-A-05	5/20/2019 15:11	A	0.5	11.2	5.60	35.79	6.84	19.12
TO55-S4-L1-Tx-04-A-09	5/20/2019 15:10	A	0.9	11.2	10.08	55.26	9.89	17.90
TO55-S4-L1-Tx-04-B-01	5/20/2019 14:58	B	0.1	3.1	0.31	29.49	5.10	17.30
TO55-S4-L1-Tx-04-B-05	5/20/2019 14:57	B	0.5	3.1	1.55	29.15	5.32	18.25
TO55-S4-L1-Tx-04-B-09	5/20/2019 14:56	B	0.9	3.1	2.79	36.31	6.26	17.23
TO55-S4-L1-Tx-04-C-01	5/20/2019 14:47	C	0.1	2.5	0.25	22.99	5.15	22.42
TO55-S4-L1-Tx-04-C-05	5/20/2019 14:46	C	0.5	2.5	1.25	86.46	13.23	15.30
TO55-S4-L1-Tx-04-C-09	5/20/2019 14:44	C	0.9	2.5	2.25	188.43	27.97	14.84
TO55-S4-L2-Tx-04-A-01	5/20/2019 21:46	A	0.1	5.4	0.54	38.52	9.12	23.68
TO55-S4-L2-Tx-04-A-05	5/20/2019 21:38	A	0.5	5.4	2.70	51.75	11.41	22.05
TO55-S4-L2-Tx-04-A-05	5/20/2019 21:38	A	0.5	5.4	2.70	52.15	10.99	21.08
TO55-S4-L2-Tx-04-A-09	5/20/2019 21:36	A	0.9	5.4	4.86	63.00	11.44	18.17
TO55-S4-L2-Tx-04-A-09	5/20/2019 21:36	A	0.9	5.4	4.86	72.42	9.68	13.37
TO55-S4-L2-Tx-04-B-01	5/20/2019 20:57	B	0.1	2.8	0.28	26.26	6.67	25.39
TO55-S4-L2-Tx-04-B-05	5/20/2019 20:54	B	0.5	2.8	1.40	50.17	10.17	20.28
TO55-S4-L2-Tx-04-B-09	5/20/2019 20:48	B	0.9	2.8	2.52	55.68	8.95	16.07
TO55-S4-L2-Tx-04-C-01	5/20/2019 21:18	C	0.1	2.5	0.25	97.90	13.01	13.29
TO55-S4-L2-Tx-04-C-05	5/20/2019 21:16	C	0.5	2.5	1.25	81.95	10.56	12.89
TO55-S4-L2-Tx-04-C-09	5/20/2019 21:14	C	0.9	2.5	2.25	121.73	14.59	11.99

Table A-C 5. Data log of TSS and LOI from suspended sediment samples at Pass Ronquille

Sample Name	Date/Time (UTC)	Station	Fractional Depth	Total Depth (m)	Actual depth (m)	TSS (mg/L)	LOI (mg/L)	% Organic
TO55-S4-L1-Tx-05-A-01	5/20/2019 15:28	A	0.1	3.2	0.32	23.65	5.21	22.03
TO55-S4-L1-Tx-05-A-05	5/20/2019 15:27	A	0.5	3.2	1.60	28.27	5.55	19.63
TO55-S4-L1-Tx-05-A-09	5/20/2019 15:26	A	0.9	3.2	2.88	27.17	5.86	21.56
TO55-S4-L1-Tx-05-B-01	5/20/2019 15:47	B	0.1	2.7	0.27	20.61	6.73	32.65
TO55-S4-L1-Tx-05-B-05	5/20/2019 15:46	B	0.5	2.7	1.35	33.64	8.51	25.30
TO55-S4-L1-Tx-05-B-09	5/20/2019 15:45	B	0.9	2.7	2.43	45.85	8.82	19.24
TO55-S4-L2-Tx-05-A-01	5/20/2019 19:48	A	0.1	3.1	0.31	37.65	7.81	20.74
TO55-S4-L2-Tx-05-A-05	5/20/2019 19:47	A	0.5	3.1	1.55	37.78	7.24	19.17
TO55-S4-L2-Tx-05-A-09	5/20/2019 19:46	A	0.9	3.1	2.79	58.66	8.71	14.86

Table A-C 6. Data log of TSS and LOI from suspended sediment samples at Bastian Pass

Sample Name	Date/Time (UTC)	Station	Fractional Depth	Total Depth (m)	Actual depth (m)	TSS (mg/L)	LOI (mg/L)	% Organic
TO55-S1-L1-Tx-06-A-01	3/17/2019 20:21	A	0.1	3.0	0.30	16.52	5.06	30.61
TO55-S1-L1-Tx-06-A-05	3/17/2019 20:19	A	0.5	3.0	1.50	17.87	4.41	24.68
TO55-S1-L1-Tx-06-A-09	3/17/2019 20:17	A	0.9	3.0	2.70	37.73	10.00	26.51
TO55-S1-L1-Tx-06-B-01	3/17/2019 20:09	B	0.1	3.4	0.34	7.05	2.84	40.32
TO55-S1-L1-Tx-06-B-05	3/17/2019 20:07	B	0.5	3.4	1.70	15.91	6.70	42.14
TO55-S1-L1-Tx-06-B-09	3/17/2019 20:03	B	0.9	3.4	3.06	9.33	3.03	32.53
TO55-S1-L1-Tx-06-C-01	3/17/2019 19:56	C	0.1	3.4	0.34	10.05	3.17	31.58
TO55-S1-L1-Tx-06-C-05	3/17/2019 19:53	C	0.5	3.4	1.70	5.74	3.30	57.41
TO55-S1-L1-Tx-06-C-09	3/17/2019 19:52	C	0.9	3.4	3.06	11.87	3.21	27.03
T055-S3-L1-Tx-06-A-01	5/6/2019 15:25	A	0.1	3.1	0.31	28.41	8.92	31.41
T055-S3-L1-Tx-06-A-05	5/6/2019 15:23	A	0.5	3.1	1.55	30.42	8.74	28.72
T055-S3-L1-Tx-06-A-09	5/6/2019 15:22	A	0.9	3.1	2.79	100.66	18.90	18.77
T055-S3-L1-Tx-06-B-01	5/6/2019 15:17	B	0.1	3.4	0.34	24.35	7.08	29.06
T055-S3-L1-Tx-06-B-05	5/6/2019 15:15	B	0.5	3.4	1.70	37.33	8.94	23.94
T055-S3-L1-Tx-06-B-09	5/6/2019 15:14	B	0.9	3.4	3.06	43.33	11.51	26.55
T055-S3-L1-Tx-06-C-01	5/6/2019 15:00	C	0.1	3.5	0.35	52.35	10.94	20.90
T055-S3-L1-Tx-06-C-05	5/6/2019 14:59	C	0.5	3.5	1.75	68.56	15.15	22.11
T055-S3-L1-Tx-06-C-09	5/6/2019 14:58	C	0.9	3.5	3.15	87.66	17.87	20.39
T055-S3-L2-Tx-06-C-01	5/6/2019 15:46	C	0.1	3.5	0.35	40.37	9.73	24.11
T055-S3-L2-Tx-06-C-05	5/6/2019 15:44	C	0.5	3.5	1.75	51.95	10.76	20.71
T055-S3-L2-Tx-06-C-09	5/6/2019 15:43	C	0.9	3.5	3.15	68.20	13.49	19.79
T055-S3-L3-Tx-06-A-01	5/6/2019 19:56	A	0.1	3.0	0.30	100.22	18.28	18.24
T055-S3-L3-Tx-06-A-05	5/6/2019 19:55	A	0.5	3.0	1.50	157.16	29.37	18.69
T055-S3-L3-Tx-06-A-09	5/6/2019 19:54	A	0.9	3.0	2.70	266.34	43.87	16.47
T055-S3-L3-Tx-06-B-01	5/6/2019 19:48	B	0.1	2.5	0.25	47.36	10.11	21.35
T055-S3-L3-Tx-06-B-05	5/6/2019 19:47	B	0.5	2.5	1.25	51.43	11.78	22.91
T055-S3-L3-Tx-06-B-09	5/6/2019 19:46	B	0.9	2.5	2.25	65.30	14.59	22.35

Sample Name	Date/Time (UTC)	Station	Fractional Depth	Total Depth (m)	Actual depth (m)	TSS (mg/L)	LOI (mg/L)	% Organic
T055-S3-L3-Tx-06-C-01	5/6/2019 19:41	C	0.1	2.7	0.27	120.84	24.40	20.19
T055-S3-L3-Tx-06-C-05	5/6/2019 19:40	C	0.5	2.7	1.35	125.79	23.16	18.41
T055-S3-L3-Tx-06-C-09	5/6/2019 19:39	C	0.9	2.7	2.43	156.60	29.87	19.07
T055-S3-L4-Tx-06-A-01	5/6/2019 20:41	A	0.1	2.9	0.29	119.79	20.95	17.49
T055-S3-L4-Tx-06-A-05	5/6/2019 20:40	A	0.5	2.9	1.45	140.00	22.30	15.93
T055-S3-L4-Tx-06-A-09	5/6/2019 20:39	A	0.9	2.9	2.61	249.84	42.86	17.15
T055-S3-L4-Tx-06-B-01	5/6/2019 20:33	B	0.1	3.2	0.32	56.00	12.11	21.62
T055-S3-L4-Tx-06-B-05	5/6/2019 20:32	B	0.5	3.2	1.60	67.70	14.76	21.80
T055-S3-L4-Tx-06-B-09	5/6/2019 20:31	B	0.9	3.2	2.88	100.11	19.16	19.14
T055-S3-L4-Tx-06-C-01	5/6/2019 20:20	C	0.1	3.2	0.32	87.16	16.95	19.44
T055-S3-L4-Tx-06-C-05	5/6/2019 20:19	C	0.5	3.2	1.60	97.84	19.31	19.74
T055-S3-L4-Tx-06-C-09	5/6/2019 20:18	C	0.9	3.2	2.88	117.81	21.77	18.48

Table A-C 7. Data log of TSS and LOI from suspended sediment samples at Fontanelle Pass

Sample Name	Date/Time (UTC)	Station	Fractional Depth	Total Depth (m)	Actual depth (m)	TSS (mg/L)	LOI (mg/L)	% Organic
TO55-S1-L1-Tx-07-A-01	3/17/2019 19:26	A	0.1	4.2	0.42	10.59	2.92	27.55
TO55-S1-L1-Tx-07-A-05	3/17/2019 19:24	A	0.5	4.2	2.10	20.32	4.84	23.83
TO55-S1-L1-Tx-07-A-09	3/17/2019 19:22	A	0.9	4.2	3.78	31.14	5.95	19.10
TO55-S1-L1-Tx-07-B-01	3/17/2019 17:47	B	0.1	3.5	0.35	18.38	5.51	30.00
TO55-S1-L1-Tx-07-B-01 (2)	3/17/2019 17:47	B	0.1	3.5	0.35	19.13	5.90	30.86
TO55-S1-L1-Tx-07-B-05	3/17/2019 17:42	B	0.5	3.5	1.75	21.05	5.93	28.18
TO55-S1-L1-Tx-07-B-09	3/17/2019 17:31	B	0.9	3.5	3.15	46.90	7.87	16.78
TO55-S1-L2-Tx-07-A-01	3/17/2019 21:15	A	0.1	4.1	0.41	10.31	4.32	41.94
TO55-S1-L2-Tx-07-A-05	3/17/2019 21:19	A	0.5	4.1	2.05	15.78	3.78	23.97
TO55-S1-L2-Tx-07-A-09	3/17/2019 21:17	A	0.9	4.1	3.69	31.31	6.51	20.80
TO55-S1-L2-Tx-07-B-01	3/17/2019 21:07	B	0.1	3.4	0.34	9.76	3.10	31.82
TO55-S1-L2-Tx-07-B-05	3/17/2019 21:05	B	0.5	3.4	1.70	28.94	7.60	26.25
TO55-S1-L2-Tx-07-B-09	3/17/2019 21:03	B	0.9	3.4	3.06	31.38	5.97	19.01
TO55-S1-L3-Tx-07-A-01	3/17/2019 22:58	A	0.1	4.0	0.40	8.76	3.14	35.80
TO55-S1-L3-Tx-07-A-05	3/17/2019 22:56	A	0.5	4.0	2.00	22.37	8.99	40.20
TO55-S1-L3-Tx-07-A-09	3/17/2019 22:54	A	0.9	4.0	3.60	19.01	5.27	27.75
TO55-S1-L3-Tx-07-B-01	3/17/2019 23:09	B	0.1	3.5	0.35	8.22	3.03	36.84
TO55-S1-L3-Tx-07-B-05	3/17/2019 23:07	B	0.5	3.5	1.75	12.62	3.32	26.27
TO55-S1-L3-Tx-07-B-09	3/17/2019 23:05	B	0.9	3.5	3.15	23.17	4.97	21.46
T055-S3-L1-Tx-07-A-01	5/5/2019 19:19	A	0.1	4.0	0.40	54.22	12.27	22.64
T055-S3-L1-Tx-07-A-05	5/5/2019 19:18	A	0.5	4.0	2.00	69.89	14.84	21.23
T055-S3-L1-Tx-07-A-09	5/5/2019 19:16	A	0.9	4.0	3.60	84.82	17.69	20.85
T055-S3-L1-Tx-07-B-01	5/5/2019 19:28	B	0.1	3.3	0.33	71.69	12.51	17.45
T055-S3-L1-Tx-07-B-05	5/5/2019 19:26	B	0.5	3.3	1.65	85.05	14.73	17.32
T055-S3-L1-Tx-07-B-09	5/5/2019 19:25	B	0.9	3.3	2.97	170.14	25.91	15.23
T055-S3-L2-Tx-07-A-01	5/5/2019 21:26	A	0.1	4.0	0.40	69.53	12.99	18.68
T055-S3-L2-Tx-07-A-05	5/5/2019 21:24	A	0.5	4.0	2.00	84.49	13.06	15.46

Sample Name	Date/Time (UTC)	Station	Fractional Depth	Total Depth (m)	Actual depth (m)	TSS (mg/L)	LOI (mg/L)	% Organic
T055-S3-L2-Tx-07-A-09	5/5/2019 21:23	A	0.9	4.0	3.60	108.82	19.28	17.72
T055-S3-L2-Tx-07-B-01	5/5/2019 21:36	B	0.1	3.4	0.34	78.53	13.19	16.80
T055-S3-L2-Tx-07-B-05	5/5/2019 21:34	B	0.5	3.4	1.70	78.77	13.54	17.19
T055-S3-L2-Tx-07-B-09	5/5/2019 21:33	B	0.9	3.4	3.06	105.81	17.13	16.18
T055-S3-L3-Tx-07-A-01	5/5/2019 22:08	A	0.1	4.0	0.40	67.28	12.92	19.21
T055-S3-L3-Tx-07-A-05	5/5/2019 22:06	A	0.5	4.0	2.00	95.57	16.24	17.00
T055-S3-L3-Tx-07-A-09	5/5/2019 22:05	A	0.9	4.0	3.60	109.33	17.95	16.42
T055-S3-L3-Tx-07-B-01	5/5/2019 22:18	B	0.1	3.2	0.32	69.03	13.13	19.02
T055-S3-L3-Tx-07-B-05	5/5/2019 22:16	B	0.5	3.2	1.60	87.96	15.18	17.26
T055-S3-L3-Tx-07-B-09	5/5/2019 22:15	B	0.9	3.2	2.88	121.03	19.90	16.44
T055-S3-L4-Tx-07-A-01	5/5/2019 22:43	A	0.1	3.8	0.38	76.08	14.44	18.98
T055-S3-L4-Tx-07-A-05	5/5/2019 22:41	A	0.5	3.8	1.90	84.93	16.68	19.65
T055-S3-L4-Tx-07-A-09	5/5/2019 22:40	A	0.9	3.8	3.42	122.57	22.36	18.24
T055-S3-L4-Tx-07-B-01	5/5/2019 22:53	B	0.1	2.3	0.23	88.06	16.67	18.93
T055-S3-L4-Tx-07-B-05	5/5/2019 22:52	B	0.5	2.3	1.15	101.18	19.04	18.82
T055-S3-L4-Tx-07-B-09	5/5/2019 22:51	B	0.9	2.3	2.07	112.81	20.52	18.19
T055-S3-L5-Tx-07-A-01	5/5/2019 14:09	A	0.1	4.1	0.41	80.63	15.39	19.09
T055-S3-L5-Tx-07-A-05	5/5/2019 14:07	A	0.5	4.1	2.05	93.06	17.14	18.42
T055-S3-L5-Tx-07-A-09	5/5/2019 14:06	A	0.9	4.1	3.69	286.46	43.49	15.18
T055-S3-L5-Tx-07-B-01	5/5/2019 14:28	B	0.1	3.4	0.34	14.47	5.64	38.97
T055-S3-L5-Tx-07-B-05	5/5/2019 14:27	B	0.5	3.4	1.70	10.83	4.38	40.38
T055-S3-L5-Tx-07-B-09	5/5/2019 14:25	B	0.9	3.4	3.06	88.54	16.04	18.12
T055-S3-L6-Tx-07-A-01	5/5/2019 18:01	A	0.1	3.9	0.39	43.99	9.28	21.10
T055-S3-L6-Tx-07-A-05	5/5/2019 17:59	A	0.5	3.9	1.95	45.00	9.13	20.29
T055-S3-L6-Tx-07-A-09	5/5/2019 17:58	A	0.9	3.9	3.51	82.00	13.26	16.17
T055-S3-L6-Tx-07-B-01	5/5/2019 18:12	B	0.1	3.5	0.35	42.84	8.22	19.19
T055-S3-L6-Tx-07-B-05	5/5/2019 18:11	B	0.5	3.5	1.75	52.42	9.05	17.27
T055-S3-L6-Tx-07-B-09	5/5/2019 18:10	B	0.9	3.5	3.15	51.91	10.60	20.42

Sample Name	Date/Time (UTC)	Station	Fractional Depth	Total Depth (m)	Actual depth (m)	TSS (mg/L)	LOI (mg/L)	% Organic
T055-S3-L7-Tx-07-A-01	5/5/2019 18:52	A	0.1	4.0	0.40	52.62	10.15	19.30
T055-S3-L7-Tx-07-A-05	5/5/2019 18:51	A	0.5	4.0	2.00	66.67	11.22	16.83
T055-S3-L7-Tx-07-A-09	5/5/2019 18:50	A	0.9	4.0	3.60	142.81	21.51	15.06
T055-S3-L7-Tx-07-B-01	5/5/2019 19:02	B	0.1	3.4	0.34	62.41	10.58	16.95
T055-S3-L7-Tx-07-B-05	5/5/2019 19:01	B	0.5	3.4	1.70	81.98	12.92	15.76
T055-S3-L7-Tx-07-B-09	5/5/2019 19:00	B	0.9	3.4	3.06	87.05	13.36	15.35
T055-S3-L8-Tx-07-A-01	5/5/2019 21:07	A	0.1	3.8	0.38	79.39	11.15	14.04
T055-S3-L8-Tx-07-A-05	5/5/2019 21:06	A	0.5	3.8	1.90	70.11	11.72	16.72
T055-S3-L8-Tx-07-A-09	5/5/2019 21:05	A	0.9	3.8	3.42	99.68	16.56	16.61
T055-S3-L8-Tx-07-B-01	5/5/2019 21:15	B	0.1	3.3	0.33	35.03	7.46	21.30
T055-S3-L8-Tx-07-B-05	5/5/2019 21:14	B	0.5	3.3	1.65	44.95	8.49	18.90
T055-S3-L8-Tx-07-B-09	5/5/2019 21:13	B	0.9	3.3	2.97	86.95	14.32	16.46
T055-S3-L9-Tx-07-A-01	5/5/2019 21:53	A	0.1	3.7	0.37	37.65	7.66	20.34
T055-S3-L9-Tx-07-A-05	5/5/2019 21:52	A	0.5	3.7	1.85	125.11	19.46	15.55
T055-S3-L9-Tx-07-A-09	5/5/2019 21:51	A	0.9	3.7	3.33	256.47	39.43	15.38
T055-S3-L9-Tx-07-B-01	5/5/2019 22:04	B	0.1	3.2	0.32	22.80	2.20	9.63
T055-S3-L9-Tx-07-B-05	5/5/2019 22:03	B	0.5	3.2	1.60	50.27	8.88	17.67
T055-S3-L9-Tx-07-B-09	5/5/2019 22:02	B	0.9	3.2	2.88	82.25	13.48	16.38
T055-S3-L10-Tx-07-A-01	5/5/2019 22:39	A	0.1	3.8	0.38	40.11	8.27	20.61
T055-S3-L10-Tx-07-A-05	5/5/2019 22:37	A	0.5	3.8	1.90	103.86	17.27	16.63
T055-S3-L10-Tx-07-A-09	5/5/2019 22:36	A	0.9	3.8	3.42	144.79	22.99	15.88
T055-S3-L10-Tx-07-B-01	5/5/2019 22:47	B	0.1	3.2	0.32	37.66	8.09	21.47
T055-S3-L10-Tx-07-B-05	5/5/2019 22:46	B	0.5	3.2	1.60	47.35	9.84	20.78
T055-S3-L10-Tx-07-B-09	5/5/2019 22:45	B	0.9	3.2	2.88	41.47	8.63	20.81

Table A-C 8. Data log of TSS and LOI from suspended sediment samples at Scofield Pass

Sample Name	Date/Time (UTC)	Station	Fractional Depth	Total Depth (m)	Actual depth (m)	TSS (mg/L)	LOI (mg/L)	% Organic
TO55-S1-L1-Tx-08-A-01	3/17/2019 22:15	A	0.1	2.5	0.25	16.61	2.96	17.83
TO55-S1-L1-Tx-08-A-05	3/17/2019 22:13	A	0.5	2.5	1.25	24.43	5.08	20.80
TO55-S1-L1-Tx-08-A-09	3/17/2019 22:11	A	0.9	2.5	2.25	28.85	5.79	20.08
TO55-S4-L1-Tx-08-A Surface	7/1/2019 18:45	A	0.1	2.0	0.20	22.98	5.43	23.61
TO55-S4-L1-Tx-08-A TD:2m, WD:1m	7/1/2019 18:43	A	0.5	2.0	1.00	47.98	9.89	20.62
TO55-S6-L1-Tx-08-A-01	6/14/2019 18:12	A	0.1	2.4	0.24	58.59	15.96	27.24
TO55-S6-L1-Tx-08-A-05	6/14/2019 18:11	A	0.5	2.4	1.20	55.83	15.83	28.35
TO55-S6-L1-Tx-08-A-09	6/14/2019 18:10	A	0.9	2.4	2.16	50.63	14.53	28.69

Table A-C 9. Data log of TSS and LOI from suspended sediment samples at Bay Coquette

Sample Name	Date/Time (UTC)	Station	Fractional Depth	Total Depth (m)	Actual depth (m)	TSS (mg/L)	LOI (mg/L)	% Organic
TO55-S6-L1-Tx-09-B-01	6/14/2019 19:10	B	0.1	1.9	0.19	34.38	10.31	30.00
TO55-S6-L1-Tx-09-B-05	6/14/2019 19:09	B	0.5	1.9	0.95	38.18	11.23	29.41
TO55-S6-L1-Tx-09-B-09	6/14/2019 19:08	B	0.9	1.9	1.71	36.42	10.72	29.43
TO55-S6-L2-Tx-09-A-01 Surface	6/14/2019 20:25	A	0.1		Surface	92.77	19.47	20.99
TO55-S6-L2-Tx-09-B-01 Surface	6/14/2019 20:12	B	0.1		Surface	48.37	13.57	28.06
TO55-S6-L3-Tx-09-A-01 Surface	6/14/2019 21:15	A	0.1		Surface	32.21	10.84	33.66
TO55-S6-L3-Tx-09-B-01 Surface	6/14/2019 21:20	B	0.1		Surface	38.38	11.99	31.23

APPENDIX D: SUSPENDED SEDIMENT DATA LOG FROM TRANSECT SURVEYS – TSS AND GRAIN SIZE

Table A-D 1. Data log of TSS and grain size from suspended sediment samples at Barataria Pass. Units for D10, D50, and D90 are in μm .

Sample Name	Date Time (UTC)	Station	Fraction Depth	Total Depth (m)	Actual Depth (m)	Average TSS (mg/L)	D10	D50	D90	Mode	Skew	Kurtosis
TO55-S1-L1-Tx-02-A-01	2/5/2019 16:50	A	0.1	3.0	0.30	11.49	3.70	10.70	36.10	9.36	4.04	22.67
TO55-S1-L1-Tx-02-A-05	2/5/2019 17:30	A	0.5	3.0	1.50	17.05	3.54	12.90	54.90	9.73	2.63	8.81
TO55-S1-L1-Tx-02-A-09	2/5/2019 17:33	A	0.9	3.0	2.70	12.43	3.99	11.90	44.20	10.00	3.65	16.85
TO55-S1-L1-Tx-02-B-01	2/5/2019 18:35	B	0.1	22.2	2.22	11.73	3.55	9.65	36.10	8.29	2.74	8.64
TO55-S1-L1-Tx-02-B-05	2/5/2019 18:42	B	0.5	22.2	11.10	18.35	3.32	9.39	27.80	8.59	2.21	7.35
TO55-S1-L1-Tx-02-B-09	2/5/2019 18:50	B	0.9	22.2	19.98	16.01	3.63	11.90	47.10	9.49	2.20	5.41
TO55-S1-L1-Tx-02-C-01	2/5/2019 19:20	C	0.1	11.4	1.14	15.43	4.30	19.00	90.90	16.30	4.77	25.18
TO55-S1-L1-Tx-02-C-05	2/5/2019 19:31	C	0.5	11.4	5.70	14.53	4.26	15.70	82.90	10.80	4.97	26.56
TO55-S1-L1-Tx-02-C-09	2/5/2019 19:50	C	0.9	11.4	10.26	19.58	4.43	20.20	88.00	26.80	5.93	47.00
TO55-S5-L2-Tx-02-A-01	6/3/2019 19:51	A	0.1	3.9	0.39	14.40	2.66	17.73	95.00	35.83	1.91	4.46
TO55-S5-L2-Tx-02-A-05	6/3/2019 19:50	A	0.5	3.9	1.95	31.71	2.95	9.63	35.43	8.72	3.50	21.25
TO55-S5-L2-Tx-02-A-09	6/3/2019 19:49	A	0.9	3.9	3.51	141.76	3.56	14.97	59.47	18.13	3.07	13.12
TO55-S5-L2-Tx-02-B-01	6/3/2019 20:25	B	0.1	24.2	2.42	13.33	4.22	35.63	148.67	111.33	1.20	0.82
TO55-S5-L2-Tx-02-B-05	6/3/2019 20:13	B	0.5	24.2	12.10	64.98	2.61	9.10	43.63	6.39	3.39	17.00
TO55-S5-L2-Tx-02-B-09	6/3/2019 20:11	B	0.9	24.2	21.78	82.39	3.64	17.07	68.43	22.97	3.32	16.36
TO55-S5-L2-Tx-02-C-01	6/3/2019 20:04	C	0.1	13.1	1.31	38.01	3.36	18.37	64.97	28.97	4.16	32.44
TO55-S5-L2-Tx-02-C-05	6/3/2019 20:01	C	0.5	13.1	6.55	124.57	3.09	14.97	72.63	24.25	1.73	3.62
TO55-S5-L2-Tx-02-C-09	6/3/2019 19:58	C	0.9	13.1	11.79	59.18	3.33	22.07	97.90	35.17	2.67	11.74
TURB TO55-Tx-02D	N/D				Surface	156.71	2.34	10.80	44.40	13.00	10.74	145.90

Table A-D 2. Data log of TSS and grain size from suspended sediment samples at Quatre Bayou Pass. Units for D10, D50, and D90 are in μm .

Sample Name	Date Time (UTC)	Station	Fraction Depth	Total Depth (m)	Actual Depth (m)	Average TSS (mg/L)	D10	D50	D90	Mode	Skew	Kurtosis
TO55-S4-L2-Tx-04-A-01	5/20/2019 21:46	A	0.1	5.4	0.54	44.08	2.32	10.15	49.05	9.57	3.56	17.09
TO55-S4-L2-Tx-04-A-05	5/20/2019 21:38	A	0.5	5.4	2.70	54.25	2.44	7.86	39.43	5.69	3.69	28.68
TO55-S4-L2-Tx-04-A-09	5/20/2019 21:36	A	0.9	5.4	4.86	59.80	2.48	8.68	48.90	5.66	2.70	9.11
TO55-S4-L2-Tx-04-B-01	5/20/2019 20:57	B	0.1	2.8	0.28	29.28	2.83	10.80	59.65	7.09	2.27	5.90
TO55-S4-L2-Tx-04-B-05	5/20/2019 20:54	B	0.5	2.8	1.40	51.86	3.01	11.23	54.83	7.27	1.89	3.58
TO55-S4-L2-Tx-04-B-09	5/20/2019 20:48	B	0.9	2.8	2.52	45.85	2.76	14.87	79.00	43.83	1.43	1.44
TO55-S5-L2-Tx-04-B-09 (3)	5/20/2019 20:48	B	0.9	2.8	2.52	56.38	3.09	15.73	62.78	26.18	2.27	7.72
TO55-S4-L2-Tx-04-C-01	5/20/2019 21:18	C	0.1	2.5	0.25	91.26	3.20	16.93	83.47	26.75	1.65	2.49
TO55-S4-L2-Tx-04-C-05	5/20/2019 21:16	C	0.5	2.5	1.25	91.93	2.52	13.23	65.53	18.05	2.32	7.02
TO55-S4-L2-Tx-04-C-09	5/20/2019 21:14	C	0.9	2.5	2.25	148.86	2.56	13.70	65.87	16.42	2.03	4.58

Table A-D 3. Data log of TSS and grain size from suspended sediment samples at Fontanelle Pass. Units for D10, D50, and D90 are in μm .

Sample Name	Date Time (UTC)	Station	Fraction Depth	Total Depth (m)	Actual Depth (m)	Average TSS (mg/L)	D10	D50	D90	Mode	Skew	Kurtosis
TO55-S1-L1-Tx-07-B-01	3/17/2019 17:47	B	0.1	3.5	0.35	15.03	2.51	7.96	29.30	7.04	3.07	11.92
TO55-S1-L1-Tx-07-B-05	3/17/2019 17:42	B	0.5	3.5	1.75	21.26	1.97	6.38	15.80	10.40	0.89	0.11
TO55-S1-L1-Tx-07-B-09	3/17/2019 17:31	B	0.9	3.5	3.15	50.36	2.15	8.21	34.60	6.60	3.02	11.22
TURB TO55-Tx-07-WS (451out)	3/12/2019 17:30			Surface		21.00	3.04	9.92	32.10	10.40	2.36	6.88

APPENDIX E: WATER SAMPLE DATA LOG FROM TRANSECT SURVEYS – NUTRIENTS

Table A-E 1. Data log of water samples from transect surveys collected for nutrients.

Inlet	Station	Fractional #	Replicate	Date Time (UTC)	Unfiltered (organic + inorganics)	Filtered (inorganics only)	SiO ₄ -Si
					TN/TP	NH ₄ -N / NO ₃ +NO ₂ -N / PO ₄ -P	
Tx-02	B	0.1	A	6/3/2019 17:39	S5-Tx-02-B-01-A-TNTP	S5-Tx-02-B-01-A-NP	S5-Tx-02-B-01-A-Si
Tx-02	B	0.1	B	6/3/2019 17:39	S5-Tx-02-B-01-B-TNTP	S5-Tx-02-B-01-B-NP	S5-Tx-02-B-01-B-Si
Tx-02	B	0.1	C	6/3/2019 17:39	S5-Tx-02-B-01-C-TNTP	S5-Tx-02-B-01-C-NP	S5-Tx-02-B-01-C-Si
Tx-02	B	0.5	A	6/3/2019 17:37	S5-Tx-02-B-05-A-TNTP	S5-Tx-02-B-05-A-NP	S5-Tx-02-B-05-A-Si
Tx-02	B	0.5	B	6/3/2019 17:37	S5-Tx-02-B-05-B-TNTP	S5-Tx-02-B-05-B-NP	S5-Tx-02-B-05-B-Si
Tx-02	B	0.5	C	6/3/2019 17:37	S5-Tx-02-B-05-C-TNTP	S5-Tx-02-B-05-C-NP	S5-Tx-02-B-05-C-Si
Tx-02	B	0.9	A	6/3/2019 17:35	S5-Tx-02-B-09-A-TNTP	S5-Tx-02-B-09-A-NP	S5-Tx-02-B-09-A-Si
Tx-02	B	0.9	B	6/3/2019 17:35	S5-Tx-02-B-09-B-TNTP	S5-Tx-02-B-09-B-NP	S5-Tx-02-B-09-B-Si
Tx-02	B	0.9	C	6/3/2019 17:35	S5-Tx-02-B-09-C-TNTP	S5-Tx-02-B-09-C-NP	S5-Tx-02-B-09-C-Si
Tx-04	B	0.1	A	5/20/2019 20:57	S4-Tx-04-B-01-A-TNTP	S4-Tx-04-B-01-A-NP	S4-Tx-04-B-01-A-Si
Tx-04	B	0.1	B	5/20/2019 20:57	S4-Tx-04-B-01-B-TNTP	S4-Tx-04-B-01-B-NP	S4-Tx-04-B-01-B-Si
Tx-04	B	0.1	C	5/20/2019 20:57	S4-Tx-04-B-01-C-TNTP	S4-Tx-04-B-01-C-NP	S4-Tx-04-B-01-C-Si
Tx-04	B	0.5	A	5/20/2019 20:54	S4-Tx-04-B-05-A-TNTP	S4-Tx-04-B-05-A-NP	S4-Tx-04-B-05-A-Si
Tx-04	B	0.5	B	5/20/2019 20:54	S4-Tx-04-B-05-B-TNTP	S4-Tx-04-B-05-B-NP	S4-Tx-04-B-05-B-Si
Tx-04	B	0.5	C	5/20/2019 20:54	S4-Tx-04-B-05-C-TNTP	S4-Tx-04-B-05-C-NP	S4-Tx-04-B-05-C-Si
Tx-04	B	0.9	A	5/20/2019 20:48	S4-Tx-04-B-09-A-TNTP	S4-Tx-04-B-09-A-NP	S4-Tx-04-B-09-A-Si
Tx-04	B	0.9	B	5/20/2019 20:48	S4-Tx-04-B-09-B-TNTP	S4-Tx-04-B-09-B-NP	S4-Tx-04-B-09-B-Si
Tx-04	B	0.9	C	5/20/2019 20:48	S4-Tx-04-B-09-C-TNTP	S4-Tx-04-B-09-C-NP	S4-Tx-04-B-09-C-Si
Tx-07	B	0.1	A	3/17/2019 18:50	S1-Tx-07-B-01-A-TNTP	S1-Tx-07-B-01-A-NP	S1-Tx-07-B-01-A-Si
Tx-07	B	0.1	B	3/17/2019 18:50	S1-Tx-07-B-01-B-TNTP	S1-Tx-07-B-01-B-NP	S1-Tx-07-B-01-B-Si
Tx-07	B	0.1	C	3/17/2019 18:50	S1-Tx-07-B-01-C-TNTP	S1-Tx-07-B-01-C-NP	S1-Tx-07-B-01-C-Si
Tx-07	B	0.5	A	3/17/2019 18:40	S1-Tx-07-B-05-A-TNTP	S1-Tx-07-B-05-A-NP	S1-Tx-07-B-05-A-Si
Tx-07	B	0.5	B	3/17/2019 18:40	S1-Tx-07-B-05-B-TNTP	S1-Tx-07-B-05-B-NP	S1-Tx-07-B-05-B-Si

Inlet	Station	Fractional Depth	Replicate	Date Time (UTC)	Unfiltered (organic + inorganics)		Filtered (inorganics only)	
					#	TN/TP	NH ₄ -N / NO ₃ +NO ₂ -N / PO ₄ -P	SiO ₄ -Si
Tx-07	B	0.5	C	3/17/2019 18:40	S1-Tx-07-B-05-C-TNTP		S1-Tx-07-B-05-C-NP	S1-Tx-07-B-05-C-Si
Tx-07	B	0.9	A	3/17/2019 18:30	S1-Tx-07-B-09-A-TNTP		S1-Tx-07-B-09-A-NP	S1-Tx-07-B-09-A-Si
Tx-07	B	0.9	B	3/17/2019 18:30	S1-Tx-07-B-09-B-TNTP		S1-Tx-07-B-09-B-NP	S1-Tx-07-B-09-B-Si
Tx-07	B	0.9	C	3/17/2019 18:30	S1-Tx-07-B-09-C-TNTP		S1-Tx-07-B-09-C-NP	S1-Tx-07-B-09-C-Si

APPENDIX F: RTK POINTS DATA LOG

Table A-F 1. RTK points collected at the Tx-02 fixed instrumented site. The “code” column is intended for the user to provide a keyword for the position of the bottom of the pole, where “WL” corresponds to water level, “pole top” corresponds to top of the instrument track pole, “vbeam” corresponds to the vertical beam of the SL-500, and “xbar” corresponds to a crossbar on the platform the instrument was attached to.

Point Name	Date Time (UTC)	Northing	Easting	Elevation	Code
Tx02D-01	1/15/2019 22:44	3242087.535	796685.619	0.188	WL
Tx02D-02	1/15/2019 22:44	3242087.526	796685.624	0.187	WL
Tx02D-03	1/15/2019 22:44	3242087.521	796685.626	0.183	WL
Tx02D-04	1/15/2019 22:44	3242087.525	796685.624	0.185	WL
Tx02D-05	1/15/2019 22:44	3242087.522	796685.621	0.181	WL
Tx02D-06	1/15/2019 22:45	3242087.527	796685.618	0.175	WL
Tx02D-07	1/15/2019 22:45	3242087.523	796685.624	0.177	WL
Tx02D-08	1/15/2019 22:45	3242087.513	796685.629	0.162	WL
Tx02D-09	1/15/2019 22:45	3242087.519	796685.624	0.187	WL
Tx02D-10	1/15/2019 22:45	3242087.53	796685.624	0.191	WL
Tx02D-11	1/15/2019 22:45	3242087.025	796685.846	1.721	pole top
Tx02D-12	1/15/2019 22:46	3242087.011	796685.829	1.719	pole top
Tx02D-13	1/15/2019 22:46	3242087.043	796685.832	1.745	pole top
Tx02D-14	1/15/2019 22:46	3242087.035	796685.826	1.725	pole top
Tx02D-15	1/15/2019 22:46	3242087.003	796685.821	1.715	pole top
Tx02D-16	2/24/2019 21:34	3242085.94	796685.32	-0.557	vbeam
Tx02D-17	2/24/2019 21:34	3242085.974	796685.333	-0.604	vbeam
Tx02D-18	2/24/2019 21:34	3242085.975	796685.332	-0.596	vbeam
Tx02D-19	2/24/2019 21:34	3242085.977	796685.346	-0.605	vbeam
Tx02D-20	2/24/2019 21:34	3242085.965	796685.345	-0.610	vbeam
Tx02D-21	2/24/2019 21:34	3242085.97	796685.365	-0.555	vbeam
Tx02D-22	2/24/2019 21:35	3242085.23	796685.092	0.080	wl
Tx02D-23	2/24/2019 21:35	3242085.495	796685.05	0.008	wl
Tx02D-24	2/24/2019 21:35	3242085.44	796685.044	-0.019	wl
Tx02D-25	2/24/2019 21:35	3242085.482	796684.998	0.054	wl
Tx02D-26	2/24/2019 21:35	3242085.486	796684.958	0.012	wl
Tx02D-27	2/24/2019 21:35	3242085.389	796685.037	0.021	wl
Tx02D-30	4/10/2019 20:34	3242091.049	796683.094	0.348	wl
Tx02D-31	4/10/2019 20:34	3242090.789	796683.054	0.331	wl
Tx02D-32	4/10/2019 20:34	3242090.82	796683.024	0.340	wl
Tx02D-33	4/10/2019 20:34	3242090.736	796682.948	0.314	wl
Tx02D-34	4/10/2019 20:34	3242090.811	796682.948	0.352	wl
Tx02D-35	4/10/2019 20:34	3242090.861	796682.934	0.336	wl
Tx02D-36	4/10/2019 20:34	3242090.972	796682.904	0.342	wl

Point Name	Date Time (UTC)	Northing	Easting	Elevation	Code
Tx02D-37	4/10/2019 20:34	3242091.077	796682.935	0.328	wl
Tx02D-38	4/10/2019 20:34	3242091.262	796682.96	0.339	wl
Tx02D-39	4/10/2019 20:34	3242091.219	796683	0.341	wl
Tx02D-40	4/10/2019 20:35	3242091.379	796683.075	0.325	wl
Tx02D-41	4/28/2019 18:30	3242087.198	796685.571	0.159	wl
Tx02D-42	4/28/2019 18:30	3242087.206	796685.586	0.180	wl
Tx02D-43	4/28/2019 18:30	3242087.239	796685.537	0.194	wl
Tx02D-44	4/28/2019 18:30	3242087.234	796685.526	0.205	wl
Tx02D-45	4/28/2019 18:30	3242087.261	796685.525	0.260	wl
Tx02D-46	4/28/2019 18:30	3242087.233	796685.54	0.213	wl
Tx02D-47	4/28/2019 18:30	3242087.213	796685.554	0.250	wl
Tx02D-48	4/28/2019 18:30	3242087.249	796685.503	0.211	wl
Tx02D-49	4/28/2019 18:30	3242087.246	796685.529	0.191	wl
Tx02D-50	4/28/2019 18:30	3242087.268	796685.559	0.258	wl
Tx02D-51	4/28/2019 19:47	3242086.995	796685.65	1.054	xbar
Tx02D-52	4/28/2019 19:47	3242086.966	796685.668	1.040	xbar
Tx02D-53	4/28/2019 19:48	3242086.944	796685.678	1.050	xbar
Tx02D-54	4/28/2019 19:48	3242087.03	796685.624	1.044	xbar
Tx02D-55	4/28/2019 19:48	3242086.928	796685.643	1.091	xbar
Tx02D-56	4/28/2019 19:48	3242086.944	796685.621	1.037	xbar
Tx02D-57	4/28/2019 19:48	3242086.973	796685.599	1.058	xbar
Tx02D-58	4/28/2019 19:48	3242086.972	796685.564	1.059	xbar
Tx02D-59	4/28/2019 19:48	3242086.99	796685.557	1.047	xbar
Tx02D-60	4/28/2019 19:48	3242086.966	796685.605	1.019	xbar
Tx02-60	5/20/2019 13:22	3241250.924	795204.289	0.421	marina wl
Tx02-61	5/20/2019 13:22	3241250.972	795204.185	0.411	marina wl
Tx02-62	5/20/2019 13:22	3241250.987	795204.077	0.416	marina wl
Tx02-63	5/20/2019 13:22	3241250.993	795203.808	0.431	marina wl
Tx02-64	5/20/2019 13:22	3241250.993	795203.696	0.405	marina wl
Tx02-65	5/20/2019 13:30	3242097.089	796657.684	0.402	station wl
Tx02-66	5/20/2019 13:30	3242096.846	796658.398	0.431	station wl
Tx02-67	5/20/2019 13:30	3242096.69	796658.563	0.412	station wl
Tx02-68	5/20/2019 13:30	3242096.734	796658.679	0.480	station wl
Tx02-69	5/20/2019 13:30	3242096.802	796658.893	0.463	station wl
Tx02-70	5/20/2019 13:30	3242096.832	796658.958	0.428	station wl
Tx02-D-71	9/5/2019 15:34	3242088.156	796689.708	0.053	WL
Tx02-D-72	9/5/2019 15:34	3242088.184	796689.898	0.125	WL
Tx02-D-73	9/5/2019 15:34	3242088.159	796689.76	0.078	WL
Tx02-D-74	9/5/2019 15:34	3242088.045	796689.823	0.075	WL
Tx02-D-75	9/5/2019 15:34	3242087.992	796689.927	0.120	WL

Point Name	Date Time (UTC)	Northing	Easting	Elevation	Code
Tx02-D-76	9/5/2019 15:34	3242088.093	796689.814	0.077	WL
Tx02-D-77	9/5/2019 15:34	3242088.03	796689.909	0.065	WL
Tx02-D-78	9/5/2019 15:34	3242087.875	796689.928	0.075	WL
Tx02-D-79	9/5/2019 15:34	3242088.031	796689.826	0.140	WL
Tx02-D-80	9/5/2019 15:34	3242087.893	796689.96	0.148	WL
Tx02D-81	9/17/2019 23:05	3242062.919	796718.961	0.259	wl
Tx02D-82	9/17/2019 23:05	3242062.779	796719.503	0.261	wl
Tx02D-83	9/17/2019 23:05	3242062.743	796719.419	0.234	wl
Tx02D-84	9/17/2019 23:05	3242063.034	796719.353	0.312	wl
Tx02D-85	9/17/2019 23:05	3242063.028	796719.333	0.122	wl
Tx02D-86	9/17/2019 23:05	3242062.73	796719.565	0.246	wl
Tx02D-87	9/17/2019 23:05	3242062.811	796719.456	0.268	wl
Tx02D-88	9/17/2019 23:05	3242062.893	796719.398	0.355	wl
Tx02D-89	9/17/2019 23:05	3242062.876	796719.533	0.277	wl
Tx02D-90	9/17/2019 23:05	3242062.938	796719.453	0.400	wl
Tx02D-91	9/25/2019 19:23	3242086.01	796687.478	0.290	WL
Tx02D-92	9/25/2019 19:23	3242086.009	796687.479	0.294	WL
Tx02D-93	9/25/2019 19:23	3242086.009	796687.482	0.294	WL
Tx02D-94	9/25/2019 19:23	3242086.01	796687.482	0.289	WL
Tx02D-95	9/25/2019 19:23	3242086.011	796687.478	0.281	WL
Tx02D-96	9/25/2019 19:23	3242086.016	796687.479	0.288	WL
Tx02D-97	9/25/2019 19:23	3242086.004	796687.477	0.290	WL
Tx02D-98	9/25/2019 19:23	3242086.006	796687.479	0.276	WL
Tx02D-99	9/25/2019 19:23	3242086.001	796687.483	0.272	WL
Tx02D-100	9/25/2019 19:23	3242086.008	796687.464	0.260	WL
Tx02D-101	9/25/2019 21:05	3242060.744	796664.115	0.153	WL
Tx02D-102	9/25/2019 21:05	3242060.744	796663.935	0.164	WL
Tx02D-103	9/25/2019 21:05	3242060.812	796663.797	0.199	WL
Tx02D-104	9/25/2019 21:05	3242060.294	796661.699	0.156	WL
Tx02D-105	9/25/2019 21:05	3242060.176	796661.418	0.123	WL
Tx02D-106	9/25/2019 21:05	3242060.019	796661.09	0.169	WL
Tx02D-107	9/25/2019 21:05	3242060.076	796660.761	0.196	WL
Tx02D-108	9/25/2019 21:05	3242060.09	796660.644	0.183	WL
Tx02D-109	9/25/2019 21:05	3242059.998	796660.43	0.080	WL
Tx02D-110	9/25/2019 21:05	3242059.811	796660.335	0.101	WL
Tx02D-111	9/25/2019 21:05	3242059.849	796660.035	0.169	WL
Tx02D-112	9/25/2019 21:05	3242059.893	796659.741	0.194	WL

Table A-F 2. RTK points collected at the Tx-04 fixed instrumented site

Point Name	Date Time (UTC)	Northing	Easting	Elevation	Code
Tx04D-01	1/16/2019 21:56	3246695.367	805038.94	0.075	WL
Tx04D-02	1/16/2019 21:56	3246695.439	805039.012	0.106	WL
Tx04D-03	1/16/2019 21:56	3246695.408	805039.005	0.089	WL
Tx04D-04	1/16/2019 21:56	3246695.449	805039.029	0.092	WL
Tx04D-05	1/16/2019 21:56	3246695.396	805039.046	0.097	WL
Tx04D-06	1/16/2019 21:56	3246695.408	805039.028	0.105	WL
Tx04D-07	1/16/2019 21:56	3246695.346	805038.996	0.101	WL
Tx04D-08	1/16/2019 21:56	3246695.413	805038.964	0.129	WL
Tx04D-09	1/16/2019 21:56	3246695.417	805038.981	0.105	WL
Tx04D-10	1/16/2019 21:56	3246695.355	805038.883	0.060	WL
Tx04D2-01	3/22/2019 21:07	3246719.132	805027.94	0.078	wl 2106gmt
Tx04D2-02	3/22/2019 21:07	3246719.146	805027.923	-0.007	wl 2106gmt
Tx04D2-03	3/22/2019 21:07	3246719.133	805027.942	0.075	wl 2106gmt
Tx04D2-04	3/22/2019 21:07	3246719.12	805027.953	0.041	wl 2106gmt
Tx04D2-05	3/22/2019 21:08	3246719.125	805027.999	0.029	wl 2106gmt
Tx04D2-06	3/22/2019 21:08	3246719.161	805027.989	-0.012	wl 2106gmt
Tx04D2-07	3/22/2019 21:08	3246719.174	805028.005	0.003	wl 2106gmt
Tx04D2-08	3/22/2019 21:08	3246719.173	805027.956	0.075	wl 2106gmt
Tx04D2-09	3/22/2019 21:08	3246719.167	805027.974	0.067	wl 2106gmt
Tx04D2-10	3/22/2019 21:08	3246719.129	805027.982	0.086	wl 2106gmt
Tx04D-20	4/28/2019 17:55	3246798.244	805062.551	0.122	wl
Tx04D-21	4/28/2019 17:55	3246798.347	805062.246	0.183	wl
Tx04D-22	4/28/2019 17:55	3246798.499	805061.983	0.240	wl
Tx04D-23	4/28/2019 17:55	3246798.654	805061.687	0.223	wl
Tx04D-24	4/28/2019 17:55	3246798.821	805061.382	0.182	wl
Tx04D-25	4/28/2019 17:55	3246798.94	805061.107	0.216	wl
Tx04D-26	4/28/2019 17:55	3246799.714	805059.636	0.231	wl
Tx04D-27	4/28/2019 17:55	3246799.897	805059.368	0.227	wl
Tx04D-28	4/28/2019 17:55	3246800.048	805059.101	0.238	wl
Tx04D-29	4/28/2019 17:55	3246800.587	805058.1	0.271	wl
Tx04D-30	4/28/2019 17:55	3246800.761	805057.823	0.248	wl

Table A-F 3. RTK points collected at the Tx-07 fixed instrumented site

Point Name	Date Time (UTC)	Northing	Easting	Elevation	Code
Tx07D-01	1/11/2019 21:18	3241377.866	829931.316	0.022	WL2117gmt
Tx07D-02	1/11/2019 21:18	3241377.845	829931.324	0.018	WL2117gmt
Tx07D-03	1/11/2019 21:18	3241377.869	829931.33	0.013	WL2117gmt
Tx07D-04	1/11/2019 21:18	3241377.867	829931.356	0.013	WL2117gmt
Tx07D-05	1/11/2019 21:18	3241377.899	829931.356	0.012	WL2117gmt
Tx07D-06	1/11/2019 21:18	3241377.888	829931.358	0.031	WL2117gmt
Tx07D-07	1/11/2019 21:18	3241377.882	829931.361	0.028	WL2117gmt
Tx07D-08	1/11/2019 21:18	3241377.865	829931.373	0.029	WL2117gmt
Tx07D-10	1/26/2019 20:21	3241375.103	829931.846	-0.033	wl2019gmt
Tx07D-11	1/26/2019 20:21	3241375.077	829931.749	-0.083	wl2019gmt
Tx07D-12	1/26/2019 20:21	3241375.225	829931.82	-0.138	wl2019gmt
Tx07D-13	1/26/2019 20:21	3241375.127	829931.805	-0.079	wl2019gmt
Tx07D-14	1/26/2019 20:21	3241375.254	829931.736	-0.065	wl2019gmt
Tx07-15	3/12/2019 19:52	3241377.282	829930.689	0.162	wl
Tx07-16	3/12/2019 19:52	3241377.315	829930.606	0.168	wl
Tx07-17	3/12/2019 19:52	3241377.289	829930.617	0.163	wl
Tx07-18	3/12/2019 19:52	3241377.243	829930.618	0.152	wl
Tx07-19	3/12/2019 19:52	3241377.224	829930.585	0.136	wl
Tx07-20	3/12/2019 19:52	3241377.198	829930.581	0.108	wl
Tx07-21	3/12/2019 19:52	3241377.503	829930.722	-1.154	vbeam
Tx07-22	3/12/2019 19:52	3241377.513	829930.716	-1.144	vbeam
Tx07-23	3/12/2019 19:52	3241377.498	829930.718	-1.173	vbeam
Tx07-24	3/12/2019 19:52	3241377.499	829930.733	-1.178	vbeam
Tx07-25	3/12/2019 19:52	3241377.509	829930.721	-1.176	vbeam
Tx07D-55	5/5/2019 22:25	3241373.494	829930.177	-0.040	WL2225gmt
Tx07D-56	5/5/2019 22:25	3241373.467	829930.17	-0.048	WL2225gmt
Tx07D-57	5/5/2019 22:25	3241373.454	829930.177	-0.043	WL2225gmt
Tx07D-58	5/5/2019 22:25	3241373.484	829930.15	-0.040	WL2225gmt
Tx07D-59	5/5/2019 22:25	3241373.475	829930.118	-0.061	WL2225gmt
Tx07-60	7/18/2019 20:33	3241377.498	829931.407	0.247	WL
Tx07-61	7/18/2019 20:33	3241377.504	829931.411	0.227	WL
Tx07-62	7/18/2019 20:33	3241377.455	829931.456	0.236	WL
Tx07-63	7/18/2019 20:33	3241377.436	829931.456	0.224	WL
Tx07-64	7/18/2019 20:33	3241377.477	829931.406	0.207	WL
Tx07-65	7/18/2019 20:33	3241377.456	829931.396	0.245	WL
Tx07-66	7/18/2019 20:33	3241377.439	829931.365	0.214	WL
Tx07-67	7/18/2019 20:33	3241377.406	829931.417	0.229	WL
Tx07-68	7/18/2019 20:33	3241377.371	829931.47	0.223	WL
Tx07-69	7/18/2019 20:33	3241377.332	829931.5	0.208	WL
Tx07-70	7/18/2019 20:33	3241377.413	829931.432	0.180	WL

Tx07-71	7/18/2019 22:32	3241377.175	829931.244	0.089	wl
Tx07-72	7/18/2019 22:32	3241377.091	829931.296	0.128	wl
Tx07-73	7/18/2019 22:32	3241377.047	829931.193	0.092	wl
Tx07-74	7/18/2019 22:32	3241377.109	829931.143	0.103	wl
Tx07-75	7/18/2019 22:32	3241377.021	829931.122	0.111	wl
Tx07-76	7/18/2019 22:32	3241377.062	829931.12	0.091	wl
Tx07-77	7/18/2019 22:33	3241377.079	829931.119	0.095	wl
Tx07-78	7/18/2019 22:33	3241377.064	829931.124	0.098	wl
Tx07-79	7/18/2019 22:33	3241377.058	829931.12	0.083	wl
Tx07-80	7/18/2019 22:33	3241376.954	829931.27	0.111	wl
Tx07D-81	9/8/2019 15:37	3241383.017	829970.691	0.167	wl
Tx07D-82	9/8/2019 15:37	3241383.029	829970.658	0.186	wl
Tx07D-83	9/8/2019 15:37	3241383.103	829970.642	0.170	wl
Tx07D-84	9/8/2019 15:37	3241383.074	829970.625	0.151	wl
Tx07D-85	9/8/2019 15:37	3241383.136	829970.585	0.163	wl
Tx07D-86	9/8/2019 15:37	3241383.107	829970.464	0.142	wl
Tx07D-87	9/8/2019 15:37	3241383.016	829970.328	0.165	wl
Tx07D-88	9/8/2019 15:37	3241383.108	829970.255	0.099	wl
Tx07D-89	9/8/2019 15:37	3241383.117	829970.172	0.124	wl
Tx07D-90	9/8/2019 15:37	3241383.141	829970.064	0.134	wl
Tx07D-91	9/8/2019 22:34	3241375.444	829932.748	-0.099	wl
Tx07D-92	9/8/2019 22:34	3241375.466	829932.743	-0.090	wl
Tx07D-93	9/8/2019 22:34	3241375.481	829932.761	-0.101	wl
Tx07D-94	9/8/2019 22:34	3241375.463	829932.75	-0.114	wl
Tx07D-95	9/8/2019 22:34	3241375.438	829932.76	-0.095	wl
Tx07D-96	9/8/2019 22:34	3241375.427	829932.755	-0.110	wl
Tx07D-97	9/8/2019 22:34	3241375.433	829932.75	-0.085	wl
Tx07D-98	9/8/2019 22:34	3241375.429	829932.746	-0.097	wl
Tx07D-99	9/8/2019 22:34	3241375.404	829932.745	-0.109	wl
Tx07D-100	9/8/2019 22:34	3241375.416	829932.746	-0.095	wl
Tx07D-101	9/26/2019 19:59	3241374.4	829932.065	0.137	WL
Tx07D-102	9/26/2019 19:59	3241374.402	829932.046	0.136	WL
Tx07D-103	9/26/2019 19:59	3241374.391	829932.054	0.163	WL
Tx07D-104	9/26/2019 19:59	3241374.382	829932.049	0.111	WL
Tx07D-105	9/26/2019 19:59	3241374.4	829932.032	0.134	WL
Tx07D-106	9/26/2019 19:59	3241374.345	829931.992	0.129	WL
Tx07D-107	9/26/2019 19:59	3241374.335	829931.968	0.112	WL
Tx07D-108	9/26/2019 19:59	3241374.37	829931.986	0.141	WL
Tx07D-109	9/26/2019 19:59	3241374.382	829931.992	0.122	WL
Tx07D-110	9/26/2019 19:59	3241374.364	829932.021	0.118	WL

APPENDIX G: CURRENT METER FILE LOG (AQUADOPP, SL-500, AND AWAC)

Table A-G 1. List of current meter files (Aquadopp, SL-500, and AWAC)

Inlet	Station	Filename	Start date time (UTC)	End date time (UTC)
	Name			
Barataria Pass	Tx-02	BP01001.arg	01/15/2019 15:00:00	01/19/2019 23:00:00
Barataria Pass	Tx-02	BP02006.arg	02/24/2019 21:00:00	03/14/2019 21:00:00
Barataria Pass	Tx-02	BP02007.arg	03/14/2019 21:12:33	03/21/2019 00:12:33
Barataria Pass	Tx-02	BP3001.arg	04/10/2019 19:00:00	04/13/2019 10:00:00
Barataria Pass	Tx-02	BP3002.arg	04/13/2019 12:04:06	04/23/2019 22:04:06
Barataria Pass	Tx-02	BP3003.arg	04/26/2019 09:53:19	04/27/2019 22:53:19
Barataria Pass	Tx-02	BP3004.arg	04/27/2019 23:57:41	04/28/2019 19:57:41
Barataria Pass	Tx-02	BP4001.arg	04/28/2019 22:00:00	05/03/2019 15:00:00
Barataria Pass	Tx-02	BP4002.arg	05/03/2019 16:18:00	05/15/2019 15:18:00
Barataria Pass-LSU	Tx-02	BPJU1902.WPR	06/26/2019 22:23:23	09/05/2016 12:51:23
Barataria Pass-LSU	Tx-02	BPAUG03.WPR	09/05/2019 13:51:03	09/17/2019 22:28:03
Barataria Pass-LSU	Tx-02	BPSEPT02.WPR	09/17/2019 23:20:49	09/25/2019 20:10:49
Quatre Bayou Pass	Tx-04	QB01001.arg	01/16/2019 22:00:00	01/26/2019 15:00:00
Quatre Bayou Pass	Tx-04	Tx04D201	03/22/2019 21:00:00	04/10/2019 21:00:00
Fontanelle Pass	Tx-07	EJ01001.arg	01/26/2019 20:00:00	03/12/2019 17:30:00
Fontanelle Pass	Tx-07	EJ02001.arg	03/12/2019 19:00:00	05/05/2019 19:00:00
Fontanelle Pass	Tx-07	EJ03001.arg	05/05/2019 20:30:00	07/01/2019 13:30:00
Fontanelle Pass	Tx-07	EJ04001.arg	07/01/2019 16:00:00	07/18/2019 20:00:00
Fontanelle Pass	Tx-07	EJ05001.arg	07/18/2019 21:00:00	09/08/2019 21:00:00
Fontanelle Pass	Tx-07	EJ06001.arg	09/08/2019 23:00:00	09/26/2019 18:00:00

APPENDIX H: YSI FILE LOG

Table A-H 1. List of raw YSI files

Inlet	Station	Filename Name	Start date time (UTC)	End date time (UTC)
Barataria Pass	Tx-02	TO55Tx02D_14C101014_011519_191200_all	01/15/2019 19:36:00	02/24/2019 9 20:24:00
Barataria Pass	Tx-02	TO55Tx02D_14C101014_022419_212400	02/24/2019 22:00:00	03/22/2019 9 21:12:00
Barataria Pass	Tx-02	TO55Tx02D2_14C101014_032219_221200	03/22/2019 22:36:00	04/10/2019 9 19:24:00
Barataria Pass	Tx-02	TO55Tx02D_14D102135_041019_202000	04/10/2019 21:20:01	04/28/2019 9 18:20:01
Barataria Pass	Tx-02	TO55Tx02D_14D102135_042819_194000.bin	04/28/2019 19:40:00	05/15/2019 9 16:50:00
Barataria Pass	Tx-02	Tx02D_14D102136_051519_184000.bin	05/15/2019 20:00:00	07/18/2019 9 15:00:00
Barataria Pass	Tx-02	TO55Tx02D_14D102135_090519_060000	09/05/2019 16:00:01	09/25/2019 9 18:20:01
Quatre Bayou Pass	Tx-04	TO55Tx04D_14D102135_011619_204800	01/16/2019 22:00:01	03/05/2019 9 01:00:01
Quatre Bayou Pass	Tx-04	tx04D2_14D102136_032219_201006	03/22/2019 21:10:06	04/10/2019 9 21:22:06
Fontanelle Pass	Tx-07	TO55Tx07D_14C101015_011119_210000	01/11/2019 21:24:00	01/20/2019 9 03:00:00
Fontanelle Pass	Tx-07	TO55Tx07D_14M101280_031219_191200	03/12/2019 20:12:00	03/17/2019 9 16:24:00
Fontanelle Pass	Tx-07	TO55Tx07D_14M101280_031219_191200_all.bi n	03/12/2019 20:12:00	05/05/2019 9 20:49:00
Fontanelle Pass	Tx-07	TO55Tx07D_14M101280_050519_211200.bin	05/05/2019 22:24:00	06/05/2019 9 10:24:00
Fontanelle Pass	Tx-07	Tx07D_14D102134_071819_222000.bin	07/18/2019 22:40:00	09/08/2019 9 20:00:00
Fontanelle Pass	Tx-07	TO55_Tx07D_14D102306_090819_120000.bin	09/08/2019 21:20:00	09/26/2019 9 18:40:00

Table A-H 2. List of processed YSI files

Inlet	Station	Filename Name	Start date time (UTC)	End date time (UTC)
Barataria Pass	Tx-02	TO55-Tx02D_2019	01/15/2019 20:00:00	09/25/2019 18:00:00
Quatre Bayou Pass	Tx-04	TO55-Tx04D_2019	01/16/2019 22:00:00	04/10/2019 21:00:00
Fontanelle Pass	Tx-07	TO55-Tx07D_2019	01/11/2019 21:00:00	09/26/2019 19:00:00

APPENDIX I: SUSPENDED SEDIMENT DATA LOG FOR YSI TURBIDITY CALIBRATION

Table A-I 1. Data log of suspended sediment samples for YSI turbidity calibration analyzed for TSS, the corresponding YSI turbidity value in FNU is also shown, matched by closest date and time. These data are contained in the same file as TSS/LOI/grain size file.

Inlet	Bottle	Sample #	Bottle Date Time (UTC)	TSS (mg/L)	YSI Date Time (UTC)	Turb (FNU)
2	TURB	TO55-Tx-02-D	1/15/19 21:16	18.40	1/15/2019 21:12	19.05
2	TURB	TO55-Tx-02-D	1/16/19 16:03	9.21	1/16/2019 16:00	5.99
2	TURB	TO55-Tx-02-D	2/5/19 17:58	18.97	2/5/2019 18:00	6.52
2	TURB	TO55-Tx-02D	2/24/2019 20:12	156.71	2/24/2019 20:12	108.46
2	TURB	TO55-Tx-02-D	2/24/19 21:38	162.70	2/24/2019 21:48	91.51
2	TURB	TO55-Tx-02-D	3/22/19 15:50	23.69	3/22/2019 15:36	13.47
2	TURB	TO55-Tx-02-D	3/22/2019 21:40	20.17	3/22/2019 22:36	14.06
2	TURB	TO55-Tx-02	4/28/2019 18:25	17.47	4/28/2019 18:20	9.12
2	TURB	TO55-Tx-02	4/28/2019 19:52	23.63	4/29/2019 20:20	10.96
2	TURB	TO55-Tx-02-D	5/15/2019 19:55	57.73	5/15/2019 20:00	35.03
2	TURB	TO55-Tx-02D	9/5/2019 15:35	21.33	9/5/2019 15:40	12.17
2	TURB	TO55-Tx-02-D	3:37:00 PM	39.83	ND	ND
4	TURB	TO55-Tx-04-D	1/16/19 21:50	11.10	1/16/19 21:48	8.51
4	TURB	TO55-Tx-04-D	3/22/19 21:10	8.09	3/22/19 21:10	31.76
4	TURB	TO55-Tx-04	4/28/2019 17:50	17.97	ND	ND
7	TURB	TO55-Tx-07-D	1/11/19 21:25	11.00	1/11/2019 21:24	6.82
7	TURB	TO55-Tx-07-D	1/26/19 20:10	16.69	ND	ND
7	TURB	TO55-Tx-07-WS (451out)	3/12/19 17:30	21.00	ND	ND
7	TURB	TO55-Tx-07-D	3/12/19 19:55	22.01	3/12/2019 20:00	34.51
7	TURB	TO55-Tx-07-D surf	3/17/19 17:05	14.85	3/17/2019 17:00	4.04
7	TURB	TO55-Tx-07-D	3/17/19 22:40	20.89	3/17/2019 22:48	14.87
7	TURB	TO55-Tx-07	5/6/2019 17:56	29.29	5/6/2019 18:00	38.14
7	TURB	TO55-Tx-07-D	5/6/2019 19:03	34.15	5/6/2019 19:00	35.86
7	TURB	TO55-Tx-07	5/6/2019 21:08	25.05	5/6/2019 21:24	46.44
7	TURB	TO55-Tx-07	5/6/2019 22:15	34.72	5/6/2019 22:12	37.54
7	TURB	TO55-Tx-07	5/6/2019 22:39	54.93	5/6/2019 22:36	34.11
7	TURB	TO55-Tx-07-D	6/4/2019 22:05	35.05	ND	ND
7	TURB	TO55-Tx-07	7/18/2019 20:23	54.47	ND	ND
7	TURB	TO55-Tx-07	7/18/2019 22:26	50.20	7/18/2019 22:40	56.25
7	TURB	TO55-Tx-07D	9/8/2019 15:25	57.50	9/8/2019 15:40	51.79
7	TURB	TO55-Tx-07	9/8/2019 22:30	53.92	9/8/2019 22:40	50.14



**THE WATER INSTITUTE
OF THE GULF®**

1110 RIVER ROAD S., SUITE 200
BATON ROUGE, LA 70802

(225) 448-2813
WWW.THEWATERINSTITUTE.ORG